RADIATION FROM N_2, CO, CH_4 AND C_2H_4 PRODUCED BY ELECTRON IMPACT

J. F. M. AARTS

RADIATION FROM N_2, CO, CH_4 AND C_2H_4 PRODUCED BY ELECTRON IMPACT

PROEFSCHRIFT

TER VERKRIJGING VAN DE GRAAD VAN DOCTOR IN DE WISKUNDE EN NATUURWETENSCHAPPEN AAN DE RIJKS-UNIVERSITEIT TE LEIDEN, OP GEZAG VAN DE RECTOR MAGNIFICUS DR. C. SOETEMAN, HOOGLERAAR IN DE FACULTEIT DER LETTEREN, TEN OVERSTAAN VAN EEN COMMISSIE UIT DE SENAAT TE VERDEDIGEN OP WOENSDAG 16 DECEMBER 1970 TE KLOKKE 16.15 UUR

DOOR

JACQUES FRANCISCUS MARIA AARTS

GEBOREN TE VOORBURG IN 1941

PROMOTOREN: PROFESSOR DR. J. KISTEMAKER

PROFESSOR DR.L.J. OOSTERHOFF

This work has been done under supervision of

Dr.F.J. de Heer

Aan mijn ouders

Aan Joke

The work described in this thesis is part of the research program of the "Stichting voor Fundamenteel Onderzoek der Materie" (Foundation for Fundamental Research on Matter) and the "Stichting Scheikundig Onderzoek in Nederland" (Netherlands Foundation for Chemical Research) and was made possible by financial support from the "Nederlandse Organisatie voor Zuiver-Wetenschappelijk Onderzoek" (Netherlands Organization for the Advancement of Pure Research).

CONTENTS

CHAPTER I

INTRODUCTION

1. *General.* The impact of electrons on molecules can give rise to electronic excitation and ionization processes. The experimental work on some simple molecules, described in this thesis, deals with those electronic transitions leading to excited states, which allow the measurement of the resulting radiative decay. In these experiments, the transition is produced by the impact of an electron beam of variable kinetic energy and of known current intensity on a molecular gas of known density, in a pressure range where secondary collisions can be neglected.

The results are expressed in the form of a cross section [1]) for the emission of the relevant radiation, σ_{em}, which has the dimensions of an area. The emission cross section is evaluated by the following equation:

$$\sigma_{em} = \frac{4\pi}{\omega} \frac{S(\omega)}{k(\lambda)(I/e)NL} P \qquad (1)$$

where $S(\omega)/k(\lambda)$, the intensity of the radiation into a solid angle ω, is measured by means of a monochromator and a photomultiplier; $k(\lambda)$ is the quantum yield (current detected per incoming photon per second) of the optical equipment; I/e is the incident electron beam flux; N is the target density; L is the path length along which emission is observed and P is a correction factor in the case of an anisotropic angular distribution of the radiation due to polarization. Because the detected radiation is produced by electrons scattered over all different angles,

the emission cross section is a so called total cross section.

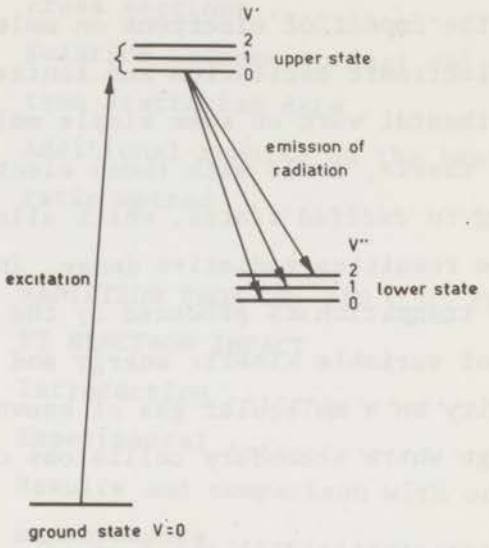

Fig. 1. Schematic diagram to illustrate the excitation and de-excitation process.

In fig. 1 we show the relation between the cross sections for excitation of an electronic state, σ_{exc}, and the corresponding emission cross sections. In the case that radiationless transitions can be neglected and radiation occurs to only one lower electronic state, the excitation cross section can be evaluated by measuring the emission cross sections for all possible transitions between the different vibrational levels of the two electronic states involved (see fig. 1):

$$\sigma_{exc} = \sum_{v'} \sigma_{exc}(v') = \sum_{v'} \sum_{v''} \sigma_{em}(v'-v'') \qquad (2)$$

where the vibrational levels v of the upper and lower

electronic states are marked with a single and a double prime respectively. The extension of this relation to cases where cascade from higher excited electronic states and/or decay to other electronic states (branching) are present, is discussed in the following chapters.

The determination of $\sigma_{em}(v'-v'')$ and $\sigma_{exc}(v')$ can provide information on the Franck-Condon factors for the relevant transitions in the de-excitation and excitation process respectively [2]. A Franck-Condon factor is the square of the integral over the product of the vibrational eigenfunctions of the two states involved.

The energy dependence of the cross sections is related to the character of the excitation process. High energy electron impact favoures optically allowed transitions. According to the Born approximation [3], which is valid in this energy region, the energy dependence of σ_{exc} is proportional to the oscillator strength of the relevant transition.

Measurements between 100 and 5000 eV have been performed on an apparatus ("high energy"), which has been used in the investigations described in ref. 4. At low impact energies optically forbidden, including spin forbidden transitions are also important in the excitation process (see for instance Brongersma [5]). The spin forbidden transitions are sometimes only detectable near the onset potential of the excitation. A "low energy" apparatus was built to study the optically forbidden excitation of molecules by the impact of electrons with energies below 100 eV (see section 2). This apparatus can also be used for the determination of the onset potential (threshold)

for the emission of radiation (either from the molecule, the molecular ion or molecular fragments). This onset potential is equal to the excitation energy of the upper molecular state involved in the excitation process.

Optical studies on the radiation from excited molecular ions and excited fragments provide information on ionization and dissociation processes, which complements that obtained in ion and electron spectroscopy and in studies where one determines the production and energy distribution of product electrons and ions [6]) (e.g. using a mass spectrometer, an electrostatic analyzer or a condensor).

Our results are most closely related to that non-optical experiments where the scattering and the energy loss of the primary electrons by the target gas is determined by means of an electron spectrometer (see for instance Lassettre [7]) and ref. 1). In these experiments one determines the differential scattering cross section $\sigma(E,\theta)$ for an energy loss E (= excitation energy of the excited state under consideration) at a scattering angle θ (with respect to the incident beam). The relation with the excitation cross section in eq. (2) is given by

$$\sigma_{exc} = \int_{\theta=0}^{\pi} \int_{\phi=0}^{2\pi} \sigma(E,\theta) \sin\theta d\theta d\phi \qquad (3)$$

where ϕ is the azimuthal angle.

Because of the limited energy resolution of the electron spectrometer, only lower excited states can be studied in this way. The optical measurements are also possible for higher excited states.

In order to obtain, as outlined above, more detailed in-

formation on the molecular excitation processes in N_2, CO, CH_4 and C_2H_4, we studied the radiation between about 500 and 10000 Å produced by electron impact between threshold and 5000 eV. The occurrence of the radiation from N_2 and CO in the upper layers of our atmosphere and that of other celestial bodies, have lead to the use of cross section data in astrophysical problems. Further, a spectroscopic investigation of molecules is of interest in radiation- and photochemistry [8]).

Measurements on radiation of the "First Negative" system of N_2^+ and the "Second Positive" group of N_2 in the visible and near ultraviolet wavelength region have been made previously by different groups. However, there were large discrepancies both in the energy dependence and the absolute values of the cross sections. We therefore decided to remeasure these bands and to extend the measurements to higher energies, allowing analysis of the results with the Bethe-Born approximation [3]). The results on dissociative excitation and ionization in N_2 are partly interpreted by means of the molecular orbital theory.

Only a few measurements on the radiation from CO, CH_4 and C_2H_4 have been carried out by other workers in a pressure region where secondary processes can be neglected. At the time that we started our work no experimental data were available for the radiation in the vacuum ultraviolet from the molecules studied here, partly due to experimental difficulties in the determination of the sensitivity of the optical equipment. For the intensity calibration in this spectral range we developed the so called branching ratio method for molecules, as described in ref. 9 and chapter IIC, section 2.2.

Generally our electron impact cross sections are compared with those in proton experiments and related with photon impact data.

In the course of our experimental investigation, similar work on N_2 and CH_4 in the vacuum ultraviolet spectral region was started by Sroka [10]), Holland [11]), Ajello [12]) and Mumma [13]). Their results will also be discussed in the following chapters. Additional measurements on N_2 in the near red, namely the Meinel system and the "First Positive" group, have been performed by McConkey and Simpson [14]), Srivastava and Mirza [15]) and Stanton and St.John [16]).

2. *The "low energy" apparatus.*

2.1. *General.* The main part of the "low energy" apparatus is shown schematically in fig. 2. The apparatus consists of a stainless steel cylindrical vessel, divided into two parts: a vacuum chamber which contains an electron source, and a collision chamber which contains an electrode system and a connection to the monochromator(s). Both chambers are connected via a collimator and a bypass. The electron beam is directed into the collision chamber and the current is measured with a Faraday cage. An axial magnetic field (maximum 380 Oe) is produced around the collision chamber in order to align the electron beam. The dimensions of the "low energy" apparatus are much smaller than those of the "high energy" apparatus [4]), which was designed originally for ionization measurements. The pressure of the target gas, introduced into the collision chamber, is measured with various pressure meters, mentioned below. The intensity of the radiation, produced along a well defined

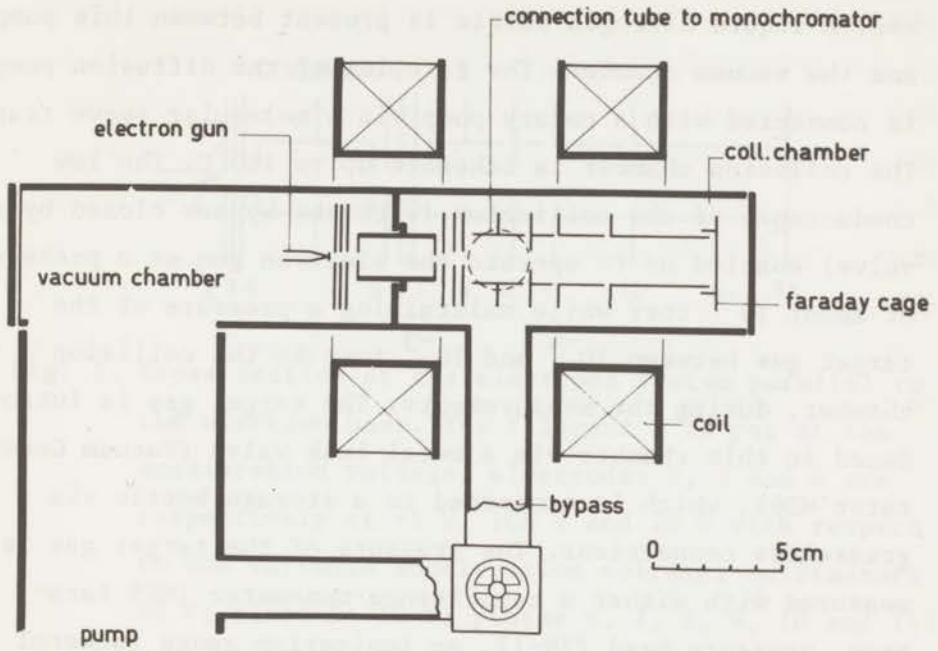

Fig. 2. The "low energy" apparatus: schematic representation of the vertical cross section through the axis. The connection tubes to the monochromators, perpendicular to this cross section, are indicated by a dotted circle.

pathlength, is measured by means of a monochromator in combination with a photomultiplier. The potential across a precision resistor, produced by the photomultiplier current, was measured with a DC voltmeter (General Radio, type 1230-A).

The emission cross sections can be evaluated by means of eq. (1). This is discussed in more detail in the following chapters.

2.2. *Vacuum.* The system is evacuated by an oil diffusion pump (Edwards E04) with a nominal pumping speed of 600 l/

sec. A liquid nitrogen baffle is present between this pump and the vacuum chamber. The foreline of the diffusion pump is connected with a rotary pump via a molecular seeve trap. The collision chamber is bakeable up to 150°C. The low conductance of the collimator (with the bypass closed by a valve) enabled us to operate the electron gun at a pressure of about 10^{-6} torr while maintaining a pressure of the target gas between 10^{-4} and 10^{-3} torr in the collision chamber, during the measurements. The target gas is introduced in this chamber via a metal leak valve (Vacuum Generator MD6), which is connected to a storage bottle via greaseless connections. The pressure of the target gas is measured with either a capacitance manometer (MKS Baratron, pressure head 77H-1), an ionization gauge (General Electric, 22GT110) or a McLeod manometer constructed in the laboratory. The McLeod manometer calibrated as described in ref. 17, served for calibration of the ionization gauge and the capacitance manometer.

2.3. *The electron source and electrode system.* The electron gun (see fig. 3), consists of a filament* (1), a grid (2), an anode (3) and a lens (4). The voltages applied to the various elements are given in fig. 3. The acceleration voltage determines, to a first approximation, the energy of the electrons in the viewing region of the monochromator (between plates 8 and 9 at earth potential). In order to eliminate the influence of contact potentials, field

* Thoriated tungsten filaments were kindly supplied by Dr. P. Zalm of the Natuurkundig Laboratorium, N.V. Philips' Gloeilampenfabrieken.

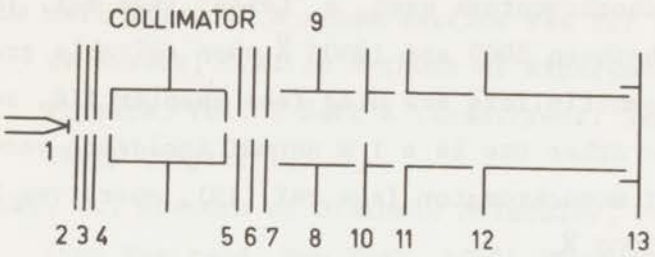

Fig. 3. Cross section of the electrode system parallel to the electron beam. The filament 1 is put at the acceleration voltage; electrodes 2, 3 and 4 are respectively at -1 V, 100 V and 20 V with respect to the variable acceleration voltage; collimator: 20 V; plate 5: 10 V; plates 6, 7, 8, 9, 10 and 11: 0 V; plate 12: 30 V and plate 13: 67.5 V.

penetration and space charge effects we calibrated the energy scale of the electron beam by means of a known threshold for emission from a target gas, i.e. He or N_2 (see chapter IV, section 2). The energy definition of the electron beam is estimated to be better than 0.5 eV. This definition can be disturbed by too large current densities and too high gas pressures (see for instance ref. 1). The currents usually varied between 1 and 20 μA.

By using a potential configuration in the collision chamber with the observation region at a lower potential than the collimator and Faraday cage, the disturbance by secondary electrons is suppressed (see chapter IIB).

2.4. *Optical detection.* To analyse the spectrum of photons, produced by the impact of the electron beam on the target gas, different grating monochromators can be

connected to either side of the collision chamber. One of the monochromators used, a "Leiss" (see ref. 18) can operate between 2000 and 10000 Å when suitable gratings and photomultipliers are used (see chapter IIC, section 2.1). The other one is a 1 m normal incidence vacuum ultraviolet monochromator (see ref. 19), operating between 500 and 2000 Å.

The intensity calibration of the equipment is discussed in the following chapters.

REFERENCES

1) For the definition of a cross section see for instance Kuyatt, C.E. in Methods of Experimental Physics, Vol. 7 Part A (Acad.Press, New York, 1968) Chapter 1.

2) Herzberg, G., Spectra of Diatomic Molecules, 2nd ed. (Van Nostrand, New York, 1966) Chapter IV.4.

3) Bethe, H.A., Ann.Physik 5 (1930) 325; see also Miller, W.F. and Platzman, R.L., Proc.Phys. Soc. 70 (1957) 299.

4) Moustafa Moussa, H.R., De Heer, F.J. and Schutten, J., Physica 40 (1969) 517.

5) Brongersma, H.H., Thesis, University of Leiden (1968); Brongersma, H.H. and Oosterhoff, L.J., Chem. Phys.Letters 3 (1969) 437.

6) Massey, H.S.W., Burhop, E.H.S. and Gilbody, H.B., Electronic and Ionic Impact Phenomena, Vol.II (Clarendon Press, Oxford, 1969) Chapters 12 and 13.

7) Lassettre, E.N., Canad.J.Chem. 47 (1969) 1733.

8) Turro, N.J., Molecular Photochemistry (Benjamin, New York, 1967), Chapter 4.

9) Aarts, J.F.M. and De Heer, F.J., J.Opt.Soc.Am. 58 (1968) 1666; see also Chapter IIIB, section 6.

10) Sroka, W., Z.Naturforsch. 24a (1969) 398, 1724.

11) Holland, R.F., J.chem.Phys. 51 (1969) 3940.

12) Ajello, J.M., J.chem.Phys. 53 (1970) 1156.

13) Mumma, M.J., Thesis, University of Pittsburgh (1970).

14) McConkey, J.W. and Simpson, F.R., J.Phys. B. 2 (1969) 923.

15) Srivastava, B.N. and Mirza, I.M., Canad.J.Phys. 47 (1969) 475.

16) Stanton, P.N. and St.John, R.M., J.Opt.Soc.Am. 59 (1969) 252.

17) Politiek, J., Thesis, University of Amsterdam (1970).

18) Schutten, J., Van Deenen, P.J., De Haas, E. and De Heer, F.J., J.Sci.Instr. 44 (1967) 153.

19) Moustafa Moussa, H.R. and De Heer, F.J., Physica 36 (1967) 646.

CHAPTER II

Part A

EMISSION CROSS SECTIONS OF THE FIRST NEGATIVE BAND SYSTEM OF N_2 BY ELECTRON IMPACT*

Synopsis

Cross sections have been measured for the emission of the First Negative Band system of N_2 when excited by electrons in the energy range of 0.1 to 6 keV. In particular the v'' progressions with the $v' = 0$ and 1 levels have been investigated. The emission cross sections can be analyzed by application of the Bethe-Born approximation. A relatively strong contribution from collision-induced dipole transitions is found in the excitation process. The energy behaviour of all vibrations is the same. The total emission cross sections of both v'' progressions account for 12.5% of the total ionization cross sections of N_2. Comparison is made with existing electron, proton and photon impact data.

1. *Introduction.* Studies on the excitation of N_2 by electron impact are of astrophysical interest. In the present study we investigated the formation of N_2^{+*} in the case of electron impact on nitrogen by measuring the emission of the radiation of eight bands of the v'' progressions with $v' = 0$ and 1 of the $B^2\Sigma_u^+ - X^2\Sigma_g^+$ transition. Our impact energy range extends over 0.1–6 keV. Most previous measurements have been carried out for the 0–0 vibrational transition. There are measurements of Sheridan *et al.*[1]) who measured between threshold energy and 30 keV. A lower energy range up to about 2 keV has been used by Hayakawa and Nishimura[2]) and by McConkey *et al.*[3]). Measurements below 200 eV on different $v' = 0 - v''$ transitions are reported by Stewart[4]), McConkey and Latimer[3]) and Zapesochnyi and Skubenich[5]). Recently Nishimura[6]) measured absolute cross sections for the v'' progressions with $v' = 0$ and 1 with an impact energy of 400 eV and relative cross sections in the energy range of 80–1500 eV. Measurements of ref. 3 on the 0–0 band lead to cross sections which are about a factor of 2.5 higher than those of refs. 1, 2, 4, and 6.

There are some measurements on the v'' progression with $v' = 0$ and 1

* Physica 40 (1968) 197,

J.F.M. Aarts, F.J. De Heer, D.A. Vroom.

done by proton impact by Philpot and Hughes[7]), Sheridan and Clark[8]), Thomas *et al.*[9]), Robinson and Gilbody[10]), Dahlberg *et al.*[11]) and Dufay *et al.*[12]). These results will be compared with electron data in section 4.4.

2. *Experimental procedure.* The apparatus and experimental technique are the same as those described in ref. 13. Basically, the excitation apparatus consists of an electron gun, a collision chamber and an electron trap. Care was taken in construction and operation of the apparatus to suppress the effects of secondary electrons and to insure complete collection of the electron beam passing through the collision chamber. Electron currents from 10 μA up to 200 μA were used. The energy of the electron beam has been checked by carrying out light intensity measurements down to the threshold for excitation of N_2 to N_2^{+*}. The energy spread of the electrons appeared to be about 2 eV. The light emitted from the irradiated gas was observed at 90° to the electron beam axis and was analyzed by a Leiss monochromator equipped with a 1200 lines/mm Bausch and Lomb replica grating blazed at 2000 Å. The dispersion at the exit slit was about 27 Å per mm.

The pressure in the collision chamber was measured by a McLeod gauge, which was modified as suggested by Meinke and Reich[14]) to overcome the effect of the diffusion of mercury vapour. Normal pressures were lower than 1.5 micron. Care was taken that all measurements were performed in the pressure region where absorption of radiation by the target gas and collisions of the second kind could be neglected. Furthermore the electron currents were taken sufficiently small, so that the measured light intensities were proportional to these currents at a fixed aceeleration voltage.

The polarization of the radiation has been measured by means of a polaroid filter.

The emission cross section σ_{ij} for a certain spectral band was determined using the following equation

$$\sigma_{ij} = \frac{4\pi}{\omega} \frac{S(\omega)}{\frac{I}{e} NLk(\lambda)} \tag{1}$$

where $S(\omega)$ represents the light intensity in the space angle ω, I/e is the number of incident particles passing per second through the collision chamber, N is the number of gas particles per cubic centimeter, L is the emission path length observed by the monochromator and $k(\lambda)$ is the quantum yield of the optical equipment as determined using a standard tungsten ribbon lamp. Because the polarization of the radiation was found to be small ($\Pi < 0.03$) no corrections have been applied for polarization in eq. (1)[15]).

In molecular systems such as nitrogen, rotational structure on the vibrational bands broadens the lines and care must be taken to insure that

all the light emitted is accounted for. Spectral scannings with a dispersion of 0.5 Å were made in order to determine if there was contamination with other band systems or lines. The expected intensity alteration of 2 : 1 was observed between even and odd K'' in the rotational R subband. The presence of two weak atomic lines in the rotational structure of the 1–3 vibration was detected, while the 1–0 was contaminated with the 0–1 vibration of the second positive group. The contribution of this band to the emission cross section of the 1–0 is above 100 eV very small, due to the fact that the second positive group arises from triplet states formed in the collision via exchange of electrons. It is known that the corresponding cross sections decrease very rapidly with increasing impact energy[16]). The size of the entrance slit of the spectrograph is limited by the presence of bands or lines in the neighbourhood of the band under consideration. This width determined the opening required in the exit slit to ensure that the image of the band, entering the monochromator, was completely contained within the exit slit. The bandwidth used for each vibration is in table I together with the widths of the corresponding entrance and exit slits used in the monochromator. In the same table the bandwidth of the P branch and R branch until the rotation quantum number $K'' = 21$ are also mentioned; the wavelengths of this rotational fine structure have been measured by Coster and Brons[17]).

TABLE I

Band heads and bandwidths

Vibration	Band head near (Å)	Bandwidth literature[17]) (Å)	Bandwidth used (Å)	Entrance slit used (mm)	Exit slit used (mm)
0–0	3914	28	30	0.1	1.2
0–1	4278	34	32	0.1	1.3
0–2	4709	42	24	0.1	1.0
0–3	5228	—	27	0.25	1.25
1–0	3582	—	24	0.1	1.0
1–1	3884	26	24	0.1	1.0
1–2	4236	34	27	0.1	1.1
1–3	4652	40	27	0.25	1.25

3. *Results.* The experimental cross sections for emission of the 0–0 and 1–0 bands are listed in table II. The ratios of the emission cross sections of the different vibrational transitions, normalized on the 0–0 are in column F of table IV, together with the results of other groups.

The accuracy of our absolute emission cross sections is estimated to be about 10%, mainly due to systematic errors in the determination of the quantum yield of the monochromator and in the gas pressure measurement.

TABLE II

Emission cross sections of $B^2\Sigma_u^+ - X^2\Sigma_g^+$ bands of N_2 in units of 10^{-18} cm^2/mol

eV	0–0	1–0
100	21.2	1.53
110	21.2*	
150	18.9	1.33
200	16.4	1.11
300	13.3	0.912
400	11.4	0.785
500	9.81	0.685
600	8.85	0.615
700	7.86	0.557
800	7.27	0.508
1000	6.15	0.437
1500	4.57	0.330
2000	3.59	0.248
3000	2.63	0.185
4000	2.11	0.148
5000	1.74	0.123
6000	1.47	0.104

* maximum value.

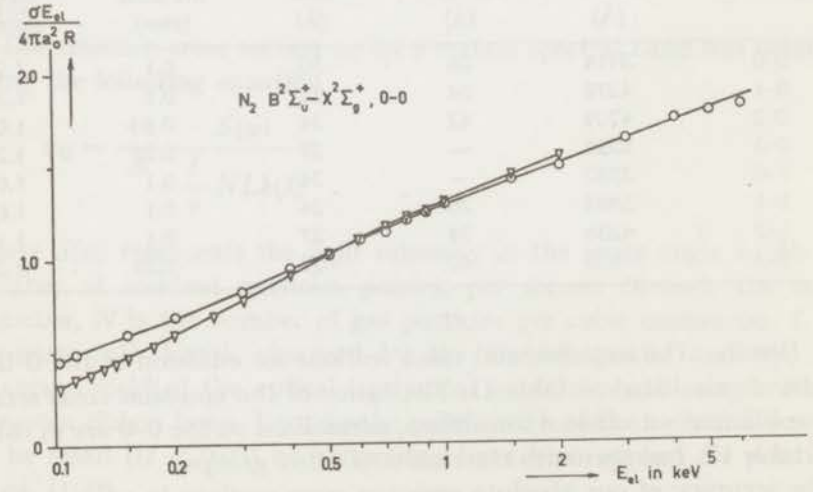

Fig. 1. The cross section for 0–0 emission in the case of electron impact on N_2, plotted as $\sigma E_{el}/4\pi a_0^2 R$ vs. ln E_{el}.
○ this work; ▽ McConkey et al.[3])

TABLE III

Cross sections of excitation of helium in 10^{-19} cm^2/atm

energy (eV)	Level					
	4^1S	5^1S	6^1S	4^1D	5^1D	6^1D
35*	2.24					
40				1.83*		
100	1.08	0.528	0.296	0.998	0.557	0.322
200	0.703			0.500	0.285	0.165
500	0.356	0.173	0.100	0.194	0.112	0.0644
1000	0.190	0.0940	0.0514	0.0918	0.0528	0.0316
2000	0.103	0.0505	0.0284	0.0524		
5000	0.0433			0.0210		

* energy at which the maximum is reached.

TABLE IV

Cross section ratios of $B^2\Sigma_u^+ - X^2\Sigma_g^+$ transitions of N_2

Vibration	proton impact				electron impact			theory
	A	B	C	D	E	F	G	H
0–0	1.00	1.00	1.00	1.00	1.00	1.00	1.00	1.00
0–1	0.31	0.31	0.25	0.39	0.32	0.32	0.3	0.31
0–2	0.063	0.074	0.066	0.10	0.075	0.060	0.05	0.061
0–3	0.010	0.011				0.0101	0.01	0.010
1–0	0.066	0.051				0.070	0.04	0.075
1–1	0.046	0.036				0.048	0.03	0.042
1–2	0.043	0.039	0.044			0.044	0.04	0.042
1–3	0.015	0.018	0.022			0.014	0.008	0.014
1–4	0.0037	0.0041						0.0035
$\frac{\sigma_{v'=1}}{\sigma_{v'=0}}$	0.125	0.10				0.127	0.088	0.120

A Dufay *et al.*[12])
B Thomas *et al.*[9])
C Robinson and Gilbody[10])
D Stewart[4])
E McConkey and Latimer[3])
F This work
G Nishimura[6])
H Nicholls[25])

The accuracy of our ratios is estimated to be about 4%. The mean deviation of our ratios of all vibrations, determined between 0.1 and 6 keV, is better than 1%. A systematic error arises in the emission cross section and in the ratio of the 1–2 vibration due to contamination with two atomic lines and could be as much as 5%. Other groups[5, 6, 7, 9, 11]) appear to have worked with slit widths principally different from our system. This may give rise to a maximum change of about 20% in their experimental cross section. The results of McConkey[3]) for the v'' progression with $v' = 0$ come very close to ours above 400 eV (see fig. 1 and table IV).

The excitation cross sections of helium, used as a second standard, appeared after careful re-examination of the apparatus to be about 20% higher than before as determined by Moustafa Moussa *et al.*[13]).

4. *Comparison with theory and other experiments*

4.1. *Bethe-Born approximation.* The excitation of the first negative band system of N_2 probably goes mainly via ionization of a valence electron (supposed to be the $2\sigma_u$ electron) of the N_2 molecule leaving the N_2^+ ion in the excited state $B^2\Sigma_u^+$. This means that when we apply the Bethe-Born approximation, we have to use the equation for ionization

$$\sigma_1 = \frac{4\pi a_0^2 R}{E_{el}} M_i^2 \ln c_1 E_{el} \tag{2}$$

where σ_1 is the ionization cross section in cm^2, a_0 is the first Bohr radius, R is the Rydberg energy, E_{el} is the electron energy, corrected for relativistic effects, c_1 is a constant and M_i^2 is the effective dipole-matrix-element squared for ionization, given by

$$M_i^2 = \int_{I.P.}^{\infty} \frac{df(E)}{dE} \frac{R}{E} \eta_1(E)\, dE \tag{3}$$

where $df(E)/dE$ is the differential oscillator strength which is a function of the excitation energy E and I.P. is the ionization potential; $\eta_1(E)$, which must be between 0 and 1, is the efficiency for ionization at excitation energy E. In our case the ionization refers to the formation of the excited $B^2\Sigma_u^+$ state of nitrogen.

From eq. (2) it can be seen that a plot of $\sigma E_{el}/4\pi a_0^2 R$ *vs.* $\ln E_{el}$, will allow determination of the value M_i^2. Such a plot is given in fig. 1 for the 0–0 band.

Eq. (2) gives the cross section of excitation of the $B^2\Sigma_u^+$ state of N_2 as a function of electron energy. We have measured the emission of eight bands from this level. Adding up all the emission from both v'' progressions and neglecting the v'' states above $v'' = 3$, we can find the corresponding excitation cross sections. In this assumption we neglect the effects of cascade of higher levels and any emission which might go to the $A^2\Pi_u$ level.

From these cross sections in the assymptotic energy region (> 0.8 keV) $M_i^2(B^2\Sigma_u^+)$ can be calculated using eq. (2). We find that in the energy region of 0.8 to 6 keV the ionization cross section of $B^2\Sigma_u^+$ amounts to about 12.5% of the total ionization cross section of N_2 measured by Schram *et al.*[18]). The corresponding M_i^2 values from electron impact, which are given in table V, have the same ratio as the cross sections.

4.2. *Photoionization and absorption.* The values of M_i^2 which have been obtained in this work can be compared with those of photoionization or photoabsorption measurements and calculations (see eqs. (2) and (3)).

A semi-empirical value of M_i^2 for total ionization can be obtained for comparison with the experimental value of Schram *et al.*[18]). We use the complete list of semi-empirical $df/d\lambda$ values (λ = wavelength) of Dalgarno *et al.*[19]) and we take for $\eta_i(E)$ the values of Samson and Cairns[20]). We then calculate $\eta_i\, df(E)/dE$ of eq. (3) and integrate. We find $M_i^2 = 3.3$ which value is 17% smaller than that of Schram *et al.*[18]). Note that the semi-empirical model of Dalgarno *et al.*[19]) is connected with the oscillator strength sum rule and with the refractive index. In their calculation it appeared to be necessary to reduce the experimental discrete oscillator strengths of Silvermand and Lassettre[21]) by 22%.

TABLE V

	electron impact	semi-empirical	proton impact
M_i^2 (total)	3.85[18])	3.3[a])	3.8[12])
M_i^2 ($B^2\Sigma_u^+$)	0.51	0.35[b])	

[a]) Derived from $df/d\lambda$ values of Dalgarno *et al.*[19]) and the η_i values of Samson and Cairns[20]).

[b]) Derived from a) and Schoen's[22]) partial photoionization cross sections.

The M_i^2 value for the $B^2\Sigma_u^+$ state can be compared with photoionization by considering the measurements of Schoen[22]). He determined relative photoionization cross sections due to the formation of the $X^2\Sigma_g^+$, $A^2\Pi_u$ and $B^2\Sigma_u^+$ states, by means of measuring the energies of electrons released from N_2 by photoionization, observing only at one direction in the wavelength region of 400 to 800 Å. From his work we estimate that $M_i^2(B^2\Sigma_u^+)/M_i^2$ (total) is about equal to 0.11, taking a constant partial ionization cross section of 0.1 below 400 Å. The ratio 0.11 has to be compared with the ratio 0.13 which is derived from our excitation measurements and the ionization measurements of Schram *et al.*[18]) (see table V). We also note that the partial photoionization cross sections of Schoen are in general agreement with those of Blake and Carver[23]) in the wavelength region of 782–580 Å. They differ about 15% with those of Frost *et al.*[24]) who measured at 584 Å over the whole sphere with a spherical electron spectrometer.

4.3. *Cross section ratios of* $B^2\Sigma_u^+ - X^2\Sigma_g^+$ *transitions.* Cross section ratios of vibrational transitions have been obtained from our experiment and are compared with those of other groups, including proton impact data and theory (see table IV). Our experimental values have been obtained by taking the average of the ratios at every impact energy used (see also section 3). Theoretical values for the ratios are calculated by

using the Franck-Condon factors of Nicholls[25]) and using the equation:

$$\sigma_{v'v''} = KN_{v'}E^3_{v'v''}\,\overline{R^e_{ij}}^2\,q_{v'v''} \tag{4}$$

where $\sigma_{v'v''}$ is the relevant cross section, K is a constant dependent on the experimental conditions, $N_{v'}$ is the population of the level v', $E_{v'v''}$ is the energy quantum of the $v'v''$ transition and $q_{v'v''}$ is the Franck-Condon factor. The electronic transition moment $\overline{R^e_{ij}}^2$ is assumed to be constant here for the whole band-system. $N_{v'=1}/N_{v'=0}$ is taken equal to the ratio of the corresponding Franck-Condon factors for excitation. This ratio is 0.120, see ref. 25. Experimentally we find 0.127 by dividing the total emission measured of the first progression by that of the zeroth progression.

As far as the ratios of the zeroth progression are concerned, there is often good agreement between different experiments and theory (see table IV). For the first progression there is more scatter between experimental data.

4.4. *Comparison between electron and proton data.* It is known that at high equal velocities protons and electrons have equal ionization or excitation efficiency. In this case for protons we can use eq. (2) replacing

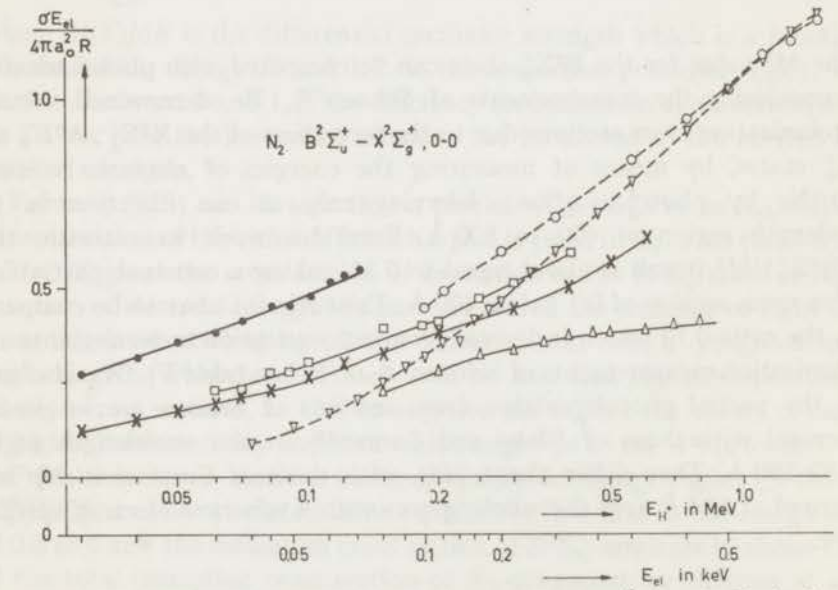

Fig. 2. The cross section for 0–0 emission plotted as $\sigma E_{el}/4\pi a_0^2 R$ vs. ln E_{el} in the case of electron and proton impact. For protons $E_{el} = (m/M)\,E_{H^+}$.

Proton data:
× Dufay *et al.*[12])
□ Robinson and Gilbody[10])
△ Thomas *et al.*[9])
● Dahlberg *et al.*[11])

Electron data:
○ this work
▽ McConkey *et al.*[3])

$v_{el.}$ by v_p. In fig. 2 the proton energies are transformed into equivalent electron energies by putting them equal to $\frac{1}{2}mv_p^2$. At lower velocities the proton cross sections will be generally higher because in the Born approximation the integration limits extend over a larger interval for protons than for electrons (see for instance Bates and Griffing[26]). Also in the case of proton excitation the capture process gives an extra contribution to the nitrogen ions: $H^+ + N_2 \rightarrow H + N_2^{+*}$. A comparison of proton and electron data is made in table IV and fig. 2. Big discrepancies appear to exist between the cross sections of the proton data. Also the energy behaviour of the high energy data of Thomas[9]) is such that no approach to electron data is present. The results of Robinson and Gilbody[10]) appear to have the best fit to the electron data of our group and those of McConkey[3]).

5. *Conclusion.* The absolute values of the cross sections of this work are over a large energy range in reasonable agreement ($< 15\%$) with those of McConkey *et al.*[1]) (see fig. 1). When scaled at equal velocities the proton impact cross sections of Robinson and Gilbody[10]) approach these electron impact cross sections at about 100 eV for electrons or 180 keV for protons (see fig. 2). The value of M_i^2 (see table V) obtained from our work for the formation of $B^2\Sigma_u^+$ is smaller by a factor of 0.13 than the M_i^2 from total ionization measurements of Schram *et al.*[18]). This factor 0.13 is about 20% larger than obtained in photoionization measurements.[22]) The absolute value of M_i^2 for total ionization determined by electron impact is about 17% larger than that obtained from semi-empirical calculations of Dalgarno *et al.*[19]) The ratio of the emission cross sections of both v'' progressions are in close agreement in many electron and proton impact experiments and in agreement with theory.

Acknowledgments. We are grateful to Professors K. Takayanagi and J. Kistemaker and Dr. M. Inokuti for valuable comments on this subject.

This work is part of the research program of the Stichting voor Fundamenteel Onderzoek der Materie (Foundation for Fundamental Research on Matter) and was made possible by financial support from the Nederlandse Organisatie voor Zuiver-Wetenschappelijk Onderzoek (Netherlands Organization for the Advancement of Pure Research).

REFERENCES

1) Sheridan, W. F., Oldenburg, O. and Carleton, N. P., Abstr. 2nd Int. Conf. Phys. Electronic and Atomic Collisions, Boulder (1961).
2) Hayakawa, S. and Nishimura, H., J. Geomagn. Geolect. **16** (1964) 72.
3) McConkey, J. W., Woolsey, J. M. and Burns, D. J., Planet. Space Sci. **15** (1967) 1332; McConkey, J. W. and Latimer, I. D., Proc. Phys. Soc. **86** (1965) 463.

4) Stewart, D. T., Proc. Phys. Soc. **A 69** (1956) 437.
5) Zapesochnyi, I. P. and Skubenich, V. V., Optics and Spectrosc. (USSR) (English Transl.) **21** (1966) 83.
6) Nishimura, H., J. Phys. Soc. Japan **24** (1968) 130.
7) Philpot, J. L. and Hughes, R. H., Phys. Rev. **133** (1964) A 107.
8) Sheridan, J. R. and Clark, K. C., Phys. Rev. **140** (1965) A 1033.
9) Thomas, E. W., Bent, G. D. and Edwards, J. L., Phys. Rev. **165** no. 1 (1968) 32.
10) Robinson, J. M. and Gilbody, H. B., Proc. Phys. Soc. **92** (1967) 589.
11) Dahlberg, D. A., Anderson, D. K. and Dayton, I. E., Phys. Rev. **164**, no. 1 (1967) 20.
12) Dufay, M., Desesquelles, J., Druetta, M. and Eidelsberg, M., Ann. Geophys. **22** (1966) 614.
13) Moustafa Moussa, H. R., De Heer, F. J. and Schutten, J., Physica, to be published; Moustafa Moussa, H. R., Thesis University of Leiden (1967).
14) Meinke, C. and Reich, G., Vakuum-Technik **12** (1963) 79.
15) Van Eck, J., De Heer, F. J. and Kistemaker, J., Physica **30** (1964) 1171.
16) Ochkur, V. I., Soviet Physics – J.E.T.P. **18** (1964) 503.
17) Coster, D. and Brons, H. H., Z. Phys. **73** (1932) 747.
18) Schram, B. L., Thesis University of Amsterdam (1966); Schram, B. L., Boerboom, A. J. H., Van der Wiel, M. J., De Heer, F. J. and Kistemaker, J., Advances in Mass Spectrometry, vol. 3 (1966) 273.
19) Dalgarno, A., Degges, T. and Williams, D. A., Proc. Phys. Soc. **92** (1967) 291.
20) Samson, J. A. R. and Cairns, R. B., J. Geophys. Res. **69** (1964) 4583.
21) Silverman, S. M. and Lassettre, E. N., J. Chem. Phys. **42** (1965) 3420.
22) Schoen, R. I., Private Communication.
23) Blake, A. J. and Carver, J. H., J. chem. Phys. **47** (1967) 1038.
24) Frost, D. C., McDowell, C. A. and Vroom, D. A., Proc. Roy. Soc. **A 296** (1967) 566.
25) Nicholls, R. W., J. Res. Nat. Bur. Stand. **65 A** (1961) 451.
26) Bates, D. R. and Griffing, G. W., Proc. Phys. Soc. **A 66** (1953) 961.

6. *Addendum.* We have remeasured the cross sections for emission of the $B^2\Sigma_u^+ - X^2\Sigma_g^+$ bands between 0.1 and 6 keV and extended the measurements to smaller energies with the "low energy" apparatus, described in chapter I. At 100, 150, and 200 eV we found emission cross sections respectively 16%, 10% and 5% lower than those given in table II. Above 200 eV the remeasured cross sections were found to be identical with those in table II. Our new values for the v'=0 - v"=0 band are given in the table below.

The measurements for the v'=0 - v"=0 band by B.N. Srivastava and I.M. Mirza (Phys.Rev. 168 (1968) 86) and W.L. Borst and E.C. Zipf (Phys.Rev. A1 (1970) 834) for electron impact at energies between 0.07 and 2.5 keV and threshold and 3 keV respectively are in good agreement, within 5%, with our data. The values of P.N. Stanton and R.M. St.John (J.Opt.Soc.Am. 59 (1969) 252), who measured between threshold and 450 eV are found to be up to at most 11% smaller than those of the former experiments. The agreement with the results of McConkey et al. [3]) is good above 300 eV; below this energy their values have a different energy dependence (see fig. 5 of the before mentioned work by Borst and Zipf).

For a comparison of our emission cross sections of the v'=0 - v"=0 band for electron and proton impact see Physica 48 (1970) 620.

Our values for the cross section ratios in table IV and M_i^2 in table V are not influenced by the change in our cross sections between 100 and 200 eV.

Emission cross sections for the v'=0 - v''=0 band of $B^2\Sigma_u^+ - X^2\Sigma_g^+$ in units of 10^{-18} cm^2/mol

20 eV	0.7
30	7.4
40	12.2
50	14.6
60	15.9
80	17.3
100	17.8
150	17.0
200	15.6

Part B

EMISSION CROSS SECTIONS OF THE SECOND POSITIVE GROUP OF NITROGEN PRODUCED BY ELECTRON IMPACT*

Synopsis

We have measured emission cross sections for the $C^3\Pi_u - B^3\Pi_g$, v'=0 - v''=0 transition of N_2 produced by 11 to 1000 eV electrons. Our cross sections decrease much faster with increasing energy than in previous experiments. This difference is probably due to a better suppression of the secondary electrons in our case.

1. *Introduction.* It is known that the cross sections, σ, for singlet-triplet transitions decrease very fast above the energy where the maximum in the cross section is reached; at sufficiently high impact energies $\sigma = A/E_{el}^3$ (see e.g. Ochkur [1]) where E_{el} is the electron energy and A a constant.

In the optical measurements this steep decrease in the cross section can easily be reduced however, due to secondary electrons, which can lead very effectively to additional excitation (see for instance Moustafa Moussa et al. [2]). For this reason we re-investigated the excitation of N_2 from $X^1\Sigma_g^+$, the ground state, to the $C^3\Pi_u$ state, by measuring the emission for v'=0 to v''=0 of the second positive group, $C^3\Pi_u - B^3\Pi_g$, with band head at 3371 Å.

* Chemical Physics Letters 4 (1969) 116
J.F.M. Aarts, F.J. De Heer.

Previous work has been reported by Stewart and Gabathuler [3]) and Zapesochnyi and Skubenich [4]). More recently Jobe et al. [5]) and Burns et al. [6]) measured emission cross sections from threshold up to about 100 eV primary electron energy.

For excitation in the energy range between 50 and 1000 eV we used the apparatus described in ref. 2. Between threshold (11 eV) and 100 eV we used an apparatus in which a better energy definition of the beam could be obtained [7]). Basically both apparatuses consist of an electron gun, a collision chamber, an electron trap and a collimating axial magnetic field (B), with a strength up to 250 Oe. The emitted radiation was observed at 90^{o} to the electron beam axis and measured with a Leiss monochromator. No corrections have been applied for the degree of polarization (Π) of the radiation; we measured that $\Pi \leq 4\%$ (see also ref. 6). The sensitivity of our optical equipment was determined by means of a tungsten standard. The pressure in the collision chamber, measured by a McLeod gauge, was varied between 10^{-4} and 10^{-3} torr. Electron currents from 1 μA, at threshold, up to 300 μA, above 500 eV, were used.

In the "high energy" apparatus, as described in ref. 2, the region from which the radiation was observed, was kept at a lower potential than the collimator and Faraday cage and other plates outside that region. This was necessary to avoid secondary electrons. For further discussion we give the scheme of the center part of the electrode configuration in fig. 1.

We analyse our cross sections on a $\sigma E_{el}/4\pi a_o^2 R$ versus $\ln E_{el}$ plot, suggested by the Bethe theory [8]), where R is

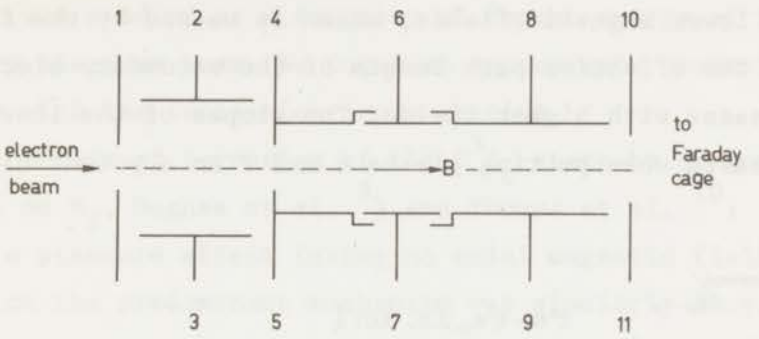

Fig. 1. Center part of the electrode system in the "high energy" apparatus [2]). Potential configuration: 1:100 V; 2:120 V; 3:40 V; 4 to 9:0 V; 10:120 V; 11:40 V. The radiation, which is observed, is emitted perpendicular to the electron beam between plates 6 and 7.

the Rydberg energy and a_o the Bohr radius. A positive or negative slope for large E_{el} in such a plot indicates an optically allowed or spin forbidden excitation process, respectively.

2. *The influence of secondary electrons.* The apparent cross section for emission was found to be independent of the primary electron beam current, except for space charge effects at too high current densities. As is shown in fig. 2 $\sigma_{apparent}$ depends on the pressure. In that figure $\sigma_{p\to 0}$ is the emission cross section obtained by extrapolation to pressure zero. Because $\sigma_{apparent}$ is independent of the electron current, recombination effects could be ruled out. It was shown that the pressure effect was caused by electrons formed in the gas via ionization of nitrogen by the

primary beam: The slopes of the lines in fig. 2 decreased with lower magnetic fields, which is caused by the fact that the effective path length of the secondary electrons increases with higher fields. The slopes of the lines also decreased when putting plates 6 and 7 on a potential nega-

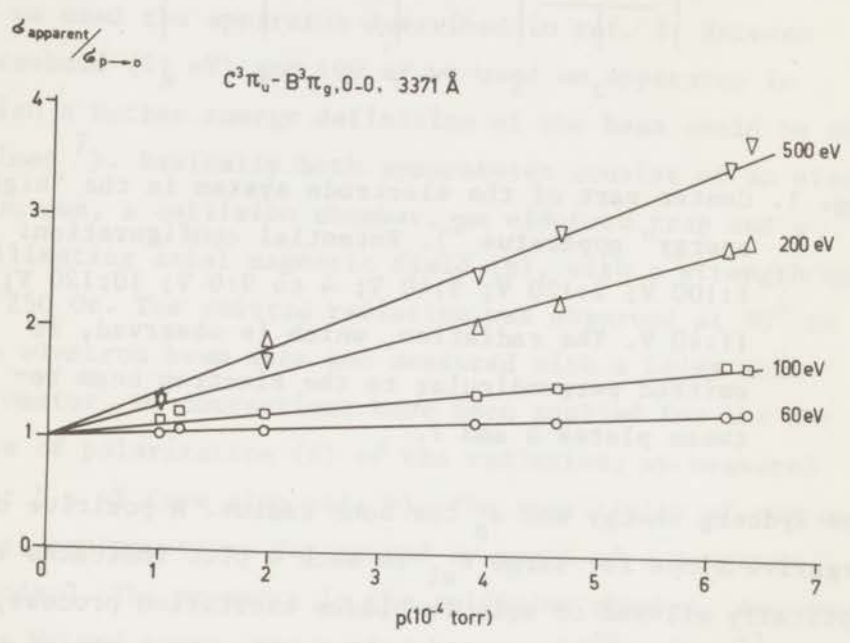

Fig. 2. Pressure dependence of the ratio of the apparent emission cross section and the emission cross section obtained by extrapolation to pressure zero at different impact energies.

tive with respect to the earthed plates 4, 5, 8 and 9 (see fig. 1), taking into account the resulting energy shift of the primary beam. This additional potential well repels the secondary electrons formed outside the region between plates 6 and 7.

A noticeable pressure dependency of $\sigma_{apparent}$ started at

about 35 eV. The absolute magnitude of the pressure effect was studied as a function of impact energy of the primary electron beam. We found an approximate proportionality with the ionization cross section.

In the case of formation of the $C^3\Pi_u$ state by proton impact on N_2, Hughes et al. [9]) and Thomas et al. [10]) found a pressure effect (using no axial magnetic field) in which the predominant mechanism was similarly ascribed to secondary electrons formed by ionization.

We found that $\sigma_{p \to 0}$ in fig. 2 also decreases with the additional potential well, but is independent of the magnetic field within the experimental error. The decrease of $\sigma_{p \to 0}$ must be due to secondary electrons from the collimator or other plates. The formation of this type of secondary electrons is independent of the pressure. The negative potential of the plates 6 and 7 was adjusted at every impact energy to the minimum in the emission of light, correcting for the energy shift of the primary beam. At 100 eV and 500 eV we applied - 10 V and - 30 V, respectively. As a consequence at 500 eV $\sigma_{p \to 0}$ decreased with a factor of 4.4 and the slope of the corresponding line in fig. 2 decreased with a factor of 4.0.

The data for $\sigma_{p \to 0}$, our emission cross sections, were taken with a magnetic field of 250 Oe.

We remark that at 500 eV and a well of - 30 V the slope in fig. 2 decreased with a factor of 2 when the magnetic field varied from 250 to 60 Oe.

Table I

Energy dependence of the emission cross sections for $C^3\Pi_u - B^3\Pi_g$, v'=0 - v''=0, normalized at the maximum

maximum in units 10^{-18} cm^2	present results	Burns et al.[6]	Jobe et al.[5]
	11.5	11.8	10.8
impact energy (eV)			
11	0	0	0
12	0.12	0.25	
13	0.52	0.65	0.27
14	1.00	1.00	
15	0.82	0.79	1.00
17	0.54	0.54	0.64
19	0.42	0.42	0.51
21	0.32	0.37	0.41
25	0.21	0.28	0.29
30	0.16	0.23	0.25
40	0.085	0.16	0.18
60	0.042	0.115	0.103
80	0.022	0.099	0.075
100	0.014	0.093	

3. Results. In table I we present our emission cross sections for the 0 - 0 transition of the second positive group as a function of electron energy, between 11 and 100 eV. The cross sections, normalized at the maximum (11.5×10^{-18} cm^2) at 14 eV are proportional to the cross sections for excitation of the triplet state $C^3\Pi_u$. In fig. 3 our data are presented by a $\sigma E_{el}/4\pi a_o^2 R$ versus $\ln E_{el}$ plot in the energy range of 50 to 1000 eV. The negative slope of our curve is typical for an excitation process with exchange of electrons. Our cross sections have a spread of about 15%. We obtained the same results

up to 100 eV both in the high and low energy apparatus, within this error. For comparison we also included in table I and fig. 3 the values of Jobe et al. [5]) and Burns

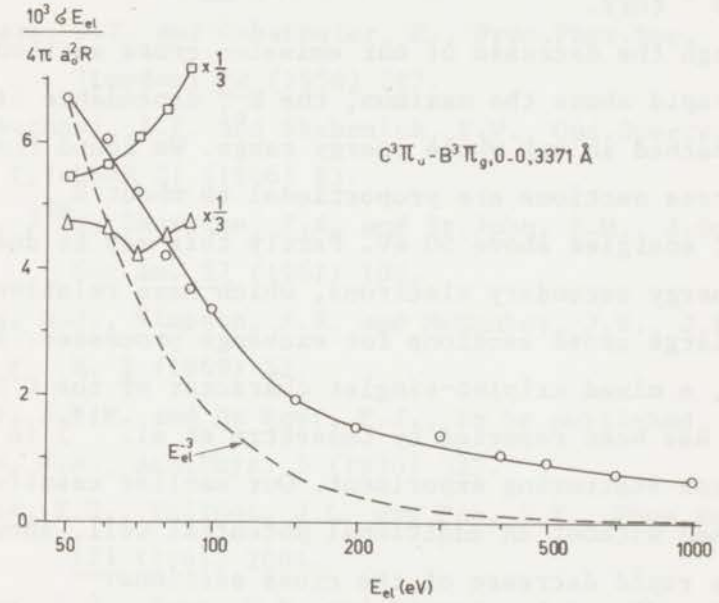

Fig. 3. Emission cross sections for the 0 - 0 vibration of the second positive group, presented in $\sigma E_{el}/4\pi a_o^2 R$ versus ln E_{el} plots: ○ present results, □ Burns et al. and △ Jobe et al. The E_{el}^{-3} dependence, normalized somewhat arbitrary at 50 eV, is given by a dotted line.

et al. [6]). In both cases the maximum cross section is in good agreement with our measurements. The numbers in table I indicate a steeper decrease of our excitation function for impact energies larger than 25 eV. This discrepancy is also apparent in fig. 3. In view of our observations, discussed in the preceding section, we attribute this discrepancy to a better suppression of seconda-

ry electrons in our experiment. Using a magnetic field of 500 Oe, Burns et al. found that the shape of the excitation curve was independent of pressure between 0.5×10^{-3} and 4.5×10^{-3} torr. Jobe et al. used pressures of 4×10^{-3} torr.

Though the decrease of our emission cross sections is very rapid above the maximum, the E_{el}^{-3} dependence is not yet reached in our whole energy range. We found that our cross sections are proportional to about $E_{el}^{-1.7}$ at impact energies above 50 eV. Partly this may be due to low energy secondary electrons, which have relatively very large cross sections for exchange processes. Besides, a mixed triplet-singlet character of the $C^3\Pi_u$ state has been reported by Lassettre et al. [11]) in an electron scattering experiment. Our earlier results [12]), obtained without an additional potential well, showed a less rapid decrease of the cross sections.

REFERENCES

1) Ochkur, V.I., Soviet Phys. JETP 18 (1964) 503.

2) Moustafa Moussa, H.R., De Heer, F.J. and Schutten, J., Physica 40 (1969) 517.

3) Stewart, D.T. and Gabathuler, E., Proc.Phys.Soc. (London) 72 (1958) 287.

4) Zapesochnyi, I.P. and Skubenich, V.V., Opt.Spectry. USSR 21 (1966) 83.

5) Jobe, J.D., Sharpton, F.A. and St.John, R.M., J.Opt. Soc.Am. 57 (1967) 106.

6) Burns, D.J., Simpson, F.R. and McConkey, J.W., J.Phys. B. 2 (1969) 52.

7) Aarts, J.F.M. and De Heer, F.J., to be published.

8) Bethe, H.A., Ann.Phys. 5 (1930) 325.

9) Hughes, R.H., Philpot, J.L. and Fan, C.Y., Phys.Rev. 123 (1961) 2084.

10) Thomas, E.W., Bent, G.D. and Edwards, J.L., Phys.Rev. 165 (1968) 32.

11) Lassettre, E.N., Skerbele, A. and Meyer, V.D., J.chem. Phys. 45 (1966) 3214.

12) Aarts, J.F.M., De Heer, F.J. and Vriens, L., VIth I.C.P.E.A.C., Boston (1969).

Part C

EMISSION CROSS SECTIONS FOR NI AND NII MULTIPLETS AND SOME MOLECULAR BANDS FOR ELECTRON IMPACT ON N_2*

Synopsis

Cross sections have been measured for the production of NI and NII multiplets between 500 and 10000 Å and of some $a^1\Pi_g$–$X\,^1\Sigma_g^+$ and $p'^1\Sigma_u^+$–$X\,^1\Sigma_g^+$ bands in the vacuum ultraviolet for 0.05–5 keV electrons incident on N_2. Most of the multiplet radiation was present in the vacuum ultraviolet region; considerable cascade contributions were found. The apparent emission cross sections for the $a^1\Pi_g$–$X\,^1\Sigma_g^+$ and $p'^1\Sigma_u^+$–$X\,^1\Sigma_g^+$ transitions were pressure dependent even at low gas densities. In the vacuum ultraviolet the cross sections were brought on an absolute scale by means of the branching ratio method for molecules, inelastic scattering data and experimental emission cross sections. At high impact energies ($\gtrsim$ 300 eV) the energy dependence of the cross sections has been analysed by means of the Bethe–Born approximation: for NI it was found that the terms involved were mainly formed via optically allowed excitation processes in the molecule; for NII optically forbidden transitions were dominant. An attempt has been made to correlate the observed dissociation fragments with intermediate molecular states. The electron impact cross sections of this work have been compared with other electron, proton and photon impact data.

1. *Introduction.* The present study on dissociative excitation and ionization of N_2 and on the radiative transitions from the excited molecular states $a^1\Pi_g$ and $p'\,^1\Sigma_u^+$ is an extension of our previous work[1–3]) on the radiation between 500 and 10000 Å produced by the impact of 0.05–5 keV electrons on N_2.

Optical studies on dissociation as described in this paper give more detailed information on the excited states of the fragments than can be obtained in mass spectrometric studies or measurements of the energy distribution of the product electrons and ions (for a review about the latter experiments see Massey *et al.*[4])). The most intense NI and NII multiplets were found in the vacuum ultraviolet wavelength region. In this part of the spectrum we also measured the radiation from the molecular states $a^1\Pi_g$ and $p'\,^1\Sigma_u^+$[5,6]). Early work concerning the multiplet radiation produced

* to be published in Physica, by J.F.M. Aarts and F.J. De Heer.

by electron impact around 8213 Å was reported by Sheridan *et al.*[7]). More recently Srivastava[8]) determined emission cross sections for two NII multiplets in the visible wavelength region for electron energies between 0.15 and 4 keV. Emission cross sections in the vacuum ultraviolet have been reported by Sroka[9]), Ajello[10]), and Mumma[11]) for electron energies between threshold and 350 eV. For proton impact similar measurements have been carried out[12–16]) with projectile velocities partly overlapping those of the electron experiments. Of the photon impact measurements, relevant to this work, we mention those of Beyer and Welge[17]); reviews are given by Huffman[18]) and Schoen[19]).

The multiplet radiation from NI and NII observed in this experiment, is schematically presented in figs. 1 and 2, respectively. For identification we used the multiplet tables of Moore[20]) and Striganov and Sventitskii[21]). In fig. 2 a few multiplets, which were observed by Sroka[9]) below 650 Å, have

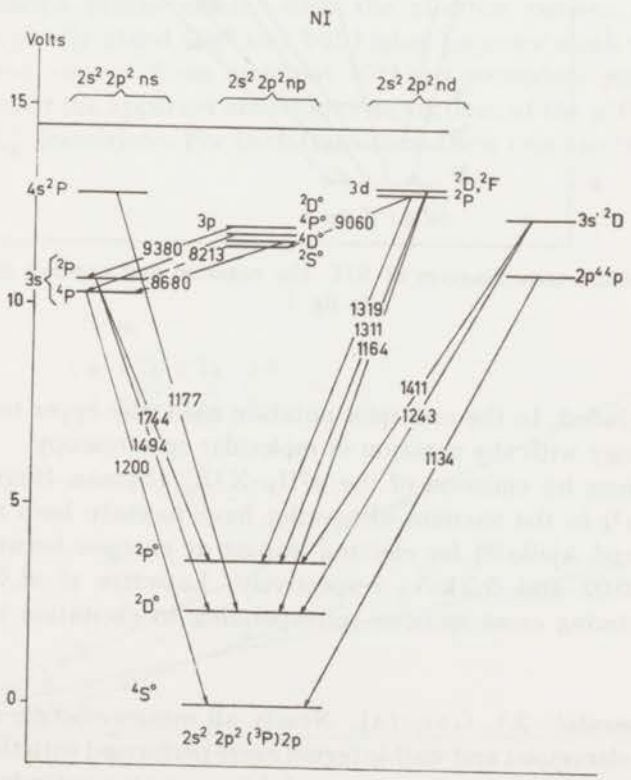

Fig. 1. Part of the term diagram of NI. The horizontal line at 14.5 eV denotes the ionization potential of N, which is the series limit of terms belonging to the configurations $(1s^2)\ 2s^2\,2p^2\,ns$ ($n = 3,4$), $2s^2\,2p^2\,np$ ($n = 2, 3$) and $2s^2\,2p^2\,nd$ ($n = 3$). Two terms, going to other limits, are given at the right side. For the notation of the terms see ref. 20. The observed multiplets are designed by arrows and averaged wavelengths.

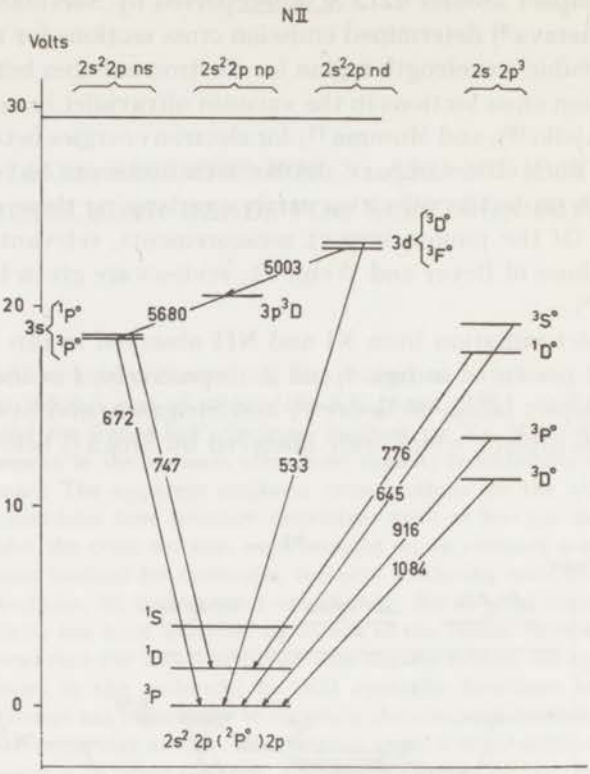

Fig. 2. Part of the term diagram of NII. The notation and symbols are similar as in fig. 1.

also been included. In the multiplet notation used, the upper term is given first, in analogy with the notation in molecular spectroscopy.

Cross sections for emission of the $a^1\Pi_g$–$X\,^1\Sigma_g^+$ (Lyman–Birge–Hopfield) band system[5]) in the vacuum ultraviolet have recently been reported by Holland[22]) and Ajello[10]) for electron impact at energies between 0.1 and 2 keV and 0.02 and 0.2 keV, respectively. Lassettre *et al.*[23]) reported electron scattering cross sections corresponding to excitation to the $a^1\Pi_g$ state.

2. *Experimental.* 2.1. General. Nearly all measurements, *i.e.* those in the vacuum ultraviolet and visible region, were performed with the apparatus described in ref. 24. The energy range of this apparatus extends from about 50 eV up to 5 keV. A few measurements, including threshold measurements, in the visible and near infrared were performed with a "low" energy apparatus[25]), operating between zero and 500 eV. Basically, both apparatuses consist of an electron gun, a collision chamber and an electron trap.

An axial magnetic field is used for the alignment of the electron beam. The emitted radiation was observed at 90° with respect to the electron beam axis. The radiation in the vacuum ultraviolet was detected by a 1 m normal incidence vacuum ultraviolet monochromator. This instrument, which is described in ref. 26, is equipped with a MgF-coated Bausch and Lomb grating of 1200 lines/mm (dispersion 8 Å/mm, blaze wavelength 1500 Å) and an EMI photomultiplier 6256S with a fluorescent screen of sodium salicylate in front of it. The radiation between 2000 and 10000 Å was measured with a Leiss monochromator[27]) equipped with one of three exchangeable Bausch and Lomb replica gratings blazed at 2000 Å (dispersion 27 Å/mm), 5000 Å (dispersion 18 Å/mm) and 7500 Å (dispersion 27 Å/mm) respectively, in combination with one of the exchangeable EMI photomultipliers 6256S and 9684A. The intensity calibration of our optical equipment is discussed in section 2.2. The emission cross sections have been evaluated from light intensity measurements in a similar way as described in refs. 1 and 24.

The multiplet radiation has been measured in a region where the light intensity varied proportionally with the electron current and the gas pressure, typically about 10^{-3} torr but higher for some weak signals in the near infrared region. Even at about 10^{-4} torr secondary pressure effects were present in the apparent emission cross sections of the $a^1\Pi_g$–$X^1\Sigma_g^+$ and $p'^1\Sigma_u^+$–$X^1\Sigma_g^+$ transitions. For both transitions these cross sections increased

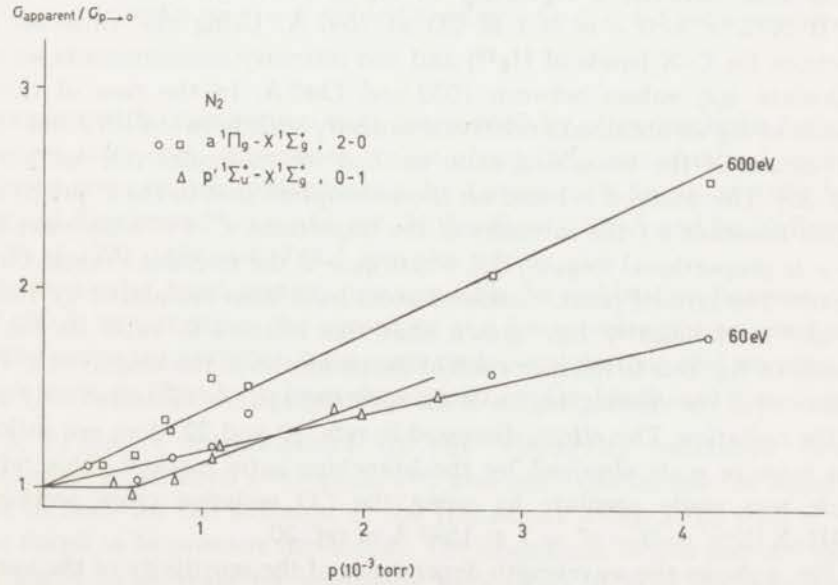

Fig. 3. Pressure dependence of the ratio of the apparent emission cross section and the emission cross section for the transitions $p'^1\Sigma_u^+$–$X^1\Sigma_g^+$, $v' = 0 - v'' = 1$ (981 Å), and $a^1\Pi_g$–$X^1\Sigma_g^+$, $v' = 2 - v'' = 0$ (1384 Å).

with increasing pressure, as can be seen in fig. 3. These pressure effects will be discussed in section 2.3.

In the evaluation of the cross sections, no corrections have been applied for the degree of polarization (Π) of the radiation[24]). This degree is generally small both for molecular radiation (see refs. 1 and 2) and for multiplet radiation (see for instance Van Brunt and Zare[28])). For the multiplet radiation of NII at 5003 Å and 5680 Å we found that $\Pi \lesssim 5\%$.

Our threshold measurements for the radiation of two NII multiplets have been performed on the "low" energy apparatus by measuring the energy difference between the onset of the NII multiplets and that for the molecular emission of the $B^2\Sigma_u^+ - X^2\Sigma_g^+$ transition, the latter having a known threshold of 18.7 eV (see ref. 4).

2.2. Intensity calibration. The sensitivity (quantum yield, k_λ) of our optical equipment between 2500 and 10000 Å was determined by means of a tungsten standard (see ref. 24). At wavelengths larger than 7000 Å, where the 9684A multiplier was used, the sensitivity could not be determined accurately because of the perturbing influence of small magnetic fields on this particular multiplier. Between 1800 and 650 Å, where we had no standard available, we determined the sensitivity in an indirect way. A calibration between 1800 and 1030 Å was obtained by measuring the emission of the molecular band systems $C^1\Pi_u - X^1\Sigma_g^+$ of H_2 (between 1030 and 1240 Å), $a^1\Pi_g - X^1\Sigma_g^+$ of N_2 (between 1270 and 1800 Å) and $A^1\Pi - X^1\Sigma^+ v' = 0 - v'' = 1$ of CO at 1597 Å. Using the emission cross sections for C–X bands of H_2[29]) and our intensity measurements we could calculate $k(\lambda)$ values between 1030 and 1240 Å. In the case of the a–X bands of N_2 we obtained a relative sensitivity scale between 1270 and 1800 Å by means of the branching ratio method for molecules (see section 6 of ref. 30). This method is based on the assumption that in the v'' progressions (with constant v') the intensity of the transitions $v' \rightarrow v''$ with wavelength $\lambda_{v'v''}$ is proportional to $q_{v'v''}/\lambda^3_{v'v''}$, where $q_{v'v''}$ is the relevant Franck–Condon factor. The latter Franck–Condon factors have been calculated by Benesch *et al.*[31]). Holland[22]) has shown that this relation is valid for the a–X bands of N_2. Due to the migration of the molecules in the long lived $a^1\Pi_g(v')$ state out of the viewing region of the spectrograph, we measured only a part of the radiation. This effect, discussed in refs. 10 and 22, does not influence the relative scale obtained by the branching ratio method. This relative scale was made absolute by using the CO emission cross section for $A^1\Pi - X^1\Sigma^+ v' = 0 - v'' = 1$ at 1597 Å of ref. 30.

Fig. 4 shows the wavelength dependence of the sensitivity of the vacuum monochromator determined as outlined above. The curves obtained from the analysis of the various band systems are seen to fit reasonably well to each other. With this indirect calibration method we found encouraging

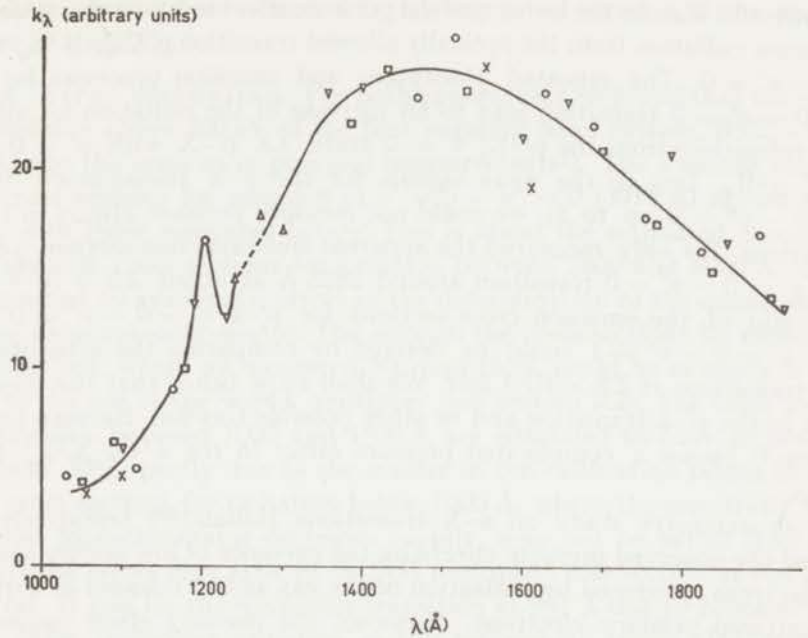

Fig. 4. Relative quantum yield of the vacuum monochromator as a function of wavelength. The right part of the curve was obtained by means of the $a\,^1\Pi_g$–$X\,^1\Sigma_g^+$ band system of N_2 and the CO emission at 1597 Å, the left part with the $C\,^1\Pi_u$–$X\,^1\Sigma_g^+$ band system of H_2 (see text). Calibration points from v'' progressions are marked respectively by ×, ○, □ and ▽ for $v' = 0, 1, 2$ and 3 and by △ for $v' = 4, 5$ and 6 together.

agreement with cross section data determined by other methods, basically different from ours. Agreement within about 15% was obtained with the emission cross section measurements by Lawrence[32]) for O_2 at 1304 Å, by Fite and Brackman[33]) (see also ref. 34) for H_2 at 1216 Å and by Holland[35]) for N_2 at 1200, 1494 and 1744 Å (see also section 3.)

No molecular band systems are available for calibration between 1000 and 650 Å. In this region the sensitivity at a few wavelengths was evaluated by measuring the radiation from some multiplets of argon and krypton, for which cross sections have been determined by De Jongh and Van Eck[36]).

2.3. Pressure dependence of the apparent emission cross sections. In Holland's[22]), Ajello's[10]) and our experiments the apparent cross sections for the emission of the transitions $a\,^1\Pi_g$–$X\,^1\Sigma_g$ with $v' < 5$ were found to be pressure dependent. The magnitude of this pressure effect was found to decrease for increasing values (up to 5) of the vibrational quantum number v' (of the $a\,^1\Pi_g$ state) and to increase for larger impact energies, E_{el} (see fig. 3). For the transition $p'\,^1\Sigma_u^+$–$X\,^1\Sigma_g^+$ $v' = 0 - v'' = 1$ we also found a pressure effect, detectable above about 5×10^{-4} torr, in-

dependent of E_{el}. In the latter case the pressure effect is due to absorption of resonance radiation from the optically allowed transition $p'^1\Sigma_u^+ - X^1\Sigma_g^+$ $v' = 0 - v'' = 0$. The repeated absorption and emission processes for the $v' = 0 - v'' = 0$ transition lead to an increase of the radiation for all the other transitions from the $p'^1\Sigma_u^+$ $v' = 0$ state, *i.e.* p'–X with $v'' \neq 0$ and $p'^1\Sigma_u^+ - a^1\Pi_g$. Due to the weak signals for the p'–a transitions[5]) (with $v' = 0 - v'' = 0$ up to 5), we could not measure pressure effects in these transitions. We only measured the apparent emission cross sections for the p'–a $v' = 0 - v'' = 0$ transition around 2825 Å at about 2.5×10^{-3} torr. The ratio of the emission cross sections for p'–a $v' = 0 - v'' = 0$ and p'–X $v' = 0 - v'' = 1$ could be derived by comparing the intensities of both transitions at 2.5×10^{-3} torr. We shall show below that the pressure effect in the p'–a transition and in other possible Gaydon–Herman singlet systems[5]) causes a complicated pressure effect in the $a^1\Pi_g - X^1\Sigma_g^+$ transitions.

In an extensive study on a–X transitions Holland[22]) tentatively explained the observed pressure effects by the presence of low energy secondary electrons, produced by ionization of the gas and/or released at surfaces by scattered primary electrons. However, the pressure effect caused by secondary electrons, as discussed by us in the case of the radiation from the $C^3\Pi_u$ state of N_2[2]), increases for increasing values of E_{el}, but does not depend on the vibrational quantum number v', contrary to the results for the a–X bands. Such a dependence on v', according to Ajello[10]), might be caused by vibrational relaxation, where in a secondary process vibrational energy of the $a^1\Pi_g$ (v') state is transferred ($v' \rightarrow v' - 1$) by collisions with ground state molecules. However, vibrational relaxation, possibly combined with the influence of secondary electrons, would also lead to different pressure effects in the v'' progressions with $v' = 5$ and 6, contrary to Holland's and our results. In both experiments these v'' progressions have no pressure effects at all. For this reason we think that for the pressure effects in the a–X bands still another process has to be considered, namely the afore-mentioned cascading transitions p'–a.

The magnitude of the pressure dependent part of the cascade (caused by resonance absorption) to the different vibrational states of $a^1\Pi_g$ will depend on v'' of the p'–a transitions, mainly determined by the relevant Franck–Condon factors. Consequently the pressure dependent part of the apparent cross section for emission of a–X is dependent on v'. Note that in our notation v' (upper level) for a–X transitions is the same as v'' (lower level) for p'–a transitions. The E_{el} dependence of the pressure effect in the a–X transitions can be understood by taking into account that the cross section for excitation to the p' and a states, and consequently the corresponding (apparent) emission cross sections, have a different energy behaviour. Excitation to the a and p' states is respectively optically forbidden and

optically allowed (see section 4.1), leading to an increase of the pressure effect at large E_{el}.

2.4. Error discussion. For both apparatuses we found that the energy dependence above 200 eV of the first negative band system, $B\,^2\Sigma_u^+ - X\,^2\Sigma_g^+$, of N_2 was the same as in previous measurements[1]). The absolute values of the cross sections for emission of $v' = 0 - v'' = 0$ (3914 Å) agreed within 10% with those measured before. This is about the estimated accuracy of our absolute cross sections for emission between 2800 and 6000 Å, mainly determined by systematic errors in the determination of the quantum yield of the Leiss monochromator. The error in the cross sections for emission in the near red, where we measured NI multiplets, could be as much as 30%, due to the use of the 9684A multiplier (see section 2.2). The cross sections for emission between 1000 and 1800 Å are estimated to have an accuracy of about 30%, partly due to the scatter in the calibration points in fig. 4. The cross sections for radiation below 1000 Å, where the sensitivity of our vacuum monochromator decreases rapidly, may not be better than 50%. Additional errors may arise in the NII multiplet cross section at 916 Å (see also ref. 9) and for the molecular transition at 981 Å due to contamination with other molecular radiation in this wavelength region. The multiplet radiation of NI at 1311, 1411 and 1494 Å is contaminated with molecular radiation of the $a\,^1\Pi_g - X\,^1\Sigma_g^+$ transition. Using calculated emission cross sections for the a–X bands (see appendix), the contamination was estimated to be less than 10%, 35% and 2%, respectively. Our threshold measurements for the onset of emission of two NII multiplets have an accuracy of about 2 eV.

3. *Results and comparison with other experiments.* In table I the emission cross sections are given for the molecular radiation: $a\,^1\Pi_g - X\,^1\Sigma_g^+$ $v' = 2 - v'' = 0$ (1384 Å), $p'\,^1\Sigma_u^+ - X\,^1\Sigma_g^+$ $v' = 0 - v'' = 1$ (981 Å) and $p'\,^1\Sigma_u^+ - a\,^1\Pi_g$ $v' = 0 - v'' = 0$ (2825 Å). The cross section for emission of p'–a, 0–0 is found to be 3% of that for the p'–X, 0–1 transition. The cross sections for the a–X, 2–0 radiation, which is contaminated with a–X, 5–2 are obtained by normalization of our relative emission cross sections (extrapolated to zero pressure) at 500 eV on the value calculated from inelastic scattering cross sections of Lassettre *et al.*[23]) and Franck–Condon factors of Benesch *et al.*[31]) (see appendix). Our emission cross sections are presented in fig. 5 in a so-called Bethe plot see section 4.1) together with the results of Holland[22]), Ajello[10]), and the values calculated from the work of Lassettre *et al.* In the whole energy range Holland's and our values are in good agreement. Below 400 eV impact energy, these values differ from the calculated ones, which are based on the Born approximation (see appendix). The energy dependence and absolute cross sections of Ajello[10]) differ from Holland and ours.

TABLE I

Emission cross sections for N_2 bands in units of 10^{-19} cm^2.

eV	$a\,^1\Pi_g - X\,^1\Sigma_g^+$ $v' = 2 - v'' = 0$, 1384 Å [a]	$p'\,^1\Sigma_u^+ - X\,^1\Sigma_g^+$ $v' = 0 - v'' = 1$, 981 Å	$p'\,^1\Sigma_u^+ - a\,^1\Pi_g$ $v' = 0 - v'' = 0$, 2825 Å
60	6.02	10.2	
80	4.72		
100	4.02		0.27
150	3.03		0.25
200	2.34	7.29	0.22
300	1.65	6.20	0.176
400	1.34	5.09	0.144
500	1.06 [b]	4.20	0.124
600	0.91		
800	0.72	2.84	0.090
1000	0.54	2.73	0.074
1500	0.40	2.00	0.060
2000	0.25	1.67	0.050

[a] uncorrected for contamination with $v' = 5 - v'' = 2$;

[b] normalized on Lassettre *et al.*[23]) taking the contamination under [a]) into account (see appendix).

The emission cross sections for the multiplet radiation of NI and NII are given in tables II and III, respectively, together with the results of Sroka[9]), Ajello[10]) and Mumma[11]) at 100 eV and of Holland[35]) at 900 eV impact energy. These tables include the onset potentials for emission measured by Sroka[9]), Mumma[11]), Beyer and Welge[17]) and ourselves, together with the calculated values. In these calculations, the minimum energies required for dissociation to N^* have been taken equal to the sum of the energy of dissociation into two $N(^4S^0)$ atoms [9.8 eV[6])] and the excitation energy of the N^* term[20]); similarly for N^{+*} it has been taken equal to the sum of the dissociative ionization energy (24.3 eV), yielding $N^+(^3P)$ and $N(^4S^0)$ and the excitation energy of the N^{+*} term. In some cases we had to take $N(^2D^0)$ instead of $N(^4S^0)$ for the second fragment in the ground state configuration, in connection with additional theoretical considerations with respect to the multiplicities of the fragments (see section 5.1). Fig. 6 is a Bethe plot, showing our data for the multiplet radiation of NII around 5003 Å, as well as electron impact data of Srivastava[8]) and proton impact data of several other groups[12–16]). A few transitions of NI have the same upper term (see fig. 1). In such a case the cross sections for one of the transitions are listed in table II and the branching ratio for the other in table IV. These ratios are compared with other experimental[9,10,35,37]) and theoretical values[38]). The emission cross sections for some NI and NII terms, connected by

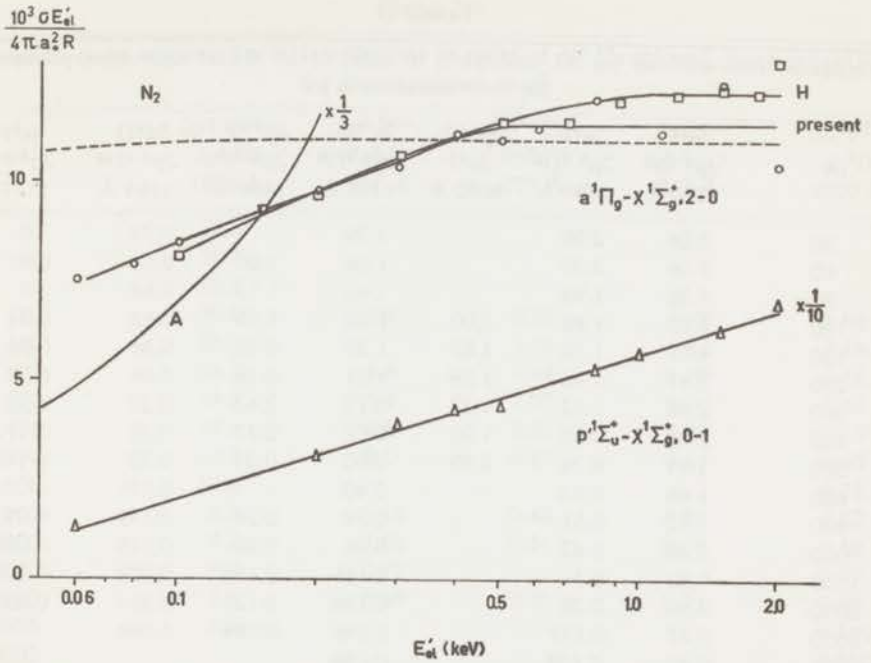

Fig. 5. Emission cross sections for the transitions $p'^1\Sigma_u^+ - X^1\Sigma_g^+$ $v' = 0 - v'' = 1$ (981 Å) and $a^1\Pi_g - X^1\Sigma_g^+$ $v' = 2 - v'' = 0$ (1384 Å) presented in $\sigma E'_{el}/4\pi a_0^2 R$ *vs.* ln E'_{el} plots. For the latter transition, our cross sections have been normalized on the dashed curve at 500 eV, which was obtained from the inelastic scattering cross sections of Lassettre *et al.*[23]) (see text). A comparison is made with the results of Ajello[10]) and Holland[22]), marked with A and H, respectively.

radiative transitions, were found to have the same energy dependence, within 5%. For such a cascade sequence we present only the cross sections for one of the transitions (in tables II and III) and give the cross section ratios between all the relevant transitions in table IV. For some multiplets of NI shown in fig. 1 no accurate measurements could be performed. The radiation of the multiplets $3d^2P - 2p^3\,{}^2P^0$ at 1319 Å and $3d^2P - 3p^2S^0$ at 9060 Å was too weak to be measured. The multiplet radiation from the $3d^2F$ term was obscured in a rather complicated part of the spectrum.

From table II we see that for a number of multiplets of NI our absolute cross sections at 100 eV and those of Mumma[11]), who also used the branching ratio method for intensity calibration (see section 2.3), agree within the experimental accuracies quoted, being about 20% in Mumma's cross sections and 30% in ours. For the multiplet $3d^2D - 2p^3\,{}^2D^0$ at 1164 Å, however, the difference between Mumma's value and ours is about a factor of 4, much larger than for the other transitions. Mumma's value was derived from the cross section at 1311 Å for $3d^2D - 2p^3\,{}^2P^0$ and Labuhn's value for the

TABLE II

Emission cross sections for NI multiplets in units of 10^{-18} cm^2 and onset potentials for their emission in eV

eV	$3s^4P-2p^3\,^4S^0$ 1200 Å	$3s^2P-2p^3\,^2D^0$ 1494 Å	$3p^4D^0-3s^4P$ 8680 Å	$3s'^2D-2p^3\,^2D^0$ 1243 Å	$2p^4\,^4P-2p^3\,^4S^0$ 1134 Å	$3d^2D-2p^3\,^2D^0$ 1164 Å	$4s^2P-2p^3\,^2D^0$ 1177 Å
50	5.06	2.00		1.79		0.73	
60	5.06	2.00		1.66	1.05	0.68	0.37
80	4.86	1.95		1.60	1.13	0.68	
100	4.72	1.88	2.00	1.52	1.05	0.62	0.44
150	4.07	1.72	1.87	1.23	0.92	0.56	0.36
200	3.47	1.43	1.59	1.01	0.78	0.46	0.29
300	2.78	1.12	1.32	0.73	0.62	0.32	0.23
400	2.20	0.88	1.07	0.59	0.47	0.25	0.172
500	1.91	0.76	0.95	0.50	0.39	0.22	0.146
600	1.66	0.63		0.40		0.191	
800	1.42	0.51		0.34	0.24	0.141	0.097
1000	1.22	0.42		0.26	0.22	0.115	0.076
1500	0.83	0.31		0.181	0.157	0.074	0.055
2000	0.65	0.25		0.136	0.121	0.064	0.039
3000	0.47	0.177		0.096	0.089	0.044	
4000	0.40	0.137		0.086			
5000	0.30	0.107		0.063			
100	38.5[9]			10.9[9]	18.9[9]		
100	7.0[10]	5.3[10]					
100	6.7[11]	2.62[11]		1.45[11]		0.163[11]	0.516[11]
900	1.16[35]	0.55[35]		0.2[35]			
onset pot.	21.5[a]			21.7[a]	20.7[a]		
	22[11]	20[11]		21[11]			
	20.0[17]	22.6[17]					
	20.0[a]	22.8[a]	21.5[a]	24.4[a]	20.6[a]	25.1[a]	25[a]

[a]) calculated values, see sections 3 and 5.1.

branching ratio of the radiation at 1311 and 1164 Å, which differs from ours (see below and table IV). The NI data of Holland[35]) at 900 eV impact energy fit between our values at 800 and 1000 eV within the experimental accuracy. Holland[23]) performed a direct intensity calibration, by determining the transmission of the monochromator and comparing the quantum yield of the photomultiplier with that of a thermopile. He quoted an experimental accuracy of about 30%. At 100 eV relatively large differences are present between Ajello's values and ours in table II (a factor of 1.5–2.8) and Sroka's values and ours in tables II and III (a factor 7 to 30). We think that the large discrepancies with Sroka[9]) are due to the fact that in his experiment

TABLE III

Emission cross sections for NII multiplets in units of 10^{-19} cm^2 and onset potentials for their emission in eV

eV	$2p^3\ ^3D^0-2p^2\ ^3P$ 1084 Å	$2p^3\ ^3P^0-2p^2\ ^3P$ 916 Å	$2p^3\ ^1D^0-2p^2\ ^1D$ 776 Å	$3s^1P^0-2p^2\ ^1D$ 747 Å	$3d^3F^0-3p^3D$ 5003 Å
50	22.8				
60	25.1				
80	28.1				
100	30.0	3.9	0.95	1.29	0.98
150	28.3		1.16	1.53	2.16
200	24.2	4.4	1.14	1.50	2.16
300	19.2	3.4	1.00	1.23	1.50
400	14.6	2.6	0.81	0.93	1.10
500	12.7	2.0	0.63	0.69	0.90
600	10.8				0.72
800	8.7	1.18	0.43	0.51	0.52
1000	7.2	1.05	0.31	0.34	0.40
1500	4.7	0.77			0.27
2000	3.6	0.59	0.21	0.21	0.20
3000	2.5				0.140
4000					0.110
5000	1.55				0.086
100	203[9])	119[9])	23[9])	32[9])	
onset pot.	40.8[9]) 35.6[a])	40.8[9]) 37.7[a])	55[9]) 44.4	55[9]) 45.0[a])	55 47.4[a])

[a]) calculated values, see sections 3 and 5.1.

the quantum yield was determined indirectly only at 584 Å and estimated at other wavelengths. Ajello[10]) performed a direct intensity calibration, rather similar to that of Holland. He compared the response of his photomultiplier at 1216 Å with that of an NO ionization chamber and made a relative calibration of his detector at other wavelengths by means of a sodium salicylate screen mounted on its window. He quoted an experimental accuracy of about 20%.

The emission cross sections for the NII multiplets around 5003 and 5680 Å of Srivastava[8]) are about a factor of 3 larger than ours (see fig. 6 and table IV). We were unable to explain these discrepancies. In fig. 6 we have also included proton impact data of Philpot and Hughes[12]), Dufay *et al.*[13]), Robinson and Gilbody[14]), Dahlberg *et al.*[15]) and Thomas *et al.*[16]); the two abcissas of fig. 6 correspond to identical velocities of the projectiles involved: $E_{H^+} = (M/m)\, E_{el}$, where M and m are the proton and electron rest masses,

respectively. The agreement between the proton and our electron impact data is rather poor.

In table IV our branching ratios are compared with the values of Mumma, Holland and Ajello and those from available atomic transition probabilities, as calculated by Kelly[38]) and obtained in Labuhn's[37]) measurements [see also the NBS compilation[39])]. The ratios of the transition probabilities are expected to be more accurate than the estimated accuracy of 50% for the transition probabilities. Our branching ratio for the $3s^2P$ term is in reasonable agreement with the theoretical value of Kelly and the experimental values of Labuhn, Mumma, Holland and Ajello. For the branching ratio of the $3d^2D$ term our value is much smaller (~5 times) than that of Kelly and Labuhn. This discrepancy is not understood. Due to the contamination of the $3d^2D$–$2p^3\,^2P^0$ multiplet at 1311 Å with a molecular band from the $a^1\Pi_g$–$X^1\Sigma_g^+$ transition, our value for the branching ratio of the $3d^2D$ term may be 5% too high. In the case of the $3s'^2D$ term we measured the multiplets $3s'\,^2D$–$2p^3\,^2D^0$ and $3s'\,^2D$–$2p^3\,^2P^0$. The latter multiplet radiation at 1411 Å was found to be rather weak and also contaminated with a molecular band of the before-mentioned system (see section 2.4). For this reason we

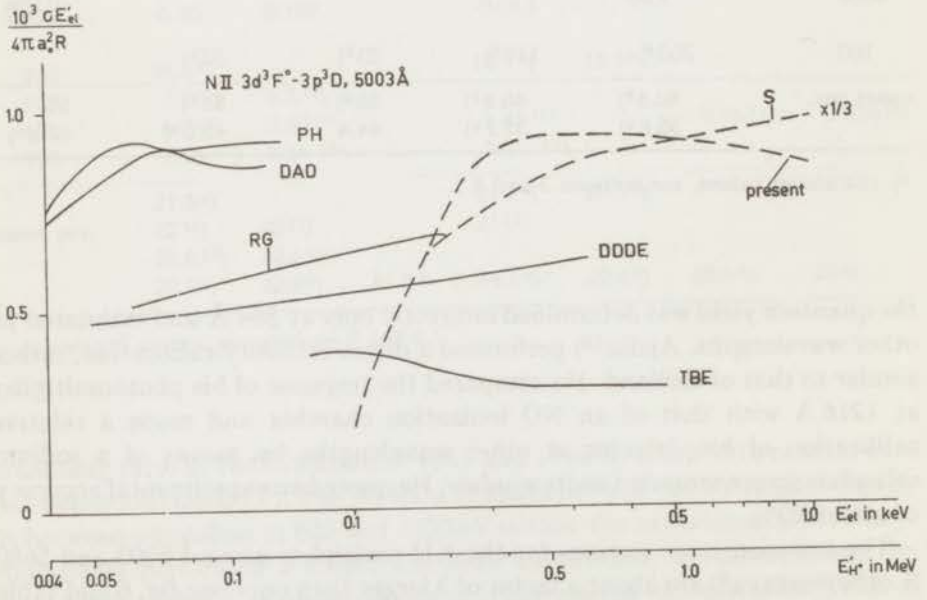

Fig. 6. Comparison of the cross sections for $N^+(3d^3F^0)$ formation in the case of proton and electron impact on N_2 presented in $\sigma E'_{el}/4\pi a_0^2 R$ *vs.* ln E'_{el} plots; the drawn lines refer to protons and the dashed lines to electrons. The two abscissas correspond to identical velocities of the projectiles involved. The abbreviations correspond with the following references: S[8]), PH[12]), DDDE[13]), RG[14]), DAD[15]), TBE[16]) and present refers to this work.

TABLE IV

Ratios of emission cross sections for NI and NII multiplets

	Branching	
NI	$3s^2P$, σ(1744 Å)/σ(1494 Å)	0.41, 0.39[38]), 0.37[37]), 0.38[10]), 0.36[11]), 0.40[35])
	$3d^2D$, σ(1311 Å)/σ(1164 Å)	0.49, 2.3[38]), 2.8[37])
	Cascade	
NI	σ(8213 Å)/σ(1200 Å)	0.055
	σ(9380 Å)/σ(1494 Å)	0.28
NII	σ(5003 Å)/σ(5680 Å)	0.99, 0.94[8])
	σ(5003 Å)/σ(672 Å)	0.74

did not give a branching ratio for these transitions in table IV. Furtheron (see section 4) the excitation cross section $\sigma(3s'\ ^2D)$ has been taken equal to the emission cross section $(3s'\ ^2D\text{–}2p^3\ ^2D^0)$.

4. *Analysis of the results with the Bethe–Born approximation.* 4.1. Bethe–Born approximation. Terms of NI arise from excitation to dissociative neutral as well as ionized molecular states; terms of NII arise only from dissociative ionized molecular states. According to the Franck–Condon principle the excitation processes can be thought of as vertical transitions in the potential energy diagram, *i.e.* the internuclear distance r does not change in the excitation process[6]). Different processes can be involved in the production of atoms: excitation to an unstable molecular state or to a stable state above its dissociation limit, or excitation to a stable state followed by predissociation or a transition to a lower unstable state. If one of the dissociation fragments is left in an excited state, multiplet radiation is emitted.

Collision induced excitation processes can be either optically allowed or forbidden. Using the Bethe–Born approximation[41]), we can determine the relative importance of these types of transitions by analysing the energy dependence of the cross sections for formation of a particular term (taking into account possible cascade contributions from other terms). In the analysis of our experimental data we use the following relations, as derived and discussed in refs. 40, 41 and 42. For optically allowed (dipole) transitions the electron impact excitation cross section σ varies at sufficiently high impact energies as

$$\sigma_n = \frac{4\pi a_0^2 R}{E'_{\mathrm{el}}} M_n^2 \ln \frac{c_n E'_{\mathrm{el}}}{R}, \qquad (1)$$

where $E'_{\mathrm{el}} = \frac{1}{2}mv^2$, v being the velocity of the incident electron, m the electron rest mass, R the Rydberg energy, a_0 the first Bohr radius and c_n a constant. For excitation to a stable molecular state n, M_n^2 is related to the optical oscillator strength f_n by $M_n^2 = f_n(R/E_n)$, where E_n is the excitation

energy. In the case of dissociative excitation to the atomic term n, M_n^2 is related to the optical oscillator strengths for all dipole transitions to molecular states which lead to formation of the particular term n and may be expressed as

$$M_n^2 = \int_{E_n}^{\infty} \eta_n(E) \frac{\mathrm{d}f(E)}{\mathrm{d}E} \frac{R}{E} \mathrm{d}E, \tag{2}$$

where E is the excitation energy transferred to the molecule, E_n the threshold energy for the process under consideration, $\eta_n(E)$ is the fraction of the intermediate molecular states which dissociate into the particular term n and $\mathrm{d}f(E)/\mathrm{d}E$ is the differential optical oscillator strength which is related to the photoabsorption cross section $\sigma_{\mathrm{ph\ abs}}(E)$, by

$$\frac{\mathrm{d}f(E)}{\mathrm{d}E} = \frac{mc}{\pi e^2 h} \sigma_{\mathrm{ph\ abs}}(E). \tag{3}$$

For optically forbidden processes the cross section varies at high impact energies as

$$\sigma \propto E_{\mathrm{el}}^{-1}. \tag{4}$$

In the case of electron exchange processes the cross section varies as

$$\sigma \propto E_{\mathrm{el}}^{-3}. \tag{5}$$

By plotting the cross sections in the form $\sigma E'_{\mathrm{el}}/4\pi a_0^2 R$ *vs.* $\ln E'_{\mathrm{el}}$, a so-called Bethe plot, we find for an optically allowed, optically forbidden and spin forbidden excitation process a curve with a positive, zero and negative slope respectively. A constant positive slope in the asymptotic region of a Bethe plot is related with M^2, whereas the intercept of the extrapolated straight-line portion with the abscissa is connected with c, cf. eq. (1). For optically allowed processes we shall find $c \simeq 1$ and for optically forbidden processes $c \gg 1$. In order to determine a particular M^2 value, we need the cross sections for formation of the corresponding term. This cross section is equal to the sum of the cross sections for emission of multiplet radiation arising from the term under consideration. Most terms of NI and all of NII are found to decay almost completely via one multiplet. In these cases, the relevant emission cross section is very nearly equal to the cross section for formation of the term under consideration.

In the excitation processes leading to the observed fragments, one-electron and two-electron transitions may be involved. In general, the cross sections for one-electron transitions are larger than those for two-electron transitions. The latter transitions are possible as a consequence of electron correlation

and configuration interaction effects (see ref. 43). For such transitions in argon, which has the same number of electrons as N_2, important contributions of optically allowed transitions have been found (see ref. 44).

4.2. Molecular radiation. The selection rules for transition in diatomic molecules (see ref. 6) predict that the formation of the $p'^1\Sigma_u^+$ and $a^1\Pi_g$ states will be optically allowed and optically forbidden, respectively. At large impact energies the relevant cross sections in fig. 5 show a straight line with a positive and a zero slope respectively, as predicted by the Bethe theory (see eqs. 1 and 4). Because we measured only a fraction of the radiation from the $p'^1\Sigma_u^+$ $v' = 0$ state, *i.e.* the p'–X 0–1 and p' — a 0–0. we can not evaluate the optical oscillator strength of the p' state with $v' = 0$ from the slope in fig. 5.

4.3. Multiplet radiation of NI. Fig. 1 shows the optically allowed ($\Delta l = \pm 1$) transitions originating from the NI terms relevant to this work. The energy dependence of the cross sections for formation of such terms in dissociative excitation of N_2, as far as could be measured, is presented by the Bethe plots in figs. 7 and 8. The M^2 and c values, given in table V, were obtained using a least-square analysis of the high-energy linear portions of these plots. These portions have a constant positive slope and c values of the order of magnitude 1 for most terms. This indicates, in spite of our limited

TABLE V

M^2 and c values for dissociative excitation and ionization of N_2

		M^2	c
NI	$3s^4P$	0.054 ± 0.002	1.2
	$3s^2P$	0.024 ± 0.001	2.8
	$2p^4\ ^4P$	0.0078 ± 0.0004	5.2
	$3d^2D$	0.0044 ± 0.0004	4.5
	$3s'\ ^2D$	0.0075 ± 0.0008	2.2
	$3p^4D^{0\,a)}$	0.035 ± 0.001	0.5
	$3p^4P^{0\,a)}$	0.0033 ± 0.0003	0.8
	$3p^2D^{0\,a)}$	0.0065 ± 0.0008	0.8
	$4s^2P$	0.0018 ± 0.0003	8.7
NII	$2p^3\ ^3D^0$	0.0080 ± 0.0016	$>10^6$
	$2p^3\ ^3P^0$	0.0022 ± 0.0004	41
	$2p^3\ ^1D^0$	0.0010 ± 0.0004	22
	$3s^1P^0$	0.0007 ± 0.0004	95

a) tentative values because of the limited experimental energy range (see fig. 7).

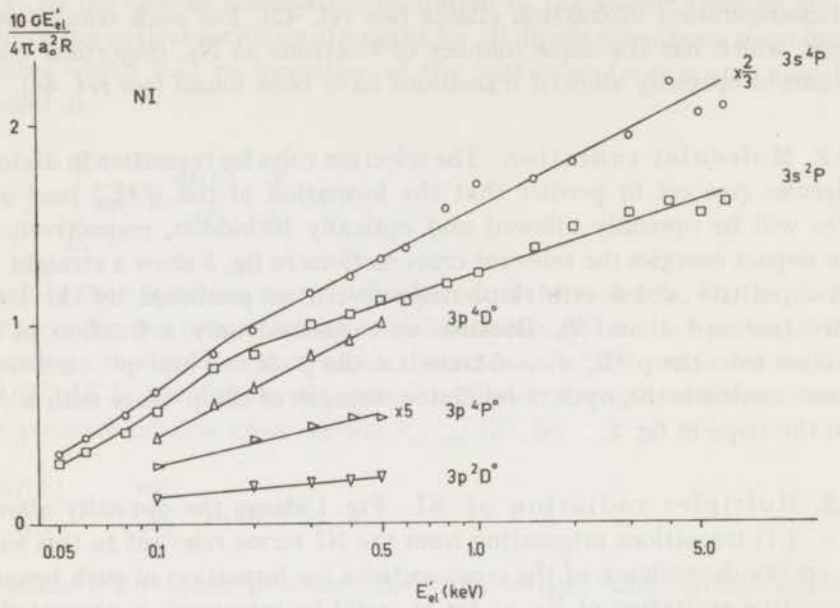

Fig. 7. Cross sections for formation of excited states of N in the case of electron impact on N_2, presented in $\sigma E'_{el}/4\pi a_0^2 R$ *vs.* ln E'_{el} plots.

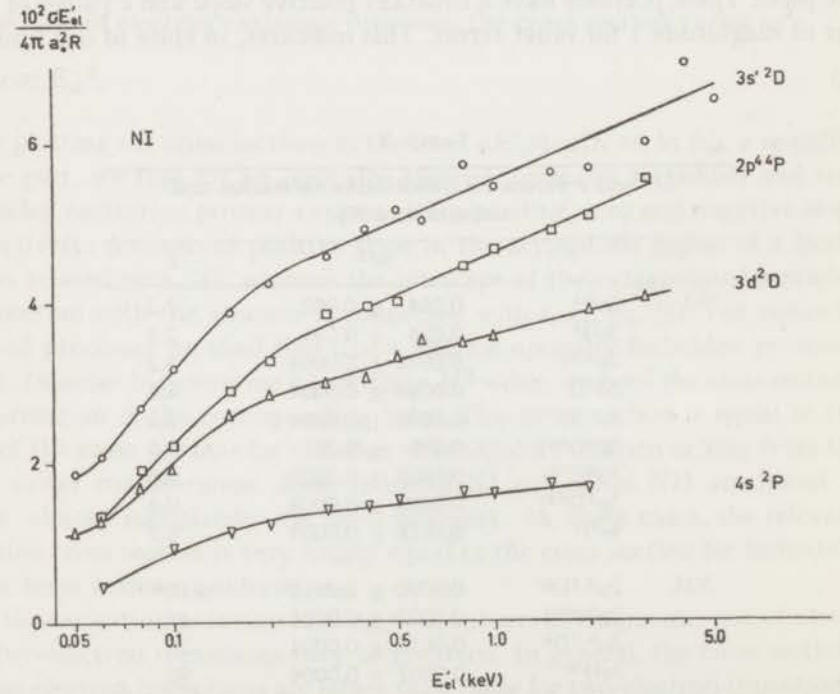

Fig. 8. Cross sections for formation of excited states of N in the case of electron impact on N_2, presented in $\sigma E'_{el}/4\pi a_0^2 R$ *vs.* ln E'_{el} plots.

energy range for some terms, that the dissociative excitation leading to these terms directly and/or via cascade, proceeds mainly via optically allowed transitions.

In our wavelength region, we did not find any of the known multiplets with $3s'^2D$, $2p^4{}^4P$, $3d^2D$, $3p^2D^0$, $3p^4P^0$, $3p^4D^0$ or $4s^2P$ as lower term. For this reason we assumed that cascade contributions to these terms could be neglected. In the case of $2p^4{}^4P$ no cascading is expected since higher terms will presumably pre-ionize, since their excitation energy is larger than the ionization energy of N [see Lawrence and Savage[45])]. As can be seen in fig. 1 the formation of the $3p^4D^0$ and $3p^4P^0$ terms leads via the multiplets $3p^4D^0$–$3s^4P$ and $3p^4P^0$–$3s^4P$, respectively, to the formation of the $3s^4P$ term; similarly the formation of the $3p^2D^0$ term leads via $3p^2D^0$–$3s^2P$ to the formation of the $3s^2P$ term. The cascade contributions to the cross sections for emission from the $3s^4P$ and $3s^2P$ terms amount to about 44% and 21%, respectively, for impact energies between 100 and 500 eV. In the case of the $3s^2P$ term cascade can also occur via the multiplets $3p^2S^0$–$3s^2P$ and $3d^2P$–$3p^2S^0$–$3s^2P$. The multiplet $3d^2P$–$3p^2S^0$ at 1319 Å was found to be weak and negligeable in the cascade contribution to the $3s^2P$ term. The multiplet $3p^2S^0$–$3s^2P$ around 13500 Å (shown in fig. 1 as a dashed line) fell outside our wavelength region.

Concluding, it was not possible to determine completely the role of cascade contributions to the $3s^2P$ term. Because the experimental cross sections for the multiplet radiation from the $3s^2P$ and $3s^4P$ terms and for the aforementioned cascade contributions to these terms, which have been determined only in a limited energy range, have an accuracy of only 30% (see section 2.4), we could not evaluate the character of the direct excitation to the $3s^2P$ and $3s^4P$ terms. However, we believe this character to be mainly optically allowed in view of the following considerations: all other relevant terms of NI, also with one electron promoted to the M shell, are found to be formed mainly via optically allowed excitation processes and Beyer and Welge have observed fluorescence of N_2 connected with the $3s^2P$ and $3s^4P$ terms. Beyer and Welge[17]) measured the undispersed fluorescence of N_2 produced by the impact of photons with wavelengths between 1000 and 450 Å. The fluorescence processes, observed in their experiment, are essentially confined to optically allowed processes (see eq. 3), due to their excitation mode. Different wavelength regions for observation were obtained by using suitable filters in front of a multiplier. They found that the radiation detected with an LiF and CaF_2 or BaF_2 window was predominantly due to the radiation at 1200 Å (from the term $3s^4P$) and 1494 Å (from the term $3s^2P$), respectively. The threshold for production of radiation at 1200 Å was found to be about 20.0 eV (622 Å), nearly equal to the calculated minimum energy 20.1 eV for dissociation of N_2 into $N(3s^4P) + N(2p^3\,{}^4S^0)$. For the fluorescence at 1200 Å absolute photodissociation cross sections were obtained by a normalization

procedure. These cross sections, given in fig. 6 of ref. 17, as a function of the wavelength of the incident radiation, showed two distinct channels for formation of the $3s^4P$ term. One channel can be assigned to the direct formation of the $3s^4P$ term and the other to that of the $3p^4D^0$ term (which decays to the $3s^4P$ term). This confirms our statement that for electron impact the $3p^4D^0$ and $3s^4P$ terms are formed by optically allowed processes.

Beyer and Welge[17]) also detected a fluorescence component at 1494 Å (from the $3s^2P$ term). The threshold for the 1494 Å production was found to be about 22.6 eV (550 Å) nearly the same as the calculated minimum energy of 22.8 eV for dissociation of N_2 into $N(3s^2P)$ and $N(2p^3\ ^2D^0)$. This observation confirms our suggestion with respect to the optically allowed character of the dissociation process leading to the $3s^2P$ term.

Since optically allowed processes are involved, our value for $M^2(3s^4P)$ can be compared with the optical data of Beyer and Welge[17]). For that purpose we use eqs. (2) and (3). Because Beyer and Welge measured between 440 Å ($E = 28.2$) and 622 Å ($E = 19.9$) it is only possible to carry out the integration in eq. (2) over a limited region of E. The M^2 value, 0.012, obtained by using the afore-mentioned E's as integration limits, has to be considered as a lower limit for M^2. In our experiment we found $M^2 = 0.054$. The large difference between our value of $M^2(3s^4P)$ and that calculated from the photodissociation cross sections[17]) suggests that in our case some other channels, involving highly excited states, are contributing to the formation of the $3s^4P$ and possibly also of other terms. One of these possible channels, K shell excitation followed by Auger transitions, will be discussed furtheron (see section 5.3). The structure in the energy dependence of the multiplet radiation at 1200 Å and 1744 Å in Ajello's[10]) measurements around 35 eV, seems to indicate a channel via dissociative ionization.

4.4. Multiplet radiation of NII. The relatively strongest multiplet radiation from NII terms is shown in fig. 2. Some weak multiplets with emission below 672 Å, measured by Sroka[9]), are also included in fig. 2. The terms with configuration $2s2p^3$ are probably cascade free (see ref. 45). In the case of the $3p^3D$ and $3s^3P^0$ terms cascade contributions can be expected (see fig. 2). By means of lifetime measurements Hesser and Lutz[46]) found that the $3s^3P^0$ term is formed mainly via cascade. This is confirmed in our experiment. At all impact energies used we found that the emission cross sections for the multiplets $3p^3D$–$3s^3P^0$ ($\lambda = 5680$ Å) and $3s^3P^0$–$2p^2\ ^3P$ ($\lambda = 672$ Å) are respectively a factor 1.01 ± 0.05 and 1.6 ± 0.7 larger than those for $3d^3F^0$–$3p^3D$ ($\lambda = 5003$ Å) in table III. The threshold for the radiation from the $3d^3F^0$ and $3p^3D$ terms was found to be 55 eV, nearly equal to the value of 53 eV for the $3s^3P^0$ term, measured by Sroka[9]). From this evidence and the fact that no other (branching) transitions are known for the $3d^3F^0$ and $3p^3D$ terms, we conclude that the $3p^3D$ and $3s^3P^0$ terms

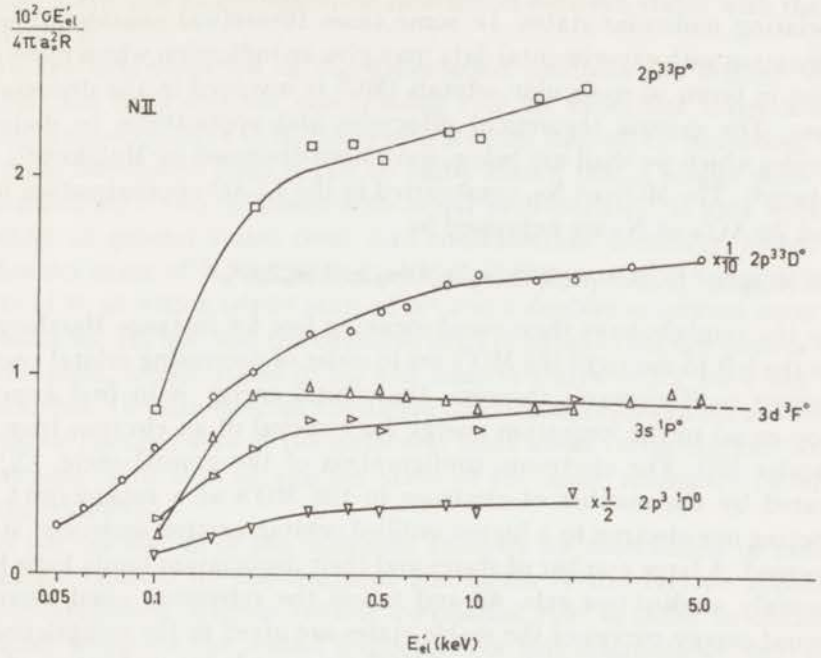

Fig. 9. Cross sections for formation of excited states of N^+ in the case of electron impact on N_2, presented in $\sigma E'_{el}/4\pi a_0^2 R$ *vs.* ln E'_{el} plots.

are to a large extent formed via a sequence of multiplets originating from the $3d^3F^0$ term, which is formed in the collision process.

In fig. 9 our cross section for formation of the NII terms are presented in Bethe plots. At high impact energies, the curves for the $2p^3\,^3D^0$, $2p^3\,^3P^0$, $2p^3\,^1D^0$ and $3s^1P^0$ terms have a small positive slope. The corresponding M^2 and c values are given in table V. The large c values for most terms indicate that the relevant terms are mainly formed via optically forbidden transitions in the collision processs.

The curve of the $2p^3\,^3D^0$ term reaches its asymptotic region at rather large impact energies, about 800 eV. This behaviour in a Bethe plot may be an indication that one of the contributing dissociative molecular states has a large excitation energy. This will be discussed further in section 5.3. The curve for the $3d^3F^0$ term in figs. 6 and 9 has a small negative slope above about 200 eV. This indicates that the formation of the $3d^3F^0$ term is optically forbidden.

5. *Correlation of the NI and NII terms with dissociative molecular states.*
5.1. Theoretical introduction. The occurrence of excited states of N and N^+ will be connected with the formation of some specific intermediate

dissociating molecular states. In some cases theoretical considerations in combination with experimental data may give an indication which molecular state(s) in terms of molecular orbitals (MO) is involved in the dissociation process. The general theoretical principles and applications to diatomic molecules which we shall use below, have been discussed by Mulliken[47]) and Herzberg[6]). The MO's of N_2, constructed in the LCAO approximation from 2s and 2p AO's of N, are expressed as

$$KK(\sigma_g 2s)^2\ (\sigma_u 2s)^2\ (\pi_u 2p)^4\ (\sigma_g 2p)^2\ (\pi_g 2p)^0\ (\sigma_u 2p)^0, \qquad (6)$$

where the symbols have their usual meaning (see for instance Herzberg[6])). From the left to the right the MO's are in order of decreasing orbital energy. According to Koopman's theorem, the orbital energy is in first approximation equal to the ionization energy for removal of an electron from the particular MO. The electronic configuration of the ground state, $^1\Sigma_g^+$, is indicated by the number of electrons in the MO's as a superscript†. By promoting one electron to a higher unfilled orbital, excited molecular states are formed. A large number of states and their dissociation limits have been extensively studied (see refs. 48 and 6 and the references cited therein). Potential energy curves of the stable states are given in the compilation of Gilmore[49]). Assignments in terms of MO's were made by application of MO theory, correlation rules and empirical data. Mulliken remarks that his catalogue[48]) of observed and predicted states, which can be roughly divided in valence-shell and Rydberg states, is probably only complete for electronic states with energies below about 12 eV, that is for valence-shell states which dissociate into N atoms with configuration $2s^22p^3$, *i.e.* $^4S^0$ and $^2D^0$. The configuration of valence-shell states, like $a\,^1\Pi_g$, contains only electrons in the MO's given in expression (6).

Molecular Rydberg states like $p'\,^1\Sigma_u^+$, have a configuration with one outer electron in a Rydberg MO, which in the LCAO approximation can be constructed from AO's with a principal quantum number $n > 2$. The latter states of N_2 dissociate or tend to dissociate into atoms of which one has a configuration $2s^22p^3$ and the other $2s^22p^2$ (ns, np or nd) with $n > 2$. These Rydberg states with one outer electron will have about the same equilibrium internuclear distance and vibrational constants as one of the ionized states (see refs. 5 and 6), *e.g.* $X\,^2\Sigma_g^+$, $A\,^2\Pi_u$, $B\,^2\Sigma_u^+$, $C\,^2\Sigma_u^+$ or $D\,^2\Pi_g$.

For a few states of N_2 (and N_2^+) whose configuration is of the type $\ldots.(\sigma_g 2s)^2\ (\sigma_u 2s)\ \ldots.$ or $\ldots.\ (\sigma_g 2s)(\sigma_u 2s)^2\ \ldots.$, it has been assumed that one of the corresponding dissociation products has one electron missing from a 2s AO (see ref. 48). It should be mentioned, however, that the MO assignments refer to small and moderate internuclear distances. At larger internuclear distance this configuration might give a poor description of the

† The superscript is omitted in the case that there is only one electron in an MO.

actual state, due to configuration interaction between states with the same symmetry.

In the determination of the dissociation products the Wigner–Witmer correlation rules and the non-crossing rule for molecular states with the same symmetry, have to be taken into account (see ref. 6). According to one of these correlation rules it can be easily shown that a singlet state of N_2 correlates with two N atoms with equal multiplicities: in this work only doublet or quartet states come into consideration. Similarly, in our case, a doublet state of N_2^+ correlates with a singlet state of N^+ and a doublet state of N, or with a triplet state of N^+ and a doublet or quartet state of N. Because we did not find the characteristics of a spin exchange process in our Bethe plots, triplet states of N_2 and quartet states of N_2^+ have not to be considered. Deviations from the above correlation rules can occur when the potential energy curve of the molecular state under consideration "avoids" a crossing with that of another state of the same symmetry (mixing of configurations).

In the calculation of the minimum energies for observation of multiplet radiation emitted by one fragment (see tables II and III) we applied the above-mentioned Wigner–Witmer correlation rule in order to obtain the possible terms for the second fragment. For this fragment we used in our calculation the lowest allowed term. For most multiplets of NII the observed threshold is larger than the calculated value. This difference may be due to the unknown kinetic energy imparted to the dissociation fragments, our choice of the lowest allowed term for the second dissociation fragment and the accuracy of the threshold measurement. It is known that this accuracy is difficult to evaluate in the case of dissociative excitation and ionization (see ref. 4).

5.2. NI. The thresholds for the multiplet radiation from the NI terms, listed in table I, are nearly equal to the calculated minimum energies. This indicates that at least some part of the observed multiplet radiation is due to dissociation processes leading to the term under consideration and $N(^4S^0)$ or $N(^2D^0)$ with configuration $2s^22p^3$. The corresponding molecular states will have one electron in a Rydberg orbital (Rydberg states), except those leading to $N(2p^4\,^4P)$.

It might be expected that the different terms of NI originate from a number of Rydberg series, which converge to one or more states of N_2^+. These latter states should also be dissociative, in view of the similarity of the relevant Rydberg states with an ionized state[5]). Because we found that the terms of NI are formed mainly via optically allowed transitions (see section 4.3), the formation of these dissociative states of N_2^+ should also proceed via optically allowed transitions. Consequently, only doublet states of N_2^+ have to be taken into account. The optically allowed formation of the relevant

dissociative Rydberg states and the related N_2^+ states indicate that in the optical absorption spectrum of N_2 continua (not discrete bands) correspond to the formation of these states. In this absorption spectrum[18, 19]) some weak continua have been found above 617 Å (= 20.1 eV), which correspond to dissociation into N fragments in the ground state configuration. In the same wavelength region discrete bands of Rydberg series have been found, which converge either to the $X\,^2\Sigma_g^+$, $A\,^2\Pi_u$ or $B\,^2\Sigma_u^+$ states of N_2^+. Below 617 Å Codling[50]) has found the absorption bands of Rydberg series converging to the $C\,^2\Sigma_u^+$ state, but not those related to the $D\,^2\Pi_g$ state. Therefore we should expect continua for the latter Rydberg and N_2^+ states. However, due to the lack of sufficient measurements below 600 Å, no continua can be identified in this region. Considering the location of the potential energy curve of the $D\,^2\Pi_g$ state, which is shallow with a large equilibrium internuclear distance at 22.0 eV for $v' = 0$ (see ref. 49), dissociation of this state into N ($^4S^0$) + N^+ (^3P) might be expected for "vertical transitions" in the excitation process. In this process parts of the $D\,^2\Pi_g$ curve above the dissociation limit at 24.3 eV can be reached. This dissociation process, already suggested by Moran *et al.*[51]) for collision induced dissociation of N_2^+ ions, can explain the dissociative ionization by photons with an energy larger than 24.3 eV, observed by Comes and Lessmann[52]). On the basis of the above evidence, we consider the dissociative $D\,^2\Pi_g$ state as one of the possible limits of the Rydberg series of states, which lead to dissociation into N($^4S^0$) and a number of excited states of N. In our case the formation of these states can lead to the multiplet radiation from NI terms with quartet multiplicity in general (see discussion with respect to the Wigner–Witmer correlation rule in section 5.1).

Similar arguments as for the $D\,^2\Pi_g$ and related Rydberg states can be applied for the less known states of N_2^+ (see Gilmore[49])): $^2\Delta_u$, $^2\Sigma_u^-$ and $^2\Pi_u$ and their corresponding Rydberg states. The latter states of N_2^+ have as their dissociation limit N ($^2D^0$) and N^+(^3P) at 26.7 eV. In this case dissociation of the corresponding Rydberg series of states may be expected into N ($^2D^0$) and excited states of N with doublet multiplicity.

Concluding we assign at least a part of the multiplet radiation of NI to the formation of dissociative Rydberg states; some of these states converge to the $D\,^2\Pi_g$ state.

Considering the electronic configuration of the $D\,^2\Pi_g$ state, which is supposed to be a mixing between two MO configurations (see Gilmore[49])), we obtain for the MO configuration of the related Rydberg series:

$$(\sigma_g 2s)^2\,(\sigma_u 2s)^2\,(\pi_u 2p)^2\,(\sigma_g 2p)^2\,(\pi_g 2p)(R)$$

and

$$(\sigma_g 2s)^2\,(\sigma_u 2s)^2\,(\pi_u 2p)^4\,(\pi_g 2p)(R), \qquad (7)$$

where R is the desigmation of a Rydberg MO.

From expressions (6) and (7) it can be seen that the excitation process will be a two-electron transition (see also section 4.1).

For the dissociation leading to $N(2p^4\ ^4P)$ we might expect $N(2p^3\ ^4S^0)$ as the second fragment; this in view of the small difference between the observed threshold and the calculated minimum energy (see table II) Considering the $2s2p^4$ configuration of the first term it has been assumed (see section 5.1) that the relevant intermediate molecular state is formed by promotion of one electron from the ($\sigma_u 2s$) MO to a higher valence-shell MO. In this case promotion of an electron from the ($\sigma_g 2s$) MO is ruled out because of the rather high calculated[53]) orbital energy of the latter (see also Siegbahn *et al.*[54])). Considering the selection rules for diatomic molecules this means that an optically allowed transition can only occur from the ($\sigma_u 2s$) to the ($\pi_g 2p$) MO. The resulting molecular state, $^1\Pi_u$, with MO configuration

$$(\sigma_g 2s)^2\ (\sigma_u 2s)(\pi_u 2p)^4\ (\sigma_g 2p)^2\ (\pi_g 2p) \qquad (8)$$

is predicted by Mulliken[48]). He estimated for this state a minimum energy of 12.15 eV.

A state of the same species, $b^1\Pi_u$ found in absorption ($v' = 0$ at 12.50 eV) has been interpreted by Dressler[55]) as being the lower of a pair of electronic states, resulting from a strong interaction between two $^1\Pi$ valence states, derived from the configuration in expression (8) and:

$$(\sigma_g 2s)^2\ (\sigma_u 2s)^2\ (\pi_u 2p)^3\ (\sigma_g 2p, (\pi_g 2p)^2.$$

The second unknown $^1\Pi_u$ state, which must also have an appreciable admixture of configuration (8), is expected to have a very large excitation energy[55]). In view of these considerations, excitation to the latter $^1\Pi_u$ state above the dissociation limit at 20.6 eV followed by (pre)dissociation may explain the multiplet radiation from $N(2p^4\ ^4P)$.

5.3. NII. Compared to the emission cross sections for N terms (table II) those for N^+ terms (table III) are relatively small, except for the $2p^3\ ^3D^0$ term. The sum of our N^+ cross sections in table III amounts to about 6% of the total cross sections for dissociative ionization of N_2 in N^+ ions with kinetic energies above 0.25 eV, as measured by Rapp *et al.*[56]) between threshold and 1000 eV. This means that electron impact produces a considerable amount of N^+ ions in non-radiative states. These ions may have the configuration $2s^22p^2$ and $2s2p^3$ with terms ^3P, ^1D, ^1S and $^5S^0$ (not shown in fig. 2), respectively.

Some of the terms of N^+ with configuration $2s^22p(3s$ or $3d)$ probably arise via a molecular state, formed by a two-electron transition. As is clear from the MO's occupied in the ground state, one electron will be removed and another electron promoted to a Rydberg MO (shake-up at ionization), *i.e.* formation of a Rydberg state of N_2^+ (related to a state of N_2^{2+}).

A possible mechanisme for formation of terms with configuration $2s2p^3$ was already mentioned in section 5.1, *i.e.* formation of an unstable state with a vacancy in either the ($\sigma_g 2s$) or ($\sigma_u 2s$) MO. In view of the rather large cross section of the $2s2p^3\ ^3D^0$ term and its threshold of about 40.8 eV [9], we believe that the one-electron transition, ejection of an electron from the ($\sigma_g 2s$) MO, is involved in the formation of this particular term. In the case of dissociative ionization of CO (see ref. 30), NO and O_2 (to be published), we also found relative large cross sections for formation of one term of CII, NII and OII, each with one electron missing from the 2s AO. Similarly, molecular states of CO^+, NO^+ and O_2^+ related to the before-mentioned N_2^+ state are believed to be involved in these dissociation processes.

Another mechanism may proceed via the formation of highly excited states of N_2 or N_2^+, *e.g.* promotion to an unfilled MO or ejection of an electron from the K shell, followed by Auger processes. Some of these Auger transitions can lead to dissociative molecular states of N_2^{2+} (and probably also of N_2^+) as has been found by Siegbahn *et al.* [54], Stalherm *et al.* [57] and Van der Wiel *et al.* [58]. Considering the relatively high thresholds for such processes – about 400 eV for ejection or excitation of an electron from the K shell – it is clear that this mechanism may contribute only at high impact energies. An indication for such a contribution may be the energy dependence of the cross section for formation of the $^3D^0$ term (see fig. 9). The asymptotic region in the Bethe plot for this term is reached at impact energies as high as about 800 eV.

The available measurements on dissociative ionization, either by electron or photon impact, are not extensive enough to provide more information about the processes occurring.

Acknowledgements. We are indebted to Professor J. Kistemaker and Professor K. Dressler and Dr. T. R. Govers for their critical comments on the manuscript and to Dr. D. A. Vroom for his contribution to the analytical procedure in the appendix. We are grateful to Drs. J. P. De Jongh, Dr. J. Van Eck and Dr. R. F. Holland for providing us experimental results before publication.

This work is part of the research program of the Stichting voor Fundamenteel Onderzoek der Materie (Foundation for Fundamental Research on Matter) and the Stichting Scheikundig Onderzoek in Nederland (Netherlands Foundation for Chemical Research) and was made possible by financial support from the Nederlandse Organisatie voor Zuiver Wetenschappelijk Onderzoek (Netherlands Organization for the Advancement of Pure research).

APPENDIX

For the normalization of our emission cross section $a\,^1\Pi_g$–$X\,^1\Sigma_g^+$, 2–0 at 500 eV, we have used the experimental inelastic differential cross sections for the transition $a\,^1\Pi_g \leftarrow X\,^1\Sigma_g^+$ of Lassettre and Krasnow[23]). They presented generalized oscillator strengths $f(K)$ for an impact energy of 523 eV over a limited range of K values, where K is the momentum transfer. For the calculation of the total cross sections, however, all values are needed between K_{min} and K_{max}. For the region where the Born approximation is valid, Vriens[59]) (see also refs. 60 and 30) has given analytical expressions for $f(K)$ in which the parameters can be fitted to the experimental data. For optically forbidden transitions, as considered here, we used the expansion

$$f(x) = \frac{x}{(1+x)^6} \sum_{\nu=0}^{\infty} c_\nu \left(\frac{x}{1+x}\right)^\nu, \tag{A.1}$$

where $x = (Ka_0/\alpha)^2$ and $\alpha = (Q/R)^{\frac{1}{2}} + [Q - E_n)/R]^{\frac{1}{2}}$.

Here a_0 and R have been defined in eq. (1) of section 4.1; Q is the ionization energy for removal of an electron from the (σ_g2p) MO (15.6 eV), E_n is the excitation energy for the transition a–X, and the c_ν's with integer ν are the fitting parameters. Using for E_n the value of 9.10 eV (the centre of the band) we calculated for α^2a value of 2.58.

With $c_0 = 0.564$, $c_1 = 0.565$, $c_2 = 0.966$ and $c_\nu = 0$ for $\nu \geqslant 3$, eq. (A.1) reproduces the experimental $f(K)$ values of Lassettre and Krasnow at most K values within 1%, except for the three largest K values, where the experimental $f(K)$ values are up to 11% larger. For dipole forbidden transitions the excitation cross section is expressed as (see ref. 60)

$$\sigma = \frac{4\pi a_0^2 R^2}{E_n E_{el}} [C - \eta\,(E_n, E_u)], \tag{A.2}$$

where

$$C = \sum_{\mu=0}^{\infty} \sum_{\nu=\mu}^{\infty} \frac{(-1)^\mu}{5+\mu} \binom{\nu}{\mu} c_\nu$$

and

$\eta(E_n, E_{el})$ can be approximated at large E_{el} by

$$\eta(E_n, E_{el}) = \frac{c_0 E_n^2}{4\alpha^2 E_{el} R}.$$

From eq. (A.2) and the afore-mentioned c_ν values, we calculated that the total excitation cross section of the $a\,^1\Pi_g$ state is given by:

$$\sigma_{E_{el}}(a) = \frac{7.15 \times 10^{-15}}{E_{el}} \left(0.1408 - \frac{0.129}{E_{el}}\right) \text{cm}^2,$$

where E_{el} is expressed in eV. Substituting for E_{el} 500 eV we obtain for σ(a) a value of 2.01×10^{-18} cm^2, which is 5% larger than the value calculated by Stolarski *et al.*[61]). For our normalization (at 500 eV), the total excitation cross section σ(a) needs to be related with the emission cross section of a particular band σ(a–X, v'–v'').
This relation can be expressed as:

$$\sigma(\text{a–X}, v'\text{–}v'') = \sigma(\text{a}, v') \frac{A_{v'v''}}{\sum_{v''} A_{v'v''}} = \sigma(\text{a}) \frac{I_{v'}}{\sum_{v'} I_{v'}} \frac{A_{v'v''}}{\sum_{v''} A_{v'v''}}, \qquad \text{(A.3)}$$

where

$$A_{v'v''} \propto q_{v'v''} |R_e(r)|^2 / \lambda^3_{v'v''}.$$

Here $A_{v'v''}$ is the spontaneous transition probability for the transition $v' \rightarrow v''$ with wavelength $\lambda_{v'v''}$, $q_{v'v''}$ is the Franck–Condon factor, $I_{v'}/\sum_{v'} I_{v'}$ is the probability for excitation to the v' level of the $a^1\Pi_g$ state and $R_e(r)$ is the electronic transition matrix element as a function of r.

Because the emission of a–X, 2–0 is contaminated with that of a–X, 5–2 around 1384 Å, we calculated the emission cross sections for both transitions with eq. (A.3). In the calculation of the branching ratios $A_{20}/\sum_{v''} A_{2v''}$ and $A_{52}/\sum_{v''} A_{5v''}$, we used as values for $q_{v'v''}$ those calculated by Benesch *et al.*[31]) and for $\lambda_{v'v''}$ those of ref. 5. In the determination of these ratios we took R_e to be constant, as found experimentally by Holland[22]). The ratios $I_2/\sum_{v'} I_{v'}$ and $I_5/\sum_{v'} I_{v'}$ were obtained from the relative intensity measurements of Lassettre *et al.*[23]). Neglecting cascade (from p'–a, 0–2) we derived a value of 1.06×10^{-19} cm^2 for the sum of the emission cross sections of a–X, 2–0 and a–X, 5–2 at 500 eV impact energy. The latter transition contributes about 18% to this value.

REFERENCES

1) Aarts, J. F. M., De Heer, F. J. and Vroom, D. A., Physica **40** (1968) 197.
2) Aarts, J. F. M. and De Heer, F. J., Chem. Phys. Letters **4** (1969) 116.
3) Aarts, J. F. M., De Heer, F. J. and Vriens, L., Proc. ICPEAC VI MIT-Press (Cambridge, 1969) p. 423.
4) Massey, H. S. W., Burhop, E. H. S. and Gilbody, H. B., Electronic and Ionic Impact Phenomena, Vol. II Clarendon Press, (Oxford, 1969) Chapters 12 and 13.
5) For a compilation see: Lofthus, A., The Molecular Spectrum of Nitrogen, Spectroscopic Rep. No. 2 (University of Oslo, 1960).
6) Herzberg, G., Spectra of Diatomic Molecules, 2nd ed. Van Nostrand, (New York, 1966).
7) Sheridan, W. F., Oldenburg, O. and Carleton, N. P., ICPEAC II, Berg, (New York, 1961) p. 159.
8) Srivastava, B. N., J. quant. Spectrosc. radiative Transfer **9** (1969) 1639.
9) Sroka, W., Z. Naturforsch. **24a** (1969) 398.

10) Ajello, J. M., J. chem. Phys. **53** (1970) 1156.
11) Mumma, M. J., Thesis, University of Pittsburgh (1970).
12) Philpot, J. L. and Hughes, R. H., Phys. Rev. **133** (1964) A107.
13) Dufay, M., Desesquelles, J., Druetta, M. and Eidelsberg, N., Ann. Geophysique **22** (1966) 614.
14) Robinson, J. M. and Gilbody, H. B., Proc. Phys. Soc. **92** (167) 589.
15) Dahlberg, D. A., Anderson, D. K. and Dayton, I. E., Phys. Rev. **164** (1967) 20.
16) Thomas, E. W., Bent, G. D. and Edwards, J. L., Phys. Rev. **165** (1968) 32.
17) Beyer, K. D. and Welge, K. H., J. chem. Phys. **51** (1969) 5323.
18) Huffman, R. E., Canad. J. Chem. **47** (1969) 1823.
19) Schoen, R. I., Canad. J. Chem. **47** (1969) 1879.
20) Moore, C. E., A Multiplet Table of Astrophysical Interest, Observatory, (Princeton, 1945);
Moore, C. E., An Ultraviolet Multiplet Table, Nat. Bur. Stand. Circ. 488 (U.S. Government Printing Office (Washington, 1950).
21) Striganov, A. R. and Sventitskii, N. S., Tables of Spectral Lines of Neutral and Ionized Atoms, IFI (New York. 1968).
22) Holland, R. F., J. chem. Phys. **51** (1969) 3940.
23) Lassettre E. N. and Krasnow, M. E., J. chem. Phys. **40** (1964) 1248;
Lassettre, E. N., Skerbele, A., Dillon, M. A. and Ross, R. J., J. chem. Phys. **48** (1968) 5066.
24) Moustafa Moussa, H. R., De Heer, F. J. and Schutten, J., Physica **40** (1969) 517.
25) Aarts, J. F. M., Thesis, University of Leiden, to be published.
26) Moustafa Moussa, H. R. and De Heer, F. J., Physica **36** (1967) 646.
27) Schutten, J., Van Deenen, P. J., De Haas, E. and De Heer, F. J., J. sci. Instrum. **44** (1967) 153.
28) Van Brunt, R. J. and Zare, R. N., J. chem. Phys. **48** (1968) 4304.
29) De Heer, F. J. and Carrière, J. D., J. chem. Phys., to be published.
30) Aarts, J. F. M. and De Heer, F. J., J. chem. Phys. **52** (1970) 5354.
31) Benesch, W., Vanderslice, J. T., Tilford, S. G. and Wilkinson, P. G., Astrophys. J. **143** (1966) 236.
32) Lawrence, G. M., Phys. Rev., A 2 (1970) 97.
33) Fite, W. L. and Brackmann, Phys. Rev. **112** (1958) 1151.
34) Carrière, J. D. and De Heer, F. J., to be published.
35) Holland, R. F., private communication.
36) De Jongh, J. P. and Van Eck, J., private communication.
37) Labuhn, F., Z. Naturforsch. **20a** (1965) 998.
38) Kelly, P. S., Astrophys. J. **140** (1964) 1247.
39) Wiese, W. L., Glennon, B. M. and Smith, M. W., Atomic Transition Probabilities H to Ne, Vol. I, NSRDS-NBS-4, US Government Printing Office (Washington, 1965).
40) Bethe, H. A., Ann. Physik **5** (1930) 325.
41) Miller W. F. and Platzman, R. L., Proc. Phys. Soc. **70** (1957) 299.
42) Vroom, D. A. and De Heer, F. J., J. chem. Phys. **50** (1969) 580.
43) Fano, U. and Cooper, J. W., Rev. mod. Phys. **40** (1968) 441.
44) Van der Wiel, M. J., El-Sherbini, Th. M. and Vriens, L., Physica **42** (1969) 411.
45) Lawrence, G. M. and Savage, B. D., Phys. Rev. **141** (1966) 67.
46) Hesser, J. E. and Lutz, B. L., J. Opt. Soc. Amer. **58** (1968) 1513.
47) Mulliken, R. S., J. Am. Chem. Soc. **88** (1966) 1849 and the references cited therein.
48) Mulliken, R. S., in The Threshold of Space, Pergamon Press (New York, 1957) p. 169.

49) Gilmore, F. G., J. quant. Spectrosc. radiative Transfer **5** (1965) 369.
50) Codling, K., Astrophys. J. **143** (1966) 552.
51) Moran, T. F., Petty, F. C. and Hedrick, A. F., J. chem. Phys. **51** (1969) 2112.
52) Comes, F. J. and Lessmann, W., Z. Naturforsch. **19a** (1964) 65.
53) Cade, P. E., Sales, K. D. and Wahl, A. C., J. chem. Phys. **44** (1966) 1973.
54) Siegbahn, K. *et al.*, ESCA Applied to Free Molecules, North-Holland (Amsterdam, 1969) p. 63.
55) Dressler, K., Canad. J. Phys. **47** (1969) 547.
56) Rapp, D., Englander-Golden, P. and Briglia, D. D., J. chem. Phys. **42** (1965) 4081.
57) Stalherm, D., Cleff, B., Hillig, H. and Mehlhorn, W., Z. Naturforsch. **24a** (1969) 1728.
58) Van der Wiel, M. J., El-Sherbini, Th. M. and Brion, C. E., Chem. Phys. Letters, to be published.
59) Vriens, L., Phys. Rev. **160** (1967) 100.
60) Vriens, L., Simpson, J. A. and Mielczarek, S. R., Phys. Rev. **165** (1968) 7.
61) Stolarski, R. S., Dulock Jr, V. A., Watson, C. E. and Green, A. E. S., J. Geophysical Res. **72** (1967) 3953.

CHAPTER III

Part A

EMISSION CROSS SECTIONS OF THE $A\,^2\Pi$ AND $B\,^2\Sigma^+$ STATES OF CO^+ *

Synopsis

Absolute emission cross sections for production of radiation of the $A\,^2\Pi$ and $B\,^2\Sigma^+$ states of CO^+ have been determined for 0.05–5 keV electrons incident on CO. The results are analyzed by means of the Bethe approximation. A strong contribution from collision-induced dipole transitions is found in the excitation processes. Cross sections for formation of the $A\,^2\Pi$, $B\,^2\Sigma^+$ and $X\,^2\Sigma^+$ states have been calculated. In some cases the variation of the electronic transition matrix element R_e could be determined from ratios of cross sections for specified vibrational transitions. The apparent cross sections for emission of the $A\,^2\Pi$–$X\,^2\Sigma^+$ band system were found to be dependent both on the gas pressure and the electron current used. These effects are connected with an excitation transfer process and a pressure effect found in lifetime measurements. A comparison is made with existing proton- and photon- impact data and also with electron data of N_2.

1. *Introduction.* The near ultraviolet and visible part of the spectrum of CO is dominated by the transitions $B\,^2\Sigma^+$–$X\,^2\Sigma^+$ and $A\,^2\Pi$–$X\,^2\Sigma^+$ of CO^+, respectively called the first negative group and the comet-tail bands[1]). The latter system, discovered in the tails of comets is thought to arise after resonance absorption of sunlight by CO^+ ions in the ground state, $X\,^2\Sigma^+$, leading to formation of the $A\,^2\Pi$ state. Next, resonance radiation is emitted and repeatedly absorbed and reemitted (see Herzberg[2])). Only a few laboratory studies have been made on the formation of the mentioned CO^+ bands by photon, electron and proton impact and on the radiative lifetime of the $A\,^2\Pi$ and $B\,^2\Sigma^+$ states. Relative measurements on band intensities of the A–X transition were done by Robinson and Nicholls[3]), using electrons between 60 and 100 eV. Skubenich and Zapesochny[4]) measured some emission cross sections for the $A\,^2\Pi$ and $B\,^2\Sigma^+$ states by electron impact between the threshold and 160 eV. Poulizac *et al.*[5]) measured emission cross sections for many bands of the A–X and B–X transitions and also weak

* Physica 49 (1970) 425,
J.F.M. Aarts, F.J. De Heer.

bands of B–A transitions, called the Baldet–Johnson system, by proton impact between 30 and 600 keV. Radiative lifetimes for several comet-tail bands were measured by Bennett and Dalby[6]), Fink and Welge[7]) and Desesquelles *et al.*[8]).

Photoelectron energy spectra by the impact of photons on CO are reported by Schoen[9]) and Berkowitz *et al.*[10]).

We studied the production of the $A\,^2\Pi$ and $B\,^2\Sigma^+$ states resulting from 0.05–5 keV electron impact by detecting the radiation of the following transitions: $A\,^2\Pi$–$X\,^2\Sigma^+$, $B\,^2\Sigma^+$–$X\,^2\Sigma^+$ and $B\,^2\Sigma^+$–$A\,^2\Pi$. Absolute emission cross sections for these band systems have been determined. Pressure and current effects, which were present in the measurements of the comet-tail bands, have been studied in detail.

2. *Experimental.* The apparatus and experimental technique are the same as those described in ref. 11. Basically the apparatus consists of an electron gun, a collision chamber and an electron trap and an axial magnetic field is used for the alignment of the electron beam. The emitted radiation was observed at 90° with respect to the electron beam axis by means of a Leiss monochromator. Radiation has been measured from A–X transitions between 3200 and 5500 Å and from B–X transitions between 2100 and 2600 Å. In order to avoid second-order radiation of the B–X transitions, A–X transitions between 4000 and 5200 Å have been measured with a glass window behind the entrance slit of the monochromator. This window absorbs radiation below 3300 Å and transmits about 85% of the radiation above 4000 Å. No corrections have been applied for the degree of polarization (Π) of the radiation, which polarization appears generally to be small for molecular radiation. We measured that $\Pi \lesssim 3\%$ for the radiation of the comet-tail bands in the visible part of the spectrum. The sensitivity of our optical equipment (quantum yield) was determined by means of a tungsten standard between 5500 and 2500 Å. Below 3000 Å the tungsten standard was used in combination with an interference filter in order to suppress the effect of stray light. For wavelengths lower than 2500 Å we used as standard a deuterium lamp manufactured by Kern (see ref. 12). The intensity distribution of this lamp as a function of wavelength was determined by Böhm at the Landessternwarte Heidelberg–Königstuhl, by comparing this lamp with a "secondary standard" deuterium lamp, calibrated against the synchrotron radiation of Desy[12]). The comparison was performed in a setup similar as given in fig. 1 of Pitz[12]) between 1650 and 2700 Å. With the deuterium lamp we only determined the relative sensitivity of our monochromator as a function of wavelength and fitted the absolute scale to the data taken with the tungsten standard above 2500 Å.

The pressure, varied between 10^{-4} and 2×10^{-3} torr, was measured by an ionization gauge (General Electric), calibrated as described in ref. 13. The

accuracy of the pressure measurement is estimated to be 2%. Electron currents from 10 μA up to 100 μA were used. All cross sections have been determined in a region where the light intensity varied proportionally with gas pressure and electron currents. Secondary effects in the emission of the comet-tail bands appeared to be present at pressures higher than about 10^{-4} torr and electron currents higher than about 25 μA. These effects will be discussed in section 4.4.

The accuracy of our absolute emission cross sections of the A–X transition is estimated to be about 11%, mainly due to systematic errors in the determination of the quantum yield of the monochromator (10%) and an additional error of 3% in the use of a weighted sensitivity for a band with a width varying between 50 and 100 Å. A systematic error arises in the emission cross sections of the $v' = 2$–$v'' = 0$ band of A–X due to contamination from a CII multiplet and could be as much as 3%. The accuracy of our cross sections for the B–X bands between 2100 and 2600 Å depends also on the intensity calibration with our "secondary deuterium standard". We estimate that the cross sections in this wavelength region will have an accuracy of about 20%. The accuracy of our cross-section ratios for the various vibrational transitions of the A–X and B–X systems is estimated to be about 5 and 10% respectively (see tables II and IV).

3. *Results.* The experimental cross sections for emission of $A\,^2\Pi$–$X\,^2\Sigma^+$ $v' = 3$–$v'' = 0$ and $B\,^2\Sigma^+$–$X\,^2\Sigma^+$ $v' = 0$–$v'' = 0$ are listed in table I. Emission cross sections of transitions with other vibrational quantum numbers, normalized on the ones just mentioned, are given in table II, together with the results of Poulizac *et al.*[5]) and ratios derived from theory (see section 4.3). For $A\,^2\Pi$–$X\,^2\Sigma^+$ we did not study transitions above 5500 Å. Below 5500 Å overlapping of bands prevented us to measure the 1–0, 4–2, 6–3 and 3–1 transitions. For two bands of $B\,^2\Sigma^+$–$A\,^2\Pi$ we have also given the cross-section ratios with respect to the $B\,^2\Sigma^+$–$X\,^2\Sigma^+$ $v' = 0$–$v'' = 0$ transition. All our ratios listed in table II were found to be independent of the impact energy, within 3%, over the range investigated.

4. *Discussion of results.* 4.1. Comparison with the Bethe approximation. At sufficiently high impact energy, according to the Bethe theory[14]), the excitation cross section of an electronic state with vibrational quantum number v', $\sigma_{v'}$, can be expressed by

$$\sigma_{v'} = \frac{4\pi a_0^2 R}{E'_{\mathrm{el}}} M_{\mathrm{i}}^2(v') \ln c \frac{E'_{\mathrm{el}}}{R}, \qquad (1)$$

where $E'_{\mathrm{el}} = \frac{1}{2}mv^2$, m is the electron rest mass, v is the velocity of the incident electron, R is the Rydberg energy, a_0 is the first Bohr radius, c is a constant and $M_{\mathrm{i}}^2(v')$ is the squared effective dipole-matrix element for for-

mation of the ion state under consideration, given by

$$M_i^2(v') = \int_{\text{I.P.}}^{\infty} \frac{df(E)}{dE} \frac{R}{E} \eta_i(E)\, dE, \tag{2}$$

where $df(E)/dE$ is the differential oscillator strength which is a function of the excitation energy E, I.P. the ionization potential and $\eta_i(E)$ the efficiency for ionization at excitation energy E ($0 \leq \eta_i(E) \leq 1$). From eq. (1) it can be seen that a plot of $\sigma_{v'} E'_{el}/4\pi a_0^2 R$ *vs.* $\ln E'_{el}$, a so called Bethe plot, will allow determination of $M_i^2(v')$ and c. Having measured emission cross sections of v'–v'', we replace $\sigma_{v'}$ and $M_i^2(v')$ by $\sigma_{v'-v''}$ and $M_i^2(v'-v'')$ respectively in eq. (1), where $M_i^2(v'-v'')$ is defined by

$$\frac{\sigma_{v'-v''}}{\sigma_{v'}} = \frac{M_i^2(v'-v'')}{M_i^2(v')}. \tag{3}$$

In fig. 1 we present Bethe plots for A–X $v' = 3$–$v'' = 0$ and B–X $v' = 0$–$v'' = 0$. Our experimental curves are linear above 200 eV and have a positive slope, which is characteristic for an optically allowed transition in the collision process. Applying a least square analysis we calculated for A–X, 3–0 and B–X, 0–0

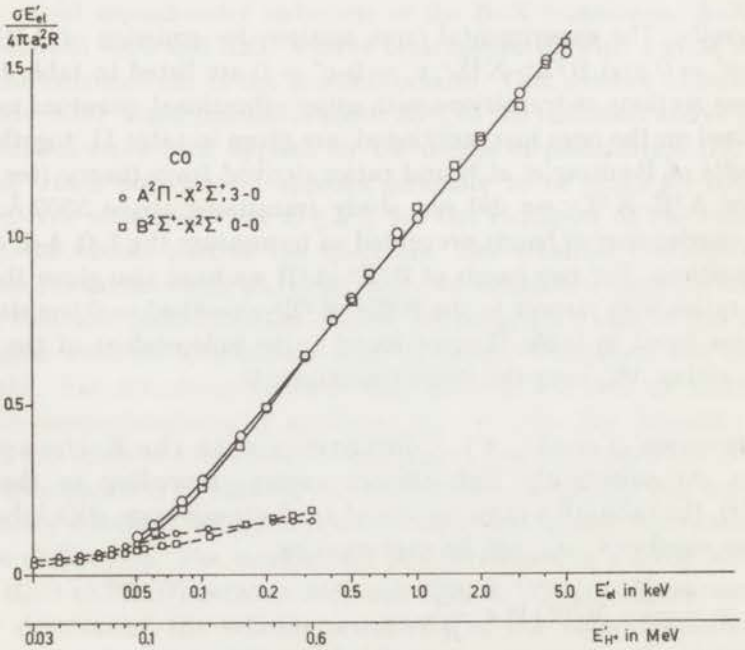

Fig. 1. Emission cross sections of CO^+ transitions presented in $\sigma E'_{el}/4\pi a_0^2 R$ *vs.* $\ln E'_{el}$ plots in the case of electron and proton impact; drawn lines refer to electrons (this work), dashed lines to protons (Poulizac *et al.*[5])). For protons $E'_{H^+} = (M/m)\, E'_{el}$
○ $A\,^2\Pi$–$X\,^2\Sigma^+$, 3–0; □ $B\,^2\Sigma^+$–$X\,^2\Sigma^+$, 0–0.

respectively $M_i^2(v'-v'') = 0.34$, $c = 0.30$ and $M_i^2(v'-v'') = 0.34$, $c = 0.29$. In fig. 1 we have also included proton impact data of Poulizac *et al.*[5]); the two abscissas of fig. 1 correspond to identical velocities of the projectiles involved: $E'_{H^+} = (M/m)E'_{el}$ where M is the proton rest mass. The agreement between electron and proton impact data is poor.

4.2. Excitation cross sections. In order to study the collision process it is important to determine the population of the different vibrational states v' of an electronic state by evaluation of the excitation cross sections $\sigma_{v'}$. They can be calculated by adding up the relevant emission cross sections $\sigma_{v'v''}$ in a v'' progression, *i.e.*:

$$\sigma_{v'} = \sum_{v''} \sigma_{v'v''} - \sigma'_{v'}. \tag{4}$$

The cross section $\sigma'_{v'}$ is a correction for contribution of cascade to v' from vibrational states of other higher lying electronic states. We have applied eq. (4) in the case of the $B\,^2\Sigma^+$ state for $v' = 0$ and $v' = 1$. No cascade is known and so we take $\sigma'_{v'} = 0$. We add up the emission cross sections of the progressions with $v' = 0$ and 1 of the B–X and B–A transitions (see table II), neglecting emission cross sections with $v'' > 4$ and 5 for $v' = 0$ and $v' = 1$ respectively. The total excitation cross section for the $B\,^2\Sigma^+$ state is approximately equal to the sum of $\sigma_{v'=0}$ and $\sigma_{v'=1}$. We find that $\sigma(B\,^2\Sigma^+)$ is 2.42

TABLE I

Emission cross sections for CO^+ bands in units of 10^{-18} cm^2

eV	$A\,^2\Pi$–$X\,^2\Sigma^+$ $v' = 3$–$v'' = 0$	$B\,^2\Sigma^+$–$X\,^2\Sigma^+$ $v' = 0$–$v'' = 0$
50	10.2	8.95
60	11.4	10.0
80	12.6	11.5
100	13.1	12.0
120	13.1	12.2
150	12.9	12.0
200	11.9	11.8
300	10.2	10.2
400	8.94	8.95
500	7.82	7.69
600	7.08	7.05
800	6.03	5.85
1000	5.04	5.17
1500	3.80	3.86
2000	3.09	3.12
3000	2.30	2.23
4000	1.83	1.82
5000	1.50	1.52

TABLE II

Emission cross-section ratios for CO^+ bands

	$v'-v''$	λ_{mean} (Å) [a]	Present	Poulizac *et al.* [c]	Theory [d]
$A\,^2\Pi-X\,^2\Sigma^+$	0–0	4900		0.26	0.071
	0–1	5500	0.20	0.74	0.182
	0–2	6250		0.85	0.205
	0–3	7168*		0.52	0.135
	0–4	8430*		0.28	0.057
	1–0	4550		0.84	0.46
	1–1	5050	0.54	0.92	0.58
	1–2	5680		0.32	0.172
	1–4	7466*		0.130	0.086
	1–5	8820*		0.185	0.108
	2–0	4260	1.08 [b]	1.35 [b]	0.93
	2–1	4700	0.42	0.67†	0.40
	2–3	5880		0.335†	0.225
	2–4	6710		0.215†	0.119
	2–6	9254*		0.135†	0.039
	3–0	4000	1.00	1.00	1.00
	3–2	4852		0.274†	0.230
	3–3	5412	0.145	0.165†	0.154
	3–5	6930*		0.132†	0.103
	3–6	8138		0.088†	0.040
	4–0	3785	0.69	0.68	0.69
	4–2	4518		0.32	0.24
	5–0	3595	0.38	0.24	0.38
	6–0	3420	0.16		0.166
	7–0	3277	0.056		0.063
	7–1	3518	0.082		0.094
$B\,^2\Sigma^+-X\,^2\Sigma^+$	0–0	2190	1.00	1.00	1.00
	0–1	2300	0.53	0.54	0.555
	0–2	2419	0.13	0.086	0.146
	0–3	2550	0.020	0.026	0.0258
	1–0	2112	0.29	0.130	0.259
	1–1	2214	0.044	0.034	0.0411
	1–2	2325	0.20	0.18	0.198
	1–3	2446	0.106	0.070	0.113
	1–4	2578	0.029	0.034	0.0343
$B\,^2\Sigma^+-A\,^2\Pi$	0–0	3960	0.053		
	0–1	4220	0.032		

[a] obtained from the compilation of Krupenie[1]; additional comet-tail transitions at wavelengths marked with an asterisk were found by Poulizac *et al.*[5];

[b] contamination from a C II multiplet;

[c] ref. 5, numbers marked with a dagger were determined at one impact energy, 400 keV;

[d] based on a calculation using Franck-Condon factors of refs. 16 and 20 (see section 4.3).

TABLE III

CO cross sections for total ionization, dissociative ionization and excitation to the $A\,^2\Pi$, $B\,^2\Sigma^+$ and $X\,^2\Sigma^+$ states of CO^+ in units of 10^{-17} cm^2

eV	$\sigma_{tot.ion.}$ [a]	$\sigma_{diss.ion.}$ [b]	$\sigma_{A\,^2\Pi}$ [c]	$\sigma_{B\,^2\Sigma}$ [c]	$\sigma_{X\,^2\Sigma}$ [d]
50	21.2	3.08	8.2	2.16	7.8
60	23.4	4.14	9.2	2.42	7.7
80	25.9	5.37	10.1	2.78	7.6
100	26.5	6.00	10.5	2.90	7.1
150	25.7	6.17	10.4	2.90	6.3
200	22.4	5.26	9.6	2.86	4.7
300	18.4	4.25	8.2	2.47	3.5
400	15.8	3.49	7.2	2.17	3.0
500	13.6	2.90	6.3	1.86	2.6
600	12.3	2.54	5.7	1.70	2.4
800	9.89	1.99	4.8	1.42	1.6
1000	8.34	1.59	4.0	1.25	1.4
1500			3.1	0.934	
2000	4.90		2.5	0.755	
3000	3.50		1.85	0.539	
4000	2.80		1.47	0.440	
5000	2.33		1.21	0.368	

[a] obtained from the cross sections of Rapp and Englander-Golden[17] and Schram *et al.*[18] (see text);
[b] obtained from the fraction for dissociative ionization of Rapp *et al.*[19] and $\sigma_{tot.ion.}$;
[c] this work;
[d] obtained by subtraction of $\sigma_{diss.ion.}$, $\sigma_{A\,^2\Pi}$ and $\sigma_{B\,^2\Sigma}$ from $\sigma_{tot.ion.}$.

TABLE IV

Cross-section ratios for excitation to the $A\,^2\Pi$ and $B\,^2\Sigma^+$ states of CO^+

	v'	Present [a]	Poulizac *et al.* [b]	Berkowitz *et al.* [c]	Theory [d]
$A\,^2\Pi$	0	0.42	1.49	0.76	0.413
	1	0.83	1.32	1.14	0.92
	2	1.16	1.60	1.25	1.13
	3	1.00	1.00	1.00	1.00
	4	0.72	0.58		0.73
	5	0.47			0.467
	6	0.26			0.270
	7	0.128			0.145
$B^2\Sigma^+$	0	1.00	1.00		1.00
	1	0.37	0.28		0.360

[a] see section 4.3;
[b] ref. 5;
[c] ref. 10;
[d] ref. 20.

TABLE V

Comparison of cross sections of CO and N_2 for total ionization, excitation to the A, B and X states and dissociative ionization in units of 10^{-17} cm^2

CO		$\sigma_{\text{tot.ion.}}$ [a]	$\sigma_{A\,^2\Pi}$ [b]	$\sigma_{B\,^2\Sigma^+}$ [b]	$\sigma_{X\,^2\Sigma}$ [b]	$\sigma_{\text{diss.ion.}}$ [c]
	100 eV	26.5	10.5	2.90	7.1	6.00
	500	13.6	6.3	1.86	2.6	2.90
	1000	8.34	4.0	1.25	1.4	1.59
	M_i^2		2.7	0.82		
	c		0.30	0.29		
N_2		$\sigma_{\text{tot.ion.}}$ [a]	$\sigma_{A\,^2\Pi_u}$	$\sigma_{B\,^2\Sigma_u^+}$ [d]	$\sigma_{X\,^2\Sigma_g^+}$	$\sigma_{\text{diss.ion.}}$ [c]
	100 eV	25.3	see text	2.78		5.55
	500	13.0		1.54		2.61
	1000	8.02		0.96		1.50
	M_i^2	3.95		0.51		
	c	0.95		0.57		

[a] obtained from the cross sections of Rapp and Englander-Golden[17]) and Schram *et al.*[18]) (see section 4.2);

[b] this work;

[c] obtained from $\sigma_{\text{tot.ion.}}$ and fractions of Rapp *et al.*[19]);

[d] these cross sections were recently remeasured and found at impact energies above 200 eV to be identical with those published in ref. 25. At 100 eV we measured a value 2.78 or 16% lower than in ref. 25.

times σ(B–X, 0–0), the emission cross sections being given in table I. The values for $\sigma(B\,^2\Sigma^+)$ are given in table III, whereas the ratio of $\sigma_{v'=1}$ and $\sigma_{v'=0}$ is presented in table IV. Similarly (see eq. (3))

$$M_i^2(B\,^2\Sigma^+) = 2.42\, M_i^2(\text{B–X, 0–0}) = 0.82 \qquad \text{(see table V)}.$$

For the $A\,^2\Pi$–$X\,^2\Sigma^+$ transition we measured only one or two emission cross sections of a progression, because the relevant radiation is spread over a larger wavelength region than is included in the present experiment. In this case the other (not measured) emission cross sections in a progression are estimated by using

$$\sigma_{v'v''} \propto N_{v'} A_{v'v''} / \sum_{v''} A_{v'v''} \propto q_{v'v''} |R_e(r_{v'v''})|^2 / \lambda^3_{v'v''}. \tag{5}$$

Here $N_{v'}$ is the population of v', $A_{v'v''}$ is the spontaneous transition probability for the electronic transition with $v' \rightarrow v''$ and wavelength $\lambda_{v'v''}$, $q_{v'v''}$ is the Franck–Condon factor and R_e the electronic transition matrix element as a function of the internuclear separation r. In a progression with v' constant, $N_{v'}$ and $\sum_{v''} A_{v'v''}$ are both constant. Assuming that $R_e(r)$ varies slowly with r, we can replace r by a fixed value $\bar{r}_{v'v''}$, called the r-centroid (see Fraser[15])). If one emission cross section is measured in a progression

we can calculate the others if we make use of Franck–Condon factors, calculated by Nicholls[16]) and assume that R_e is constant in a progression. Then eq. (4) can be applied again for the calculation of $\sigma_{v'}$. Due to the cascading transitions B–A a small cascade correction ($\sigma'_{v'}$) has to be introduced (see eq. (4)), which amounts to 7% and 2% for $\sigma_{v'=0}$ and $\sigma_{v'=1}$ respectively and which is assumed to be neglectable for higher vibrational states. The calculated $\sigma_{v'}$ values are given in table IV relative to $\sigma_{v'=3}$. Their sum is approximately equal to the total excitation cross section of the $A\,^2\Pi$ state. We find that $\sigma(A\,^2\Pi)$, given in table III, is 8.0 times σ(A–X, 3–0), given in table I. Similarly (see eq. (3))

$$M_i^2(A\,^2\Pi) = 8.0 \times M_i^2(\text{A–X, 3–0}) = 2.7 \qquad \text{(see table V)}.$$

The cross sections for formation of CO^+ ions in the $X\,^2\Sigma^+$ state can be estimated by using different experimental cross sections: The total ionization cross section of CO has been measured by Rapp and Englander-Golden[17]) in the energy range of 14 to 1000 eV. We only use their data up to 100 eV because there is some evidence that at higher energies their cross sections are affected by secondary electrons. The ionization cross sections of Rapp and Englander-Golden for CO and N_2 differ only a factor of 1.04 above 100 eV impact energy. Schram *et al.*[18]) measured total ionization cross sections for N_2, but not for CO, above 100 eV. Their cross section for N_2 at 100 eV is only 3% smaller than that of Rapp and Englander-Golden. We transform Schram's cross sections for N_2 to those for CO by multiplying Schram's cross sections by 1.04, the ratio found by Rapp and Englander-Golden. We also multiply by 1.03 in order to get the ionization cross section of Rapp and Englander-Golden at 100 eV. In fact, we use for CO the absolute ionization cross sections of Rapp and Englander-Golden[17]) up to 100 eV and the energy dependence of the cross sections for N_2 of Schram *et al.*[18]) above 100 eV. The cross sections thus calculated are given in table III. Rapp *et al.*[19]) have measured the fraction of ions formed by dissociative ionization having energies larger than 0.25 eV. Their cross sections given in table III may therefore be lower than the complete cross sections for dissociative ionization.

We can find upper limits for the cross sections for formation of ions in the $X\,^2\Sigma^+$ state by subtracting $\sigma_{\text{diss.ion}}$, $\sigma_{A\,^2\Pi}$ and $\sigma_{B\,^2\Sigma^+}$ from $\sigma_{\text{tot.ion}}$ as shown in table III. The fractions for formation of $A\,^2\Pi$, $B\,^2\Sigma^+$, $X\,^2\Sigma^+$ and dissociated ions are respectively 39%, 10%, 37% and 15% at 50 eV and 48%, 15%, 17% and 19% at 1000 eV.

The fractions of ions formed in the different states have also been measured in photon experiments. Schoen[9]) found for 12–23 eV photons that the fractions of ions in the A, B and X states were, respectively, 58%, 35% and 7% with an accuracy of 30% for the A state and 100% for the B state. Using

photons of 584 Å, Berkowitz *et al.*[10]) found for the ratio of numbers of ions in the A and X states 0.8.

4.3. Cross-section ratios and electronic transition moments. In table II we compare our experimental emission cross-section ratios for vibrational transitions $B^2\Sigma^+$–$X^2\Sigma^+$ and $A^2\Pi$–$X^2\Sigma^+$ with those of Poulizac *et al.*[5]) and theory. In table IV we compare corresponding cross-section ratios for excitation *i.e.*, $B^2\Sigma^+ \leftarrow X^1\Sigma^+$ and $A^2\Pi \leftarrow X^1\Sigma^+$. For the latter transition photon impact data of Berkowitz *et al.*[10]) are included in table IV.

Theoretical values for the ratios are calculated by means of well known relations in a band system (see Herzberg[2])). For the excitation from the ground state of CO, $X^1\Sigma^+$ $v'' = 0$, to the vibrational level v' of the excited electronic state, we have in analogy with absorption of photons

$$\sigma_{v'} \propto N_{v'} \propto q'_{v'0} \, |R'_e(\bar{r}_{v'0})|^2, \tag{6}$$

where R'_e is the electronic transition matrix element in the excitation process. The relation for emission in a v'' progression (v' is constant) is given in eq. (5). Combining eqs. (5) and (6) we get the relation between the different progressions in a band system:

$$\sigma_{v'v''} \propto N_{v'} \frac{A_{v'v''}}{\sum\limits_{v''} A_{v'v''}}$$

$$\propto q_{v'0} |R'_e(\bar{r}_{v'0})|^2 \frac{q_{v'v''} \, |R_e(\bar{r}_{v'v''})|^2 / \lambda^3_{v'v''}}{\sum\limits_{v''} q_{v'v''} \, |R_e(\bar{r}_{v'v''})|^2 / \lambda^3_{v'v''}}. \tag{7}$$

From eqs. (6) and (7) we have obtained the theoretical ratios in tables IV and II respectively. We have taken theoretical Franck–Condon factors $q'_{v'0}$ from Wacks[20]) which agree with those calculated recently by Nicholls[21]), $q_{v'v''}$ from Nicholls[16]) and assumed that R_e and R'_e are constant. In the case of the A–X system, the wavelengths of only a few bands in the v'' progressions with $v' > 3$ have been found experimentally[1]). The remaining wavelengths needed in the summation in eq. (7) were calculated from the spectroscopic constants of the two states under consideration (see Herzberg[2])). In the calculation of the theoretical values for the emission cross-section ratios of the $B^2\Sigma^+$–$X^2\Sigma^+$ bands we corrected for the observed branching of radiation from $B^2\Sigma^+$ $v' = 0$ to the $A^2\Pi$ and $X^2\Sigma^+$ states by multiplying the cross-section ratios of the progression with $v' = 0$ by the experimental factor $\sigma(B^2\Sigma^+\text{–}X^2\Sigma^+, v' = 0 - \Sigma v'')/\sigma(B^2\Sigma^+, v' = 0)$. The assumption of constant R_e can be tested by comparing the experimental ratios of emission cross sections in a v'' progression with those calculated from eqs. (5) or (7) and similar for R'_e by comparing experimental ratios of excitation cross sections with $q'_{v'0}$. In the case of the A–X system we could not determine the variation of R_e, because for the different v'' progressions we could not measure

more than one or two bands. Only the variation of R_e and R_e' together could be studied by comparing our ratios with the theoretical values (uncorrected for cascade), calculated with eq. (7) and R_e and R_e' constant. In the range of $\bar{r}$ values[16]), with $\bar{r}_{0-1}$ and $\bar{r}_{7-0}$ as extremes, we find a variation of about 25%. When we compare the ratios for the estimated excitation cross sections (see section 4.2) with $q'_{v'0}$ we find that the largest deviation is about 13%.

As can be seen in table II our ratios of the A–X transitions deviate from those of Poulizac *et al.* [5]) especially for the 0–1, 1–1, 2–1 and 5–0 bands. This discrepancy is not understood. Large deviations also occur in the cross-section ratios for excitation to $A\,^2\Pi$ $v' = 0$ and 1 as shown in table IV. The ratios of Berkowitz *et al.*[10]), who measured photoelectrons produced by the impact of 584 Å photons on CO, are also not in agreement with our experiment. However, it is known that the ratios of the population of vibrational states, determined by photoelectron measurements, can deviate from Franck–Condon factors for excitation (see for instance Collin and Natalis[22])).

Our experimental emission cross-section ratios of the $B\,^2\Sigma^+$–$X\,^2\Sigma^+$ band system (see table II) deviate partly more than 10% (our experimental accuracy) from theoretical values for both progressions. This is probably due only to a variation of R_e over the bandsystem, because we see in table IV that our experimental ratio $\sigma_{v'=1}/\sigma_{v'=0}$ for excitation to the $B\,^2\Sigma^+$ state agrees with the ratio of theoretical Franck–Condon factors. This means that R_e' in eq. (6) is the same for excitation to $v'=0$ and $v'=1$. We de-

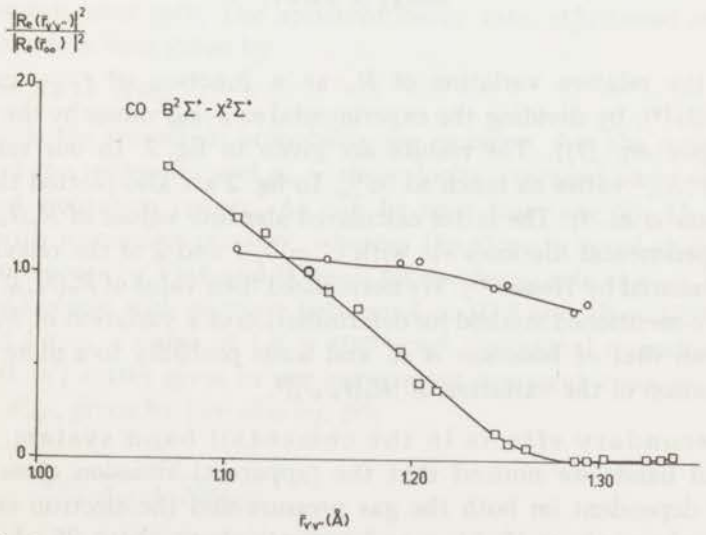

Fig. 2. Relative variation of the electronic transition moment for the transition $B\,^2\Sigma^+$–$X\,^2\Sigma^+$ as function of the r-centroid.
○ this work; □ Isaacson *et al.*[23]), normalized to unity at $\bar{r}_{00}$.

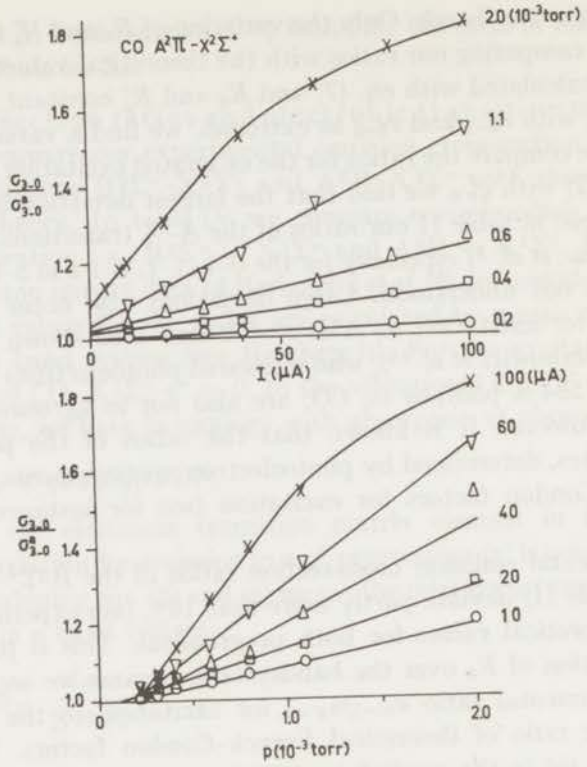

Fig. 3. The ratio of the emission cross section and the apparent emission cross section for $A^2\Pi$–$X^2\Sigma^+$, 3–0 as function of the electron current and the pressure at an impact energy of 200 eV.

termine the relative variation of R_e as a function of $\bar{r}_{v'v''}$, calculated by Nicholls[16]), by dividing the experimental $\sigma_{v'v''}/\sigma_{00}$ values by the theoretical ones (see eq. (7)). The results are given in fig. 2. In our range of r-centroids $|R_e|^2$ varies as much as 38%. In fig. 2 are also plotted the results of Isaacson *et al.*[23]). The latter calculated absolute values of $R_e(\bar{r}_{v'v''})$ from three experimental lifetimes $\tau_{v'}$ with $v' = 0$, 1 and 2 of the relevant radiation, measured by Hesser[24]). We normalized their value of $R_e(\bar{r}_{0-0})$ to unity. Our above-mentioned method for determination of a variation of R_e is more direct than that of Isaacson *et al.* and leads probably to a more accurate determination of the variation of $|R_e(\bar{r}_{v'v''})|^2$.

4.4. Secondary effects in the comet-tail band system. For the comet-tail bands we noticed that the (apparent) emission cross sections $\sigma_{v'v''}$ are dependent on both the gas pressure and the electron current at pressures above about 10^{-4} torr and currents above about 25 μA. In fig. 3 we have plotted the ratio of $\sigma_{3-0}/\sigma^a_{3-0}$ at an impact energy of 200 eV, where σ_{3-0} is the cross section in the pressure- and current-independent region and

where σ^{a}_{3-0} is the apparent cross section as a function of the gas pressure (or gas density N) and the electron current I. In a first approximation we can express our experimental results by

$$\sigma_{3-0}/\sigma^{a}_{3-0} = 1 + c_1 N + c_2 NI, \tag{8}$$

where c_1 and c_2 are constants. It will be shown below that the mechanism of the secondary effects is probably also responsible for the pressure dependence of the radiative decay rate $A_{v'}$, or lifetime $\tau_{v'}$, as measured by Fink and Welge[7]) by means of the phase-shift method. Fink and Welge found an anomalous decrease of the "apparent" decay rate, $A^{a}_{v'}$, with increasing pressure between about 5×10^{-4} and 4×10^{-3} torr and a linear increase of $A^{a}_{v'}$ between 4×10^{-3} and 18×10^{-3} torr. The minimum in $A^{a}_{v'}$ (= maximum $\tau_{v'}$) at about 4×10^{-3} torr was different for two vibrations in a progression (constant v') and was found to depend on the electron current used. Earlier lifetime measurements, reported by Bennett and Dalby[6]), are in agreement with the maximum $\tau_{v'}$ of Fink and Welge and also with recent measurements of Desesquelles *et al.*[8]), using a beam-foil technique. However, Bennett and Dalby found no pressure dependence of $\tau_{v'}$ between 2×10^{-4} and 6×10^{-3} torr.

Due to the relatively long lifetime of the $A\,^2\Pi$ (v') states, about 2×10^{-6} s, it may be expected that some of the molecules in the $A\,^2\Pi$ (v') state loose their excitation energy by collisions with molecules in the ground state $X\,^1\Sigma^+$ ($v = 0$) before decay by radiative transitions can occur (collisional quenching). These secondary reactions can have large cross sections if the difference in excitation energy of the molecular states before and after the collision is near zero. The apparent decay rate, $A^{a}_{v'}$, found in lifetime measurements is then given by

$$A^{a}_{v'} = A_{v'} + N\bar{v}\sigma_q, \tag{9}$$

where $A_{v'}$ is the transition probability for emission, $\bar{v}$ is the mean kinetic velocity of the molecules and σ_q is the velocity-averaged cross section for transfer of excitation energy. As can be seen from eq. (9) $A^{a}_{v'}$ increases linearly with increasing pressure, whereas the slope is equal to $\bar{v}\sigma_q$. From the measurements by Fink and Welge[7]) for the decay rate of $v' = 3$–$v'' = 0$, increasing linearly with pressure between 4×10^{-3} and 18×10^{-3} torr, we calculated for σ_q a value of 1.2×10^{-14} cm^2. Collisional quenching of excited $A\,^2\Pi$ (v') states gives in our experiment apparent cross sections for emission, $\sigma^{a}_{v'v''}$, given by (see also eq. (9))

$$\sigma^{a}_{v'v''} = \sigma_{v'v''}\,\frac{A_{v'}}{A_{v'} + N\bar{v}\sigma_q}$$

or

$$\frac{\sigma_{v'v''}}{\sigma^{a}_{v'v''}} = \left(1 + \frac{N\bar{v}\sigma_q}{A_{v'}}\right). \tag{10}$$

In our experiment with the 3–0 band the pressure dependence of the apparent emission cross section corresponds to the term c_1N in eq. (8). Combining eqs. (8) and (10) we get $c_1 = \sigma_q \bar{v}/A_{v'}$. Using our experimental c_1 value and for $A_{v'=3}$ the "minimum value" of Fink and Welge, we find that $\sigma_q = 1.0 \times 10^{-14}$ cm^2, which agrees quite well with the value calculated from the pressure increase of $A^a_{v'=3}$ between 4×10^{-3} and 18×10^{-3} torr in the work of Fink and Welge. In the pressure range of 5×10^{-4} to 4×10^{-3} torr Fink and Welge explained their anomalous decrease in $A^a_{v'}$ with increasing pressure by resonance absorption (see also section 1). In the collision process CO^+ ions are also formed in the $X\,^2\Sigma^+$ state (see also section 4.2). Just like in the tail of a comet, resonance absorption of $A\,^2\Pi$–$X\,^2\Sigma^+$ radiation by $X\,^2\Sigma^+$ ions should lead at increasing pressures to apparent longer lifetimes or smaller $A_{v'}$ values, as found by Fink and Welge. It can be shown that the presence of resonance absorption by the $X\,^2\Sigma^+$ ions would lead to a term c_2NI as in eq. (8) for the apparent emission cross section. If the mentioned resonance absorption is important, the magnitude of c_2 in the emission of $A\,^2\Pi$–$X\,^2\Sigma^+$ v'–v'' will depend on the value of v''. However, our measurements gave the same c_2 values in eq. (8) for $v' = 3$–$v'' = 0$ and $v' = 3$–$v'' = 3$. We think that in view of these considerations the effect of resonance absorption on the emission cross sections is not important under our experimental conditions.

We noticed that the magnitude of the term c_2NI in eq. (8) diminished when we increased the viewing region of the monochromator in a direction perpendicular to the beam. Photographs of the dimensions of the "radiating beam" made at different pressures and currents showed a broadening when the pressure and current increased. This broadening is caused by the relatively long radiative lifetime of the ion in the $A\,^2\Pi$ (v') state and a mechanism of a drift velocity of the ions out of the beam, which may be caused by space charge effects and field penetration from electrodes in the neighbourhood of the viewing region of the monochromator.

In the lifetime experiment of Fink and Welge[7]) the used potential configuration may cause a potential gradient in the collision chamber. This field penetration can be responsible for the measured decrease of $A_{v'}$ with increasing pressure below 4×10^{-3} torr. At higher pressures the escape of excited ions decreases by secondary collisions with the ground state.

4.5. Comparison of CO and N_2 data. CO and the isoelectronic molecule N_2 have comparable ion states, X, A and B, and corresponding transitions, with the exception that the weak B–A transition in CO^+ is not known in N_2^+. In table V a comparison is made between experimental total ionization cross sections and excitation cross sections of CO and N_2. Total ionization cross sections and cross sections for dissociative ionization of CO and N_2 appear to be almost equal to each other (see section 4.2 and refs. 17

and 19). The cross sections for formation of ions in the $B\,^2\Sigma^+$ state of CO^+ and the $B\,^2\Sigma_u^+$ state of N_2^+ respectively amount to 11–15% and 11–12% of the corresponding total ionization cross sections.

In the case of N_2 the experimental $A\,^2\Pi_u$ cross sections at 100 eV was found to be 4.7 ×, 2.65 × and 4.6 × 10^{-17} cm^2 as found by Stanton and St. John[26]), McConkey and Simpson[27]), and Skubenich and Zapesochny[4]). respectively. These values seem rather low with respect to the data of CO in table V. The emission cross sections of Srivastava and Mirza[28]) for $A\,^2\Pi_u$–$X\,^2\Sigma_g^+$ of N_2, which are larger than in the just before mentioned experiments, will lead to higher values of $\sigma_{A\,^2\Pi_u}$.

Berkowitz *et al.*[10]) showed in their photon impact experiments that the ratio between the excitation cross sections of the A and X ionic states is 0.78 in the case of N_2 and 0.8 in the case of CO. On the other hand, from the results in table V we find that the sum of these cross sections is approximately the same for N_2 and CO. We therefore expect that both for the A and X states the excitation cross sections for N_2 and CO are approximately equal.

Acknowledgements. We are indebted to Professor J. Kistemaker, Dr. T. R. Govers and Dr. L. Vriens for their critical comments on the manuscript. We thank Dr. W. Böhm of the group of Professor D. Labs of the Landessternwarte Heidelberg–Königstuhl for calibrating our deuterium lamps against the "secondary standard" deuterium lamp. We are grateful to Dr. T. R. Govers, Drs. C. A. van de Runstraat, Mr. C. I. M. Beenakker and Mr. H. J. Luyken for assistence in the calibration of our monochromator.

This work is part of the research program of the Stichting voor Fundamenteel Onderzoek der Materie (Foundation for Fundamental Research on Matter) and the Stichting Scheikundig Onderzoek in Nederland (Netherlands Foundation for Chemical Research) and was made possible by financial support from the Nederlandse Organisatie voor Zuiver-Wetenschappelijk Onderzoek (Netherlands Organization for the Advancement of Pure Research).

REFERENCES

1) Krupenie, P. H., The Band Spectrum of Carbon Monoxide, NSRDS–NBS 5, U.S. Government Printing Office (Washington, 1966).
2) Herzberg, G., Spectra of Diatomic Molecules, 2nd ed., Van Nostrand (Princeton, 1966).
3) Robinson, D. and Nicholls, R. W., Proc. Phys. Soc. **A75** (1960) 817.
4) Skubenich, V. V. and Zapesochny, I. P., ICPEAC V, Leningrad, eds. I. P. Flaks and E. S. Solovyov (1967) 570;
see also: Skubenich, V. V., Optics and Spectrosc. (USSR) (Engl. Transl.) **23** (1967) 540.

5) Poulizac, M. C., Desesquelles, J. and Dufay, M., Ann. d'Astrophysique **30** (1967) 301.
6) Bennett, R. G. and Dalby, E. W., J. chem. Phys. **32** (1960) 1111.
7) Fink, E. H. and Welge, K. H., Z. Naturforsch. **23a** (1968) 358.
8) Desesquelles, J., Dufay, M. and Poulizac, M. C., Phys. Letters **27A** (1968) 96.
9) Schoen, R. I., J. chem. Phys. **40** (1964) 1830.
10) Berkowitz, J., Ehrhardt, H. and Tekaat, T., Z. Phys. **200** (1967) 69.
11) Moustafa Moussa, H. R., De Heer, F. J. and Schutten, J., Physica **40** (1969) 517.
12) Pitz, E., Applied Optics **8** (1969) 255;
Böhm, W., Labs, D., Lemke, D. and Pitz, E., Forschungsbericht W 6909, 1969, Bundesministerium für wissenschaftliche Forschung.
13) Bannenberg, J. G. and Tip, A., Proc. 4th Intern. Vacuum Congress, Manchester, ed. The Institute of Physics and the Physical Society, Conference Series No. 6 (1968) 609.
14) Bethe, H. A., Ann. Physik **5** (1930) 325.
15) Fraser, P. A., Canad. J. Phys. **32** (1954) 515.
16) Nicholls, R. W., Canad. J. Phys. **40** (1962) 1772.
17) Rapp, D. and Englander-Golden, P., J. chem. Phys. **43** (1965) 1464.
18) Schram, B. L., De Heer, F. J., Van der Wiel, M. J. and Kistemaker, J., Physica **31** (1965) 94;
Schram, B. L., Moustafa, H. R., Schutten, J. and De Heer, F. J., Physica **32** (1966) 734.
19) Rapp, D., Englander-Golden, P. and Briglia, D. D., J. chem. Phys. **42** (1965) 4081.
20) Wacks, M. E., J. chem. Phys. **41** (1964) 930.
21) Nicholls, R. W., J. Phys. B. **1** (1968) 1192.
22) Collin, J. E. and Natalis, P., J. Mass Spectrometry and Ion Physics, **2** (1969) 231.
23) Isaacson, L., Marram, E. P. and Wentink Jr., T., J. quant. Spectrosc. radiative Transfer **7** (1967) 691.
24) Hesser, J. E., J. chem. Phys. **48** (1968) 2518.
25) Aarts, J. F. M., De Heer, F. J. and Vroom, D. A., Physica **40** (1968) 197.
26) Stanton, P. N. and St. John, R. M., J. Opt. Soc. Amer. **59** (1969) 252.
27) McConkey, J. W. and Simpson, F. R., ICPEAC VI Boston, ed. The MIT Press, (1969) 414.
28) Srivastava, B. N. and Mirza, I. M., Canad. J. Phys. **47** (1969) 475.

Part B

EMISSION OF RADIATION IN THE VACUUM ULTRAVIOLET BY IMPACT OF ELECTRONS ON CARBON MONOXIDE*

Synopsis

We have measured relative cross sections for emission of radiation in the vacuum ultraviolet in the case of 0.1 - 5 keV electrons on CO. The molecular transitions studied are the fourth positive band system $A^1\Pi - X^1\Sigma^+$ and the Hopfield-Birge band systems $B^1\Sigma^+ - X^1\Sigma^+$ and $C^1\Sigma^+ - X^1\Sigma^+$. Absolute values for the cross sections are obtained by normalization on those evaluated from inelastic scattering experiments of Lassettre and co-workers. The apparent cross sections for the transitions which combine with the zero vibrational level of $X^1\Sigma^+$ are found to depend strongly on the gas pressure. This is probably caused by trapping of resonance radiation. There are indications in our results, that the electronic transition moment is not constant for the different transitions in the fourth positive band system. Dissociative excitation processes have been studied by observation of atomic radiation of fragment atoms and ions. Applications in the intensity calibration in the vacuum ultraviolet wavelength region are discussed.

1. *Introduction.* Studies on excitation of CO by electron impact are both of fundamental and astrophysical interest. We measured cross sections for emission of radiation from

* The Journal of Chemical Physics, 52 (1970) 5354, J.F.M. Aarts, F.J. De Heer.

CO in the vacuum ultraviolet produced by a beam of monoenergetic electrons (100 - 5000 eV). We detected radiation for the following transitions: $A^1\Pi - X^1\Sigma^+$, $B^1\Sigma^+ - X^1\Sigma^+$, $C^1\Sigma^+ - X^1\Sigma^+$, $E^1\Pi - X^1\Sigma^+$, and $F^1\Pi - X^1\Sigma^+$ (see Herzberg [1]) and Krupenie [2])). The emission of the $E^1\Pi$ and $F^1\Pi$ states was very weak and did not allow us to measure the energy dependence of their cross sections. Dissociative excitation has been observed from several C I, C II, O I and O II multiplets (see Moore [3])).

Our optical measurements are related with the inelastic scattering experiments of Lassettre and Silverman [4]), Meyer et al. [5]) and Lassettre and Skerbele [6]) and the lifetime measurements of Hesser [7]).

2. *Experimental procedure.* The apparatus and experimental procedure are the same as those described in refs. 8 and 9. Basically, the apparatus consists of an electron gun, a collision chamber which can be filled with CO, and an electron trap. Care was taken in construction and operation of the apparatus to suppress effects of secondary electrons and to insure complete collection of the electron beam passing through the collision chamber. The emitted radiation was observed at 90° to the electron beam axis and analyzed by a vacuum monochromator [9]). No corrections have been applied for polarization of the radiation, which polarization appears generally to be small for molecular radiation.

The emission cross section σ_{ij} for a certain spectral band is determined by

$$\sigma_{ij} = \frac{4\pi}{\omega} \frac{S(\omega)}{(I/e)\ NLk(\lambda)} \qquad (1)$$

where $S(\omega)$ represents the signal of the light emitted in the space angle ω, I/e is the number of incident particles passing per second through the collision chamber, N is the density of the target gas measured with a McLeod gauge, L is the emission path length observed by the monochromator and $k(\lambda)$ is the sensitivity (quantum yield) of the optical equipment.

Because a simple light standard is not available in the vacuum ultraviolet, we could not determine $k(\lambda)$ directly. For different molecular bands we measured relative emission cross sections as a function of impact energy. We normalized some of these relative emission cross sections at 500 eV on cross sections evaluated from inelastic scattering data of Lassettre and co-workers [4,6]. This evaluation is done by calculating first the excitation cross sections and then by using branching ratios [10,11] in order to obtain the relevant emission cross sections. This procedure is explained in section 5. When measuring the signal of light $S(\omega)$ at a certain wavelength and calculating the corresponding emission cross section σ_{ij} from inelastic scattering data, it is clear that $k(\lambda)$ can be determined using eq. (1). This has been done for $B\,^1\Sigma^+ - X\,^1\Sigma^+$ (0-0) at 1150 Å, for $C\,^1\Sigma^+ - X\,^1\Sigma^+$ (0-0) at 1088 Å and for different bands of the $A\,^1\Pi - X\,^1\Sigma^+$ band system, for instance the 0-1 band at 1597 Å.

The inaccuracy of the absolute values of our cross sections thus depends on the inaccuracies in the inelastic scattering data used, which inaccuracies are claimed to be about 10%. Additional errors of about 30% may be present for the bands of the $A\,^1\Pi - X\,^1\Sigma^+$ band system due to the branching ratios (see sections 5 and 6) used in the calcu-

lation of their emission cross sections.

In order to estimate the reliability of the k(λ) values obtained from the CO bands, we also measured the emission of the Werner bands of H_2 in the wavelength region between 1000 and 1240 Å (to be published). For determination of the cross sections for emission of these bands we used the theoretical Born calculations of Khare [12]) giving the excitation cross sections of the upper state of this system. Then we used the inelastic scattering data of Geiger and Topschowsky [13]) to find the relative population of the different vibrational levels of this upper state and the Franck-Condon factors given by Spindler [14]) to calculate the emission cross sections for the relevant Werner bands. Using the semiempirical emission cross sections obtained in this way and our intensity measurements we could calculate k(λ) values between 1000 and 1240 Å. We found that the corresponding value at 1088 Å was 41% larger than that of CO and at 1150 Å 28% lower (a smaller k(λ) value means a corresponding larger cross section for CO). At other wavelengths connected with dissociative excitation (see section 4) k(λ) was obtained by interpolation. The accuracy of the interpolated k(λ) values may not be better than 100%.

3. *Transitions from the* $A^1\Pi$, $B^1\Sigma^+$, *and* $C^1\Sigma^+$ *states.*

3.1. *Introduction.* The $A^1\Pi - X^1\Sigma^+$ bands (called the fourth positive group) are most characteristic for the vacuum ultraviolet part of the spectrum. Because of the relatively large difference in equilibrium distance of the two states, about 0.1 Å [1]), many vibrations v' of the upper state $A^1\Pi$ are populated in the excitation process.

We have detected emission from v' between 0-8 to v" between 0-16. The corresponding emission covers the wavelength region from 1350 to 2400 Å.

The $B^1\Sigma^+$ and $C^1\Sigma^+$ states have about the same equilibrium distance as the ground state $X^1\Sigma^+$ [1]). This implies that mainly the v'=0 vibrational levels of the B and C states are formed in the excitation process (see also Lassettre and Skerbele [6])). The Hopfield-Birge transitions, B-X and C-X, in which the v'=0 - v"=0 bands are thus dominating, give radiation in the vacuum ultraviolet. The Ångstrom and Herzberg band system, B-A and C-A, give radiation in the visible region. Because the transition probabilities are roughly proportional to ν^3, where ν is the frequency of the radiation, the emission of the B-A and C-A transitions will be much weaker than that of the B-X and C-X transitions. This has been affirmed experimentally (section 5).

3.2. *Pressure dependence of the apparent emission cross sections.* Strong pressure effects have been found in the apparent cross sections for emission of those bands in the fourth positive group and those Hopfield-Birge bands which combine with v"=0 of the ground state. This must be due to self-absorption of radiation (resonance trapping). The effect is illustrated in fig. 1, where we plotted the ratios of the apparent emission cross sections at pressure p and at pressure zero (the latter being obtained by extrapolation) for an A-X, a B-X and a C-X band with v"=0. These ratios appeared to be independent of the electron impact energy. The pressure effect increases in the order of B-X, A-X and C-X bands. This is understandable,

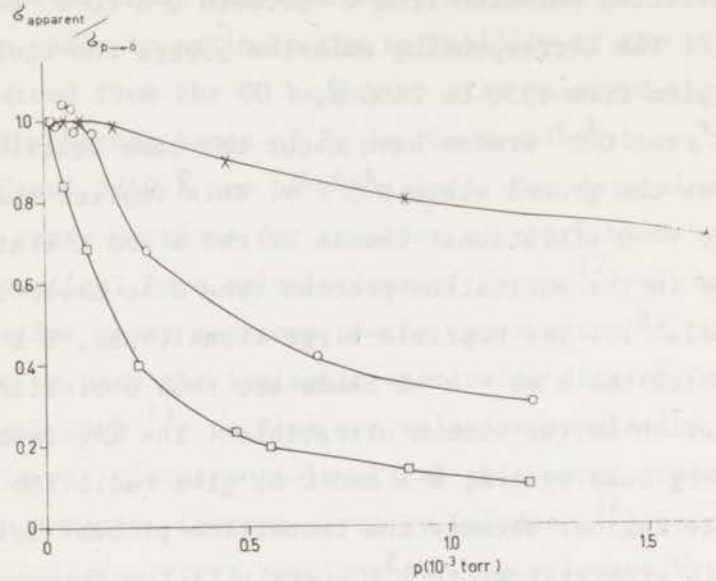

Fig. 1. Pressure dependence of the ratio of the apparent emission cross section and the emission cross section obtained by extrapolation to pressure zero for the transitions: ○, $A^1\Pi$-$X^1\Sigma^+$, 2-0, 1477 Å; ×, $B^1\Sigma^+$-$X^1\Sigma^+$, 0-0, 1150 Å; □, $C^1\Sigma^+$-$X^1\Sigma^+$, 0-0, 1088 Å.

because in this order the optical oscillator strength of the upper levels increases (see section 3.3 and ref. 6) and consequently the effect of self-absorption of radiation increases too.

3.3. *Emission cross sections and oscillator strengths.* In table I we give emission cross sections for $A^1\Pi$-$X^1\Sigma^+$ (0-1), $B^1\Sigma^+$-$X^1\Sigma^+$ (0-0) and $C^1\Sigma^+$-$X^1\Sigma^+$ (0-0) radiation. Our relative cross sections have been normalized at 500 eV on data of Lassettre and coworkers (see also section 5): From their measurements we calculated excitation cross

TABLE I

Emission cross sections in units of 10^{-18} cm^2

eV	$A^1\Pi$-$X^1\Sigma^+$ 0-1, 1596 Å a)	$B^1\Sigma^+$-$X^1\Sigma^+$ 0-0, 1150 Å	$C^1\Sigma^+$-$X^1\Sigma^+$ 0-0, 1088 Å
100	1.35	1.96	13.4
200	0.838	1.29	10.0
300	0.659		7.72
400	0.500	0.732	
500	0.438 b)	0.650 b)	5.43 b)
600	0.383	0.558	
800	0.302	0.423	4.07
1000	0.242	0.380	3.49
1500	0.182	0.259	
2000	0.145	0.225	1.96
3000	0.103	0.152	
4000	0.081	0.119	
5000	0.064	0.103	

a) uncorrected for cascade; see section 5.2;

b) normalized on Lassettre and co-workers [4,6], see section 5.

TABLE II

Optical oscillator strengths for A-X, B-X, and C-X transitions

	This work a)	Electron scattering b)	Lifetime measurements c)
$A^1\Pi$ (v'=0)	0.020	0.0181	0.0111
$B^1\Sigma^+$ (v'=0)	0.015	0.0139	0.0073
$C^1\Sigma^+$ (v'=0)	0.16	0.148	0.12

a) derived from Bethe plots (fig. 2) and normalization at 500 eV on cross sections of Lassettre and co-workers [4,6];

b) ref. 6;

c) ref. 7.

sections for different vibrational states, and we established the relation between our emission and their excitation cross sections. For the A-X band system the emission cross sections for all measured transitions (up to v'=5) appear to have the same energy dependence. For B-X and C-X we measured only one band.

The formation of the $A^1\Pi$, $B^1\Sigma^+$ and $C^1\Sigma^+$ states is optically allowed with respect to the ground state. At sufficiently high impact energy, according to the Bethe [15] theory, the excitation cross section $\sigma_{v'}$, for a state v' can be expressed by

$$\sigma_{v'}=(4\pi a_o^2 R/E_{el}')M_{v'}^2 \ln 4c(E_{el}'/R), \qquad (2)$$

where $E_{el}'=\frac{1}{2}mv^2$, m is the electron rest mass, v the velocity of the incident electron, R the Rydberg energy, a_o the first Bohr radius and c a constant. $M_{v'}^2=Rf_{v'}/E_{v'}$, where $f_{v'}$ is the optical oscillator strength for the transition and $E_{v'}$ the excitation energy.

We investigated whether the energy dependence of our emission cross sections was consistent with the optical oscillator strengths of Lassettre and Skerbele [6]. For that purpose we calculated excitation cross sections for $A^1\Pi$ v'=0, $B^1\Sigma^+$ v'=0 and $C^1\Sigma^+$ v'=0 by making use of the proportionality between excitation cross sections and cross sections for emission of radiation from the corresponding excited level (see also eqs. (11)-(13) in section 5). In fig. 2 we present the thus obtained excitation cross sections in a $\sigma E_{el}'/4\pi a_o^2 R$ versus $\ln E_{el}'$ plot. A linear relation is found in our energy region and the slopes of the lines are equal to $M_{v'}^2$, or $Rf_{v'}/E_{v'}$. Experimental results for $f_{v'}$ are given in table II, where

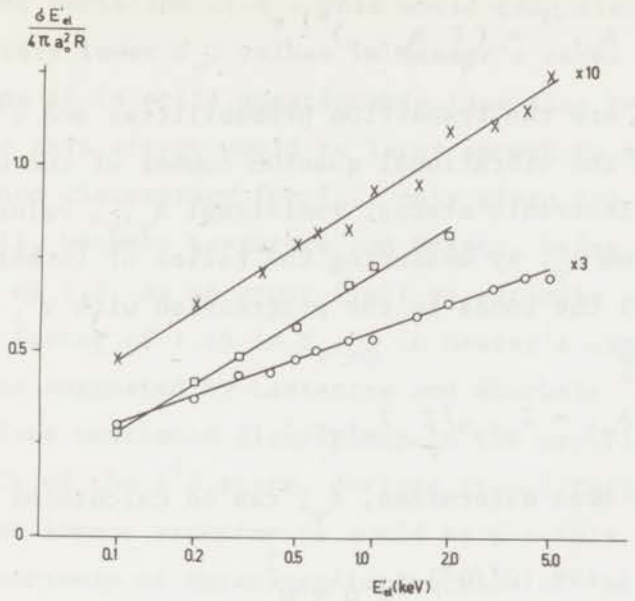

Fig. 2. Excitation cross sections normalized on data of Lassettre and co-workers, presented in $\sigma E'_{el}/4\pi a_o^2 R$ versus $\ln E'_{el}$ plots: O, $A^1\Pi$ v'=0; X, $B^1\Sigma^+$ v'=0; and □, $C^1\Sigma$ v'=0.

also values are included of Lassettre et al. [6]), and of Hesser [7]) from lifetime measurements. Oscillator strengths for $A^1\Pi$ (v'=1 and 2), which were recently obtained by Rich [16]) using a shock tube technique, are about midway between the values of Hesser and Lassettre and Skerbele. Our $f_{v'}$ values are in reasonable agreement with those of Lassettre and Skerbele; the difference is varying between 2% and 10%. Hesser's values are much lower for the $A^1\Pi$ and $B^1\Sigma^+$ states.

We shall discuss the possible causes for these discrepancies between $f_{v'}$ values of Hesser and Lassettre.

Hesser obtained $f_{v'}$ from his lifetime measurements by using different relations:

$$\sigma_{v'} = A_{v'}^{-1} = \left(\sum_{v''} A_{v'v''}\right)^{-1}, \qquad (3)$$

where $A_{v'v''}$ are the transition probabilities and v' and v'' refer to the vibrational quantum number of the upper and lower electronic states. Individual $A_{v'v''}$ values are obtained from $\tau_{v'}$ by measuring the ratios of intensities $I_{v'v''}$ of all the bands in the progression with v', using the equation

$$A_{v'v''}/A_{v'} = I_{v'v''}/\sum_{v''} I_{v'v''} \,. \qquad (4)$$

If $A_{v'0}$ has been determined, $f_{v'}$ can be calculated by

$$f_{v'} = 1.499\ (G'/G'')\ A_{v'0}\lambda_{v'0}^{2} \,. \qquad (5)$$

Here $\lambda_{v'0}$ is the wavelength of transition in centimeters, $A_{v'0}$ is given in seconds^{-1} and G' and G'' are electronic degeneracies, as defined by Mulliken [17]).

The possible experimental error in $I_{v'v''}$ and so in $A_{v'0}$ and $f_{v'}$ are dependent on the accuracy in the determination of the relative sensitivity (quantum yield) of the monochromator as a function of the wavelength. Our measurements indicate a steeper decrease of $I_{v'v''}$ with increasing value of v'' than that of Hesser. This is connected with a systematic decrease of the electronic transition matrix element R_e (see section 6) in our experiment with increasing values of the r-centroid $\bar{r}_{v'v''}$ (see Jarmain et al. [18])). The results of Hesser (given in table I of ref. 7) show in general no steep variation of $R_e(\bar{r}_{v'v''})$ with respect to the averaged value of R_e of a progression with v'. In this case Hesser's value for $A_{v'0}$, calculated with eq. (4), becomes lower than that

with our variation of R_e. This would then also lead to relatively lower $f_{v'}$ values in Hesser's case. Notwithstanding it is still questionable (see also ref. 7) whether this effect would be large enough to solve the mentioned discrepancy for $f_{v'}$, only given for v'=0 in table II, between Lassettre and Hesser, being almost a factor of 1.7. As an upper limit we estimate an increase with a factor of 1.15 in $f_{v'=0}$ in Hesser's experiment.

It was suggested by Lassettre and Skerbele [6]) that the before mentioned discrepancy in the oscillator strength of the $A^1\Pi$ state, derived from lifetime and electron impact experiments could be possibly due to the occurrence of resonance interaction of the $A^1\Pi$ state with one or more states, which do not combine via dipole transitions with any lower level, Such a mixing could increase the lifetime and consequently lowers the oscillator strength derived from it (see Douglas [19])).

In the case of the $B^1\Sigma^+$ and $C^1\Sigma^+$ states we can neglect all vibrational states except v'=0 to v"=0 for the v'=0 progression. This means that eq. (3) can be reduced to $A_{v'0} = A_{v'} = 1/\tau_{v'}$.

For the $C^1\Sigma^+$ (v'=0) state the f value found by Lassettre and by Hesser agree within 23%. We mentioned already (see section 2) that at 1088 Å our cross sections (and thus f) for the $C^1\Sigma^+$-$X^1\Sigma^+$ v'=0-v"=0 band, which are normalized on those of Lassettre et al. [4,6]), differ by 41% with those obtained by means of the normalization procedure with the Werner bands of H_2.

For the $B^1\Sigma^+$ (v'=0) state the f value found by Lassettre is almost a factor 2 higher than that of Hesser. The

TABLE III

Emission cross sections in units of 10^{-18} cm^2

eV	C II $^2D-^2P^0$ 1335 Å	C I $^3D^0$, $^3F^0-^3P$ 1278 Å	O I $^3S^0-^3P$ 1305 Å
100	4.17	0.903	0.785
150	3.88	0.732	
200	3.51	0.626	0.615
300	2.85	0.470	0.469
400	2.26	0.378	0.386
500	1.86	0.313	0.334
600	1.61	0.264	0.288
800	1.35	0.206	0.229
1000	1.10	0.170	0.181
1500	0.776	0.131	0.135
2000	0.605	0.099	0.109
3000	0.439		0.075
4000	0.337		0.060
5000	0.284		

TABLE IV

Constants for the calculation of excitation cross sections according to eqs. (2) and (8)

		$f_{v'}$ [a]	lnc	c_1	c_2	c_3
$A^1\Pi$	v'=0	0.0181	0.437	2.0	13.0	15.5
$B^1\Sigma^+$	v'=0	0.0139	- 0.47	2.65	4.00	
$C^1\Sigma^+$	v'=0	0.148	- 1.76	- 5.0	11.0	15.0

a) ref. 6.

latter reported that measurements on the $B^1\Sigma^+ - X^1\Sigma^+ v'=0 - v''=0$, at 1150 Å, were contaminated with radiation from an O I multiplet. He found that the intensity ratio of the relevant CO and O I radiation is 7 at an impact energy of 200 eV. This contamination could lead to an error in the f value obtained from the lifetime measurement. In our experiment we could not resolve the radiation of the O I multiplet. We mentioned already (see section 2) that at 1150 Å our cross sections (and thus f) normalized by means of the Werner bands are about 28% larger than those normalized on cross sections of Lassettre and co-workers. It is questionable whether the contamination with O I is large enough to explain this difference.

4. *Dissociative excitation.* We also studied excitation processes in the molecule leading to dissociation and formation of excited atoms or ions. Due to spectral overlap of some multiplets with the fourth positive group and (or) weak signals of these multiplets we only measured cross sections for the following transitions: C I $3d\,^3D^0$ (could also be $^3F^0$)$-2p^2\,^3P$ at 1278 Å, C II $2p^2\,^2D-2p^2\,^2P^0$ at 1335 Å and O I $3s\,^3S^0-2p^4\,^3P$ at 1305 Å. The emission cross sections are given in table III and again presented in fig. 3 by $\sigma E_{el}'/4\pi a_o^2 R - \ln E_{el}'$ plots. For all the transitions shown, we find a positive slope of the straight lines at high impact energies ($\gtrsim$ 300 eV). This implies (see also ref. 20) that at least one of the relevant excited dissociative states of the molecule is optically (dipole) allowed with respect to the ground state. The threshold for emission of the C II multiplet was found to

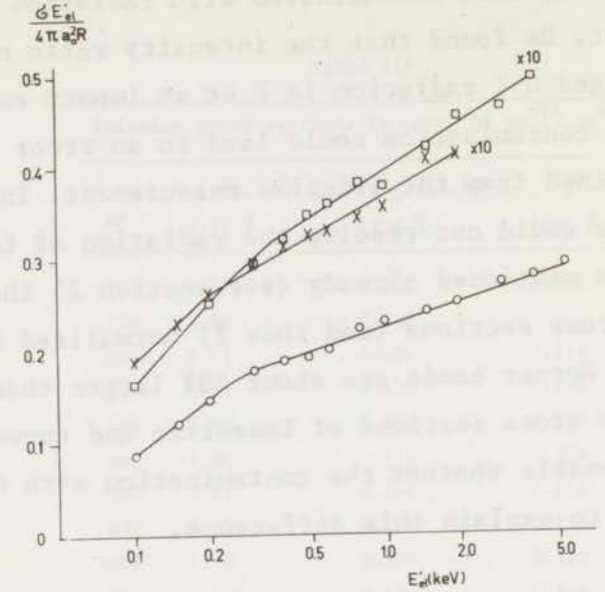

Fig. 3. Emission cross sections of C I, C II and O I multiplets, presented in $\sigma E'_{el}/4\pi a_0^2 R$ versus $\ln E'_{el}$ plots: ○, C II, $2p^2\ ^2D - 2p^2\ ^2P^o$, 1335 Å; ×, C I, $3d^3\ ^3D^o$, $^3F^o - 2p^2\ ^3P$, 1278 Å; □, O I, $3s\ ^3S^o - 2p^4\ ^3P$, 1305 Å.

lie at 33.5 ± 1 eV. The smallest possible threshold energy for the C II emission is the sum of the dissociation energy of CO, 11.09 eV [2]), the ionization energy of C I, 11.27 eV, and the excitation energy of the C II term, 9.29 eV. The sum is 31.6 eV. Our threshold of 33.5 ± 1 eV implies that in the dissociative process leading to the emission of the multiplet, oxygen is formed in the ^3P or ^1D state of O I.

5. *Normalization of our emission cross sections.*

5.1. *Evaluation of total excitation cross sections from inelastic differential cross sections.* The procedure em-

ployed is the one described by Vriens [21]) (see also Lassettre [22])) and applied by Vriens et al. [23]) and Lassettre et al. [24]). Often the experimental results on inelastic scattering of electrons are given by the generalized oscillator strength f(K), where K is the momentum transfer. The experimental f(K) values are determined only over a limited range of K values, while for calculation of the total cross sections all values are needed between K_{min} and K_{max}. Mainly for the region where the Born approximation is valid, Vriens [21]) has given analytical expressions for f(K) in which the parameters can be fitted to the experimental data. For dipole allowed transitions, considered in our case, the expansion is

$$f(x) = \frac{f(0)}{(1+x)^6}\left[1+\sum_{v=1}^{\infty} c_v \left(\frac{x}{1+x}\right)^v\right] , \qquad (6)$$

where

$$x=(Ka_o/\alpha)^2 \text{ and } \alpha=(Q/R)^{\frac{1}{2}}+[(Q-E)/R]^{\frac{1}{2}} . \qquad (7)$$

Here a_o and R have been defined in eq. (2); Q is the ionization energy of the electron involved in the excitation process, f(0) is the optical oscillator strength, and c_v are the parameters to be fitted. If the excitation refers to a certain vibrational state v', then the total excitation cross section is given by eq. (2), in which $M_{v'}^2=Rf_{v'}/E_{v'}$ ($f_{v'}=f(0)$) and c is determined by the parameters c_v of eq. (6), α and $E_{v'}$:

$$\ln c=2\ln(\alpha R/E_{v'})-(137/60)+\frac{1}{6}c_1+\frac{1}{42}c_2+\frac{1}{168}c_3 \qquad (8)$$

Lassettre and Silverman [4]) have determined f(K) values for the $A^1\Pi$, $B^1\Sigma^+$, and $C^1\Sigma^+$ states of CO. They used electrons with impact energies 416, 509, and 599 eV and

showed that to a good approximation the Born approximation was valid in this energy region. Meyer et al. [5]) extended the measurements with higher resolution, in order to determine the oscillator strengths of the different vibrational levels of the mentioned states. Later on the absolute values of f(K) have been remeasured by Lassettre and Skerbele [6]).

For our calculations of c we have used the f(K) values of Lassettre and co-workers for $A^1\Pi$ v'=0, $B^1\Sigma^+$ v'=0, and $C^1\Sigma^+$ v'=0. The results of our calculation are summarized in table IV. The values of $f_{v'}$ and c can be substituted in eq. (2) to obtain total excitation cross sections at different impact energies. Excitation cross sections of other vibrational states can be obtained by substituting the corresponding $f_{v'}$ of ref. 6 in eq. (2).

5.2. *Relation between optical and electron scattering data.* For our normalization procedure we have to relate our optical emission cross sections with the total excitation cross sections evaluated from electron scattering data. The basis formula is

$$\sigma_{ij,v'v''}=(A_{ij,v'v''}/\sum_{j,v''} A_{ij,v'v''}) \times$$

$$(\sigma_{i,v'}+\sum_{k,v'',v'} \sigma_{ki,v''v'}) , \qquad (9)$$

with j < i and k > i,

$$A_{ij,v'v''} \propto \nu_{v'v''}{}^3 q_{v'v''} \mid R_e(r) \mid^2 . \qquad (10)$$

Further $\sigma_{i,v'}$ is the excitation cross section (evaluated from inelastic scattering data) to the v' vibration-

al level of electronic state i; $\sigma_{ij,v'v''}$ is the cross section for emission of radiation from level i, v' to level j, v''. The term on the right-hand side with summation over k, v''' refers to population of level i, v' via cascade of radiation from higher excited levels k, v'''. $A_{ij,v'v''}$ represents the transition probability between levels iv' and jv'', $\nu_{v'v''}$ is the frequency of the radiation, $q_{v'v''}$ is the Franck-Condon factor and R_e is the electronic transition moment as a function of r, the internuclear separation. When R_e varies slowly with r, $R_e(r)$ is replaced by the fixed value of R_e at the r centroid of v'-v'', $\bar{r}_{v'v''}$ (see Jarmain et al. [18])).

We present the relations between emission and excitation for the relevant levels of this work. Afterwards the derivation is given. The equations are

$$\sigma(A^1\Pi\text{-}X^1\Sigma^+,\ v'=0\text{-}v''=1) = (q_{01}\nu_{01}^3 / \sum_{v''} q_{0v''}\nu_{0v''}^3)\,\sigma(A^1\Pi, v'=0), \qquad (11)$$

$$\sigma(B^1\Sigma^+\text{-}X^1\Sigma^+,\ v'=0\text{-}v''=0) = 0.86 \times 0.99\ \sigma(B^1\Sigma^+,\ v'=0), \qquad (12)$$

$$\sigma(C^1\Sigma^+\text{-}X^1\Sigma^+ v'=0\text{-}v''=0) = 0.99\ \sigma(C^1\Sigma^+, v'=0). \qquad (13)$$

In the derivation the effect of cascade has been neglected: No cascade to the $B^1\Sigma^+$ and $C^1\Sigma^+$ states is known. The cascade to the $A^1\Pi$ state goes via transitions from the $B^1\Sigma^+$ and $C^1\Sigma^+$ states, called the Ångstrom and Herzberg bands, which lie in the visible spectral region. From the calculated excitation cross sections for $A^1\Pi$ (section 5.1) and the measured emission cross sections

for the cascading transitions (to be published) we found that the cascade effect is about 1.5 % of the excitation cross section of $A^1\Pi$.

In the case of $A^1\Pi$, eq. (9) is further simplified by the fact that $A^1\Pi$ can decay only to $X^1\Sigma^+$. Then eq. (11) can be found immediately if we take the electronic transition matrix element $|R_e|^2$ constant for all relevant transitions in the A-X band system [1]). In that case the transition probabilities $A_{0v''}$ are proportional to $q_{0v''}\nu_{0v''}^3$. Franck-Condon factors, $q_{v'v''}$, for this band system have been calculated by Nicholls [25]). Our measurements indicate that $|R_e|^2$ decreases with increase of $\bar{r}_{v'v''}$ (see section 6). So we may make an error in our calculation by taking $|R_e|^2$ constant. This error will be smaller the larger the value of $q_{0v''}\nu_{0v''}^3$ in eq. (11) with respect to the denominator. The mentioned variation of $|R_e|^2$ would lead to too small cross sections in our calculation for the $A^1\Pi$-$X^1\Sigma^+ v'=0$-$v''=1$ transition (see table I). The estimated error for this transition could be as much as 15%.

The $B^1\Sigma^+$ and $C^1\Sigma^+$ states can decay both to the $X^1\Sigma^+$ and $A^1\Pi$ states. From the calculated excitation cross sections for $B^1\Sigma^+ v'=0$ and $C^1\Sigma^+ v'=0$ (section 5.1) and the measured Ångstrom and Herzberg bands we find that 86% of $B^1\Sigma^+ v'=0$ and 99% of $C^1\Sigma^+ v'=0$ decay to the $X^1\Sigma^+$ state. Computations of Franck-Condon factors of the B-X transition by Miller (see ref. 26) show that nearly 99% of the decay from $v'=0$ is in the $v'=0$-$v''=0$ band. For the C band this is assumed to be almost similar. In this case we have taken 100% of the decay from $v'=0$ in the

v'=0-v''=0 band. Using these properties it is easy to derive eqs. (12) and (13).

6. *Additional remarks on the branching ratio method.* The branching ratio method for molecules has been used to determine the sensitivity of the vacuum monochromator at different wavelengths [10,11]). In this method one uses two or more spectral bands with a common upper level. If R_e is constant their intensity ratios can be determined by making use of known Franck-Condon factors. When applying this method to the fourth positive group of CO, some irregularities were present at wavelengths below 1580 Å in fig. 1 of ref. 10. Some calibration points with v''=0 showed a much too low relative sensitivity. It has been found now that this is due to the effect of self-absorption as is described in section 3.2. With a target pressure of 10^{-4} torr this effect was eliminated. Additional measurements of the $a^1\Pi_g - X^1\Sigma_g^+$ of N_2 (Lyman-Birge-Hopfield), provided calibration points in the same wavelength region where the fourth positive group of CO radiates. Calibration points of the two band systems are consistent in the region 1400-1600 Å. Above 1600 Å the two band systems start to deviate from each other and at approximately 2000 Å the CO curve is about a factor of 3 lower than the N_2 curve. This discrepancy may be due to the fact that the electronic transition moment R_e of one or both band systems is not a constant over the range of v' and v'' transitions being considered.

We brought the calibration points obtained with the fourth positive band system between 1400 and 2000 Å on an

absolute scale at 1597 Å (see the $A^1\Pi-X^1\Sigma^+ v'=0-v''=1$ cross sections in table I). For the first negative group between 2100 and 2600 Å the absolute scale was obtained by using absolute cross sections obtained with our Leiss monochromator (to be published). We then find that the calibration points derived from the fourth positive system near 2000 Å are about a factor 3 too low with respect to those obtained from the first negative band system. This discrepancy may be due to the fact that in the $A^1\Pi-X^1\Sigma^+$ system $|R_e|^2$ decreases with increasing values of $\bar{r}_{v'v''}$.

Acknowledgments. We wish to thank professor E.N. Lassettre for valuable discussions and providing us experimental results before publication. We are indebted to professor J. Kistemaker and Dr. L. Vriens for their critical comments on the manuscript and to the latter for his contributions to the analytical procedure. We are also grateful for the comments of professor K. Dressler and Dr. J.E. Hesser about the lifetime measurements.

This work is part of the research program of the Stichting voor Fundamenteel Onderzoek der Materie (Foundation for Fundamental Research on Matter) and the Stichting Scheikundig Onderzoek in Nederland (Netherlands Foundation for Chemical Research) and was made possible by financial support from the Nederlandse Organisatie voor Zuiver-Wetenschappelijk Onderzoek (Netherlands Organization for the Advancement of Pure Research).

REFERENCES

1) Herzberg, G., Spectra of Diatomic Molecules (Van Nostrand, New York, 1950), 2nd ed.

2) Krupenie, P.H., Natl.Std.Ref.Data.Ser., Natl.Bur.Std. (U.S.) (1966).

3) Moore, C.E., Natl.Bur.Std. (U.S.), Circ. 488 (1950).

4) Lassettre, E.N. and Silverman, S.M., J.chem.Phys. 40, (1956) 1256.

5) Meyer, V.D., Skerbele, A., and Lassettre, E.N., J. chem.Phys. 43 (1965) 805.

6) Lassettre, E.N. and Skerbele, A., "Absolute Generalized Oscillator Strengths for Four Electronic Transitions in Carbon Monoxide at 500 eV Kinetic Energy", J.chem.Phys. (to be published).

7) Hesser, J.E., J.chem.Phys. 48 (1968) 2518.

8) Moustafa Moussa, H.R., de Heer, F.J. and Schutten, J., Physica 40 (1969) 517.

9) Moustafa Moussa, H.R., de Heer, F.J., Physica 36 (1967) 646.

10) Aarts, J.F.M. and de Heer, F.J., J.Opt.Soc.Am. 58 (1968) 1666.

11) McConkey, J.W., J.Opt.Soc.Am. 59 (1969) 110.

12) Khare, S.P., Phys.Rev. 149 (1966) 33.

13) Geiger, J. and Topschowsky, M., Z.Naturforsch. 21a (1966) 626.

14) Spindler Jr., R.J., J.quant.Spectry.radiative Transfer 9 (1969) 617.

15) Bethe, H.A., Ann.Physik 5 (1930) 325.

16) Rich, J.C., Astrophys.J. 153 (1968) 327.

17) Mulliken, R.S., J.chem.Phys. 7 (1939) 14.

18) Jarmain, W.R., Ebisuzaki, R. and Nicholls, R.W., Can.J.Phys. 38 (1969) 510.

19) Douglas, A.E., J.chem.Phys. 45 (1966) 1007.

20) Vroom, D.A. and de Heer, F.J., J.chem.Phys. 50 (1960) 580.

21) Vriens, L., Phys.Rev. 160 (1967) 100.

22) Lassettre, E.N., J.chem.Phys. 43 (1965) 4479.

23) Vriens, L., Simpson, J.A. and Mielczarek, S.R., Phys.Rev. 165 (1968) 7.

24) Lassettre, E.N., Skerbele, A. and Dillon, M.A., J.chem.Phys. 50 (1969) 1829.

25) Nicholls, R.W., J.quant.Spectry.radiative Transfer 2 (1962) 433.

26) Moore Jr., J.H., and Robinson, D.W., J.chem.Phys. 48 (1968) 4870.

CHAPTER IV

RADIATION FROM CH_4 AND C_2H_4 PRODUCED BY ELECTRON IMPACT*

Synopsis

The optical radiation resulting from the impact of 0-5 keV electrons on CH_4 and C_2H_4 has been investigated in the wavelength region from 1000 to 10000 Å. Only radiation from excited fragments was found. Thresholds and cross sections have been measured for the emission of the Balmer β radiation of H and the $A^2\Delta$-$X^2\Pi$ radiation of CH. The energy dependence of the cross sections at relatively high impact energies has been analysed by means of the Bethe-Born approximation. Possible mechanisms leading to the formation of the relevant fragments in the dissociative excitation of CH_4 and C_2H_4 have been considered.

1. *Introduction.* The present study on the excitation of CH_4 and C_2H_4 by electron impact is an extension of the experimental work of Vroom and De Heer [1]) on simple hydrocarbons. They determined emission cross sections for Lyman α and β and Balmer radiation from hydrogen atoms, produced in dissociative excitation of these molecules by 0.05 - 6 keV electrons. In the present work we measured the onset energy for the emission of some H lines of the Balmer series** and remeasured the emission cross sections for H_β.

* to be published in Physica, by J.F.M. Aarts, C.I.M. Beenakker and F.J. De Heer.

** The relevant H lines of the Balmer series are indicated as usual by H_α, H_β and H_γ respectively for n=3→2, 4→2 and 5→2 transitions, where n is the principal quantum number.

We investigated whether molecular radiation was produced in the excitation process between 1000 and 10000 Å. For the relatively strong radiation from the $A^2\Delta$-$X^2\Pi$ transition of CH thus found, we determined emission cross sections as well as the onset energy.

Similar measurements have been carried out by Sroka [2]. He measured emission cross sections for Lyman α, β, γ and δ radiation and multiplet radiation of CI in the vacuum ultraviolet wavelength region (900 - 1700 Å), investigating dissociative excitation of methane by electrons from threshold up to 400 eV. Carré [3] studied the same process in CH_4 and C_2H_4 for proton impact between 30 and 600 keV, partly overlapping our velocity range. He measured emission cross sections for H_β, H_γ and the $A^2\Delta$-$X^2\Pi$ and $B^2\Sigma^-$-$X^2\Pi$ transitions of CH.

2. *Experimental.* The measurements were performed with a "high" and a "low" energy apparatuses. The "low" energy apparatus [4] is basically the same as the "high" energy apparatus, fully described in ref. 5. In the former we use a capacitance manometer (MKS Baratron, type 77H-1) for the measurement of the gas pressure. The optical equipment used is described in ref. 6.

The emission cross section σ for the H and the CH radiation was determined by using the following equation:

$$\sigma = \frac{4\pi}{\omega} \frac{S(\omega)}{(I/e)NLk(\lambda)} \qquad (1)$$

where $S(\omega)$ represents the light intensity in the space angle ω, (I/e) the number of incident particles passing per second through the collision chamber, N the target

density, L the path length along which emission is observed by the monochromator and $k(\lambda)$ the quantum yield of the optical equipment determined by means of a standard tungsten ribbon lamp [5]. No corrections have been applied for the degree of polarization of the radiation, which is found to be small for the Balmer radiation [1]. The light intensities have been measured in a region where they varied proportionally with the electron current and the gas pressure ($\leq 10^{-3}$ torr). At impact energies $\geq$ 100 eV, the electron currents were of the order of 200 μA; they were smaller than 10 μA in the neighbourhood of the threshold.

With the "high" energy apparatus we measured relative emission cross sections. These relative values were normalized at 100 eV on those cross sections obtained with the "low" energy apparatus.

The uncertainty of our emission cross sections is estimated to be about 10%, mainly due to systematic errors in the intensity calibration. Additional errors of about 3% may arise in the cross section for the $A^2\Delta$-$X^2\Pi$ transition, due to the fact that this band had to be measured in parts (see below).

The onset energy for the Balmer and the CH radiation, formed by dissociative excitation in CH_4 and C_2H_4, has been determined by energy scannings on an X-Y recorder. These measurements were performed with a mixture of CH_4 or C_2H_4 and He, where the 4713 Å radiation of He (4^3S-2^3P) was used for calibration of the energy scale. The 4713 Å radiation of He has a known threshold of 23.5 eV [7a]. It is known that the accuracy of the experimental

onset energy for dissociative excitation is difficult to evaluate [8]). We estimate the accuracy for the Balmer and the CH radiation to be about 0.5 eV in the case of CH_4 and 1 eV in the case of C_2H_4.

The measurement of the $A^2\Delta$-$X^2\Pi$ transition of CH was complicated by the extension of its bands, about 200 Å broad, and the presence of the H_γ radiation at 4340 Å (see fig. 1). The most intense part of the observed radiation consists of the v'=0 - v''=0 band with a band head at

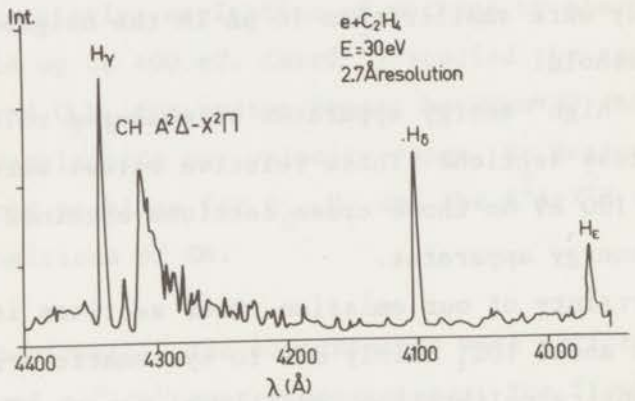

Fig. 1. Part of the emission spectrum produced by dissociative excitation of ethylene by electron impact.

4314 Å. The maximum slit width of our monochromator was 2 mm, corresponding to a bandpass of 54 Å. The following procedure was applied. The relevant wavelength region was divided into four parts, each of 50 Å width, corresponding to a width of 1.8 mm of the monochromator exit slit. The entrance slit width was taken 0.1 mm in order to reduce overlap of the chosen band parts as much as possible. The intensity of the whole CH band was determined by adding up

the intensities of the four parts of 50 Å. The ratio of the intensity of the whole band to the most intense part, including the band head but excluding H_γ, was determined for impact energies below the onset for H_γ, which is higher than the onset energy for the CH band. The dependence of the intensity on the impact energy was only determined for the most intense part. For the calculation of the cross section at different impact energies we multiplied the intensity of the most intense part by the ratio just mentioned. This ratio was almost the same for dissociative excitation of methane and ethylene. In the above procedure we assume that the rotational structure and the population of the different vibrational levels of the $A^2\Delta$ state of CH are both independent of the impact energies used.

3. *Results and comparison with other measurements.* In the spectra (1000-10000 Å) obtained by electron impact on CH_4 and C_2H_4 only radiation from fragments could be identified [7,9,10], i.e. Lyman and Balmer radiation of H, CI multiplets: $2p^3\ ^3D^o - 2p^2\ ^3P$ (1561 Å), $3s\ ^3P^o - 2p^2\ ^3P$ (1657 Å) and $3s\ ^1P^o - 2p^2\ ^1D$ (1931 Å), CH transitions: $A^2\Delta-X^2\Pi$ (4300 Å system) and $B^2\Sigma^--X^2\Pi$ (3900 Å system) and in the case of C_2H_4 Swan bands (~ 4700 Å) of C_2 as well. Except for the Swan bands the spectra obtained from CH_4 and C_2H_4 are similar. The light signals of the CI multiplets, the B-X transition of CH and the Swan bands of C_2 were too weak for cross section measurements, which were confined to H_β and $A^2\Delta-X^2\Pi$ of CH. The results for both CH_4 and C_2H_4 are given in table I.

TABLE I

Emission cross section for Balmer β radiation from H and $A^2\Delta$-$X^2\Pi$ radiation from CH fragments of CH_4 and C_2H_4 in units of 10^{-19} cm^2

eV	CH, $A^2\Delta$-$X^2\Pi$ 4200-4400 Å		H, n = 4-2 4861 Å	
	CH_4	C_2H_4	CH_4	C_2H_4
20	6.1	1.4	-	-
40	17.4	10.0	3.69	1.87
60	17.7	14.4	5.68	4.00
80	17.3	14.7	6.36	5.48
100	17.0	14.6	6.48	5.95
150	14.3	12.0	5.21	5.05
200	11.6	9.80	4.15	4.00
300	8.53	7.42	2.86	2.63
400	6.91	5.95	2.12	2.00
500	5.75	4.95	1.65	1.54
600	4.90	4.20	1.39	1.28
800	3.77	3.30	1.04	0.926
1000	3.09	2.66	0.820	0.730
1500	2.23	1.83	0.524	0.490
2000	1.73	1.47	0.396	0.365
3000	1.20	1.05	0.267	0.254
4000	0.925	0.80	0.204	0.199
5000	0.785	0.67	0.167	0.159
M^2	0.0094 ± 0.0010	0.0082 ± 0.0003		
c	15	14		

TABLE II

Observed onset energies (eV) for formation of H(n) and CH(A) fragments in dissociative excitation of CH_4 and C_2H_4

	Lyman [a]	Balmer
CH_4		
$CH_4^* \rightarrow H(n=2)$	20.7 ± 0.8	
$\rightarrow H(n=3)$	21.2 ± 0.8	21.9 ± 0.5
$\rightarrow H(n=4)$	21.7 ± 0.8	21.8 ± 0.5
$\rightarrow H(n=5)$	21.7 ± 0.8	22.3 ± 0.5
$CH_4^* \rightarrow CH(A)$	14.6 ± 0.5	
C_2H_4		
		Balmer
$C_2H_4^* \rightarrow H(n=4)$		23.2 ± 1.0
$C_2H_4^* \rightarrow CH(A)$	15.2 ± 1.0	

a) Sroka [2].

The energy dependence of these emission cross sections below 100 eV is presented in fig. 2 for CH_4 and in fig. 3 for C_2H_4. The onset energy for the emission from CH and for Balmer radiation is given in table II.

Because we found for the A-X transition of CH only radiation between 4200 Å and 4400 Å, the afore mentioned emission cross sections are equal to the cross sections for dissociative excitation to the $A^2\Delta$ state of CH. According to ref. 1, the H_β cross sections are mainly determined by the dissociative excitation to the 4s and 4d states of H. The cross sections for C_2H_4 are found to

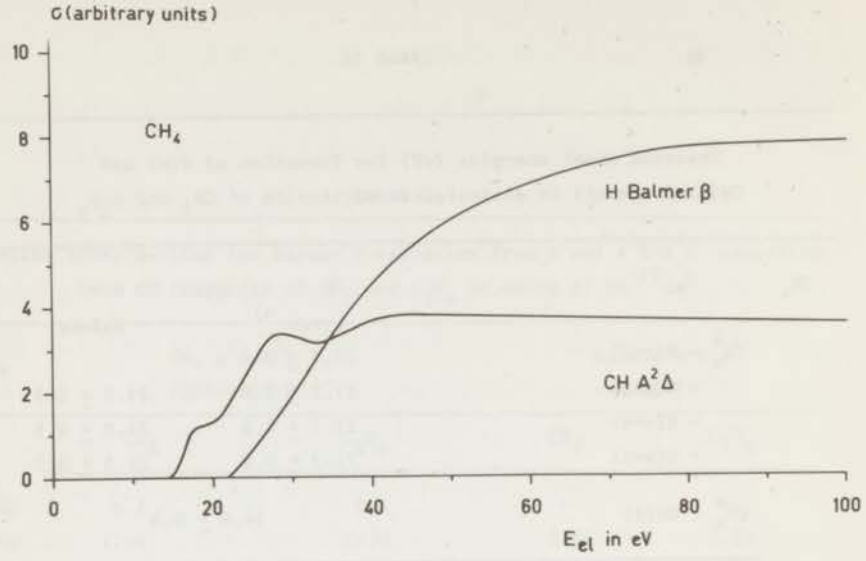

Fig. 2. Energy dependence below 100 eV of the emission cross sections for the Balmer β radiation from H and for $A^2\Delta$-$X^2\Pi$ from CH formed in dissociative excitation of methane.

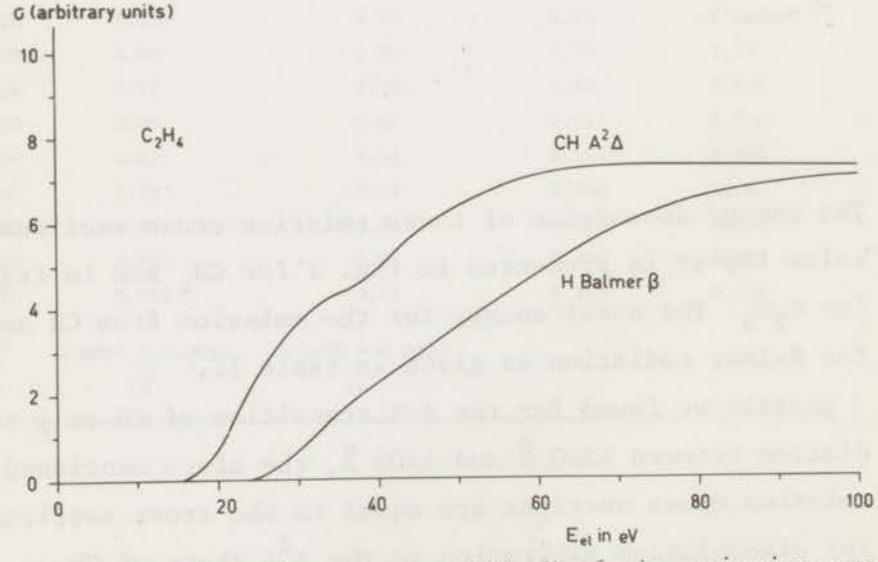

Fig. 3. Energy dependence below 100 eV of the emission cross sections for the Balmer β radiation from H and for $A^2\Delta$-$X^2\Pi$ from CH formed in dissociative excitation of ethylene.

have the same energy dependence, within about 4%, as those for CH_4 (see table I). In figure 4 we compare our data for

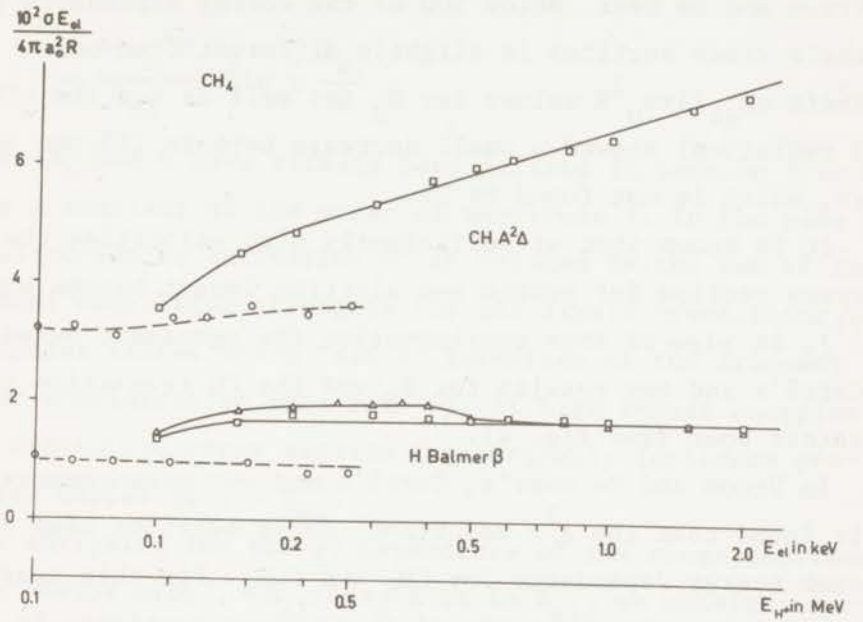

Fig. 4. Emission cross sections for the Balmer β radiation from H and $A^2\Delta$-$X^2\Pi$ radiation from CH presented in Bethe plots in the case of electron and proton impact on CH_4: solid lines refer to electrons; △, Vroom and De Heer [1]) and □, this work; dashed lines refer to protons: ○, Carré [3]). For protons $E_{el} = \frac{m}{M} E_{H^+}$.

methane above 100 eV with those of Vroom and De Heer [1]) and the proton impact data of Carré [3]) in a so called "Bethe" plot. In such a graph $\sigma E_{el}/4\pi a_o^2 R$ is plotted versus ln E_{el}, where a_o is the Bohr radius and R the Rydberg energy. The two abscissas for electrons and protons correspond to identical velocities of the projectiles involved: $E_{H^+} = \frac{M}{m} E_{el}$ where M and m are the proton and electron

masses respectively. For electron energies above 500 eV our cross sections for H_β agree within 4% with those of Vroom and De Heer. Below 500 eV the energy dependence of their cross sections is slightly different from ours. Their $\sigma E_{el}/4\pi a_o^2 R$ values for H_β (as well as for the other H radiation) showed a small decrease between 250 and 500 eV, which is not found by us.

It is known that at sufficiently high velocities the cross section for proton and electron impact become equal [11]). In view of this consideration the agreement between Carré's and our results for H_β and the CH transition is rather poor (see fig. 4).

In Vroom and De Heer's, Carré's and our measurements it is found that the $A^2\Delta$ and H(n=4) cross sections have the same energy dependence for CH_4 and C_2H_4. For this reason we discuss only the ratio of these cross sections. In the case of the H_β radiation, our ratio of 1.06 (obtained from table I) is 18% larger than that of ref. 1, which is within the quoted experimental accuracies. Carré's value is 1.15 in the comparable energy range (above about 200 keV).

In the case of the A-X radiation of CH, Carré's value of 1.9 for the ratio is much larger than our value of 0.86 (obtained from table I). This discrepancy is not understood.

4. *Analysis of the results with the Bethe-Born approximation.* In previous articles (see for instance ref. 6) we have shown the application of the Bethe theory [11]) on cross section data. At sufficiently high impact energy,

according to this theory [11]), the excitation cross section for optically allowed (dipole) transitions can be expressed by

$$\sigma = \frac{4\pi a_o^2 R}{E_{el}} M^2 \ln c \frac{E_{el}}{R} \qquad (2)$$

where a_o and R have already been defined in section 3 and c is a constant of the order of magnitude 1. In the case of dissociative excitation M^2 is related to the sum of the optical oscillator strengths for all dipole transitions to molecular states which lead to formation of the fragment under consideration (see ref. 6). At high impact energies the excitation cross section for optically forbidden processes varies as $\sigma \propto E_{el}^{-1}$.

By analysing the energy dependence of the cross sections in a "Bethe plot", $\sigma E_{el}/4\pi a_o^2 R$ vs $\ln E_{el}$, we obtain information on the type of processes involved in the (molecular) excitation process preceding the dissociation (cf. ref. 6). A constant positive slope in the asymptotic region in such a plot is connected with M^2, whereas the intercept of the extrapolated straight line portion with the abscissa is connected with c (see eq. (2)).

In the case of the formation of the CH ($A^2\Delta$) fragment in CH_4 we find a small constant positive slope for impact energies larger than 150 eV (see fig. 4); this indicates that optically allowed transitions are involved in the dissociative excitation process (compare eq. (2)). This applies also for the dissociative excitation in C_2H_4 in view of the proportionality of the relevant cross sections (see section 3). In table I we give the values of M^2 and c, determined by a least square analysis. The fact that the c

values are much larger than one, suggests that also optically forbidden transitions in CH_4 and C_2H_4 contribute to the formation of $CH(A^2\Delta)$ fragments. Another indication that more than one dissociation process leads to the formation of the particular CH fragment is the "structure" in the energy dependence below 100 eV of the relevant cross sections (see figs. 2 and 3).

In fig. 4 we see that σE_{el} for H_β radiation from CH_4 is constant above about 150 eV. In view of the proportionality of the relevant cross sections in CH_4 and C_2H_4 this applies also for the latter gas. The zero slope in this Bethe plot indicates that the dissociative excitation in CH_4 and C_2H_4 leading to H_β radiation proceeds via optically forbidden transitions, as was found before by Vroom and De Heer [1]) and Carré [3]).

In our Bethe plots there is no indication for relative strong contributions of spin forbidden transitions in the dissociative excitation processes under consideration, as they would would give a negative slope. Such transitions have been found in other electron impact experiments (see for instance ref. 12), with a detection technique, basically different from ours.

5. *Dissociation processes.*

5.1. *Methane.* Because there are only continua present in the optical absorption spectrum of CH_4 (see for instance refs. 13 and 14) and no molecular radiation of CH_4 is found, neither in the emission spectra of Sroka [2]), nor in ours, we conclude that the excited singlet states of CH_4 are unstable with respect to dissociation into

fragments (see also ref. 10).

For some dissociation processes leading to particular quantum states of the fragments, we have calculated minimum excitation energies by adding up the energy of dissociation into fragments in their ground state and the relevant excitation energies of one or more of those fragments (see table III). These calculated values are minimum values because the kinetic energy imparted to the frag-

TABLE III

Calculated minimum [a] energies (eV) for formation of H(n=4) and CH(A) fragments in dissociative excitation of CH_4 and C_2H_4

	Dissociation products [b]	
CH_4	1) $CH_4^* \rightarrow CH(X) + H_2(X) + H(n=1)$	9.2
	2) $CH(X) + 3\,H(n=1)$	13.7
	3) $CH(A) + H_2(X) + H(n=1)$	12.1
	4) $CH(A) + 3\,H(n=1)$	16.6
	5) $CH(A) + H_2(X) + H(n=4)$	24.8
	6) $CH_3(\tilde{X}) + H(n=4)$	17.2
	7) $CH_3(\tilde{B}) + H(n=4)$	22.9
	8) $CH_2(\tilde{X}) + H(n=4) + H(n=1)$	22.1
	9) $CH(X) + H(n=4) + H_2(X)$	22.0
C_2H_4	1) $C_2H_4^* \rightarrow CH(A) + CH(X) + H_2(X)$	14.5
	2) $CH(A) + CH(X) + 2\,H(n=1)$	19.0
	3) $C_2H_3(\tilde{X}) + H(n=4)$	16.6
	4) $C_2H_2(\tilde{X}) + H(n=4) + H(n=1)$	19.1
	5) $CH_2(\tilde{X}) + CH(X) + H(n=4)$	24.5

a) the kinetic energy imparted to the fragments is taken zero. The used dissociation energies (see section 5) for $0^{\circ}K$ have not been corrected for the influence of the temperature, being only a few hundredths of an eV at room temperature;

b) the quantum state of the fragments is given in parentheses.

ments and possible vibrational energy is assumed to be zero. They have been obtained by using the following data: the excitation energies of H, CH and CH_3 have been taken from the tables of refs. 7a, 15 and 10 respectively. For the dissociation energies we used D(H-H) = 4.48 eV [15], D(C-H) = 3.47 eV [15], $D(CH_3-H)$ = 4.41 eV [10], $D(CH_2-H)$ = 4.90 eV [10] and D(CH-H) = 4.46 eV, calculated as shown below. The latter two interdependent values are only approximate: the value for $D(CH_2-H)$ is an upper limit, due to the method of its determination [10]; the value of 4.46 eV, being the lower limit of D(CH-H), is derived by means of the following thermodynamic relation:

$$D(CH-H) = 4\Delta Hf^{\circ}(H) + \Delta Hf^{\circ}(C) - \Delta Hf^{\circ}(CH_4) - \\ - D(C-H) - D(CH_2-H) - D(CH_3-H) \qquad (3)$$

The thermodynamic quantities ΔHf° represent the heat of dissociation of methane into free atoms and have been taken from ref. 16. The dissociation energies on the right hand side of eq. 3 have already been given before. The accuracy of the calculated minimum excitation energies given in table III is estimated to be better than 0.2 eV in all cases except for process no. 8. In this table we did not include dissociative ionization processes. These processes require larger excitation energies and therefore they are less probable.

In order to determine some of the dissociation processes occurring, we consider also the results of flash photolysis (see for instance ref. 17) and "neutral" fragment mass spectrometry (see for instance ref. 18).

Flash photolysis experiments by Braun et al. [17] revealed that dissociation of CH_4 produced mainly CH and

hydrogen. Since the wavelength of the flash radiation was larger than 1050 Å (= 11.8 eV, the transmission limit of the LiF window), it is obvious from table III that the only process that could produce CH was:

$$CH_4 + h\nu \rightarrow CH_4^* \rightarrow CH(X^2\Pi) + H_2(X^1\Sigma_g^+) + H(n=1) \qquad (4)$$

Another experiment on fragmentation of CH_4 was carried out by Dyson [18], who bombarded CH_4 with 100 eV electrons. In this experiment the neutral fragments were detected by ionizing them by a second electron beam and making a mass spectrometer analysis. Dyson's experiment indicated a high probability for the formation of methyl radicals (and hydrogen), not found by Braun et al.:

$$e + CH_4 \rightarrow CH_4^* \rightarrow CH_3^* + H \qquad (5)$$

where the CH_3 radical is most probably in an excited state (see ref. 10). The large cross section for production of this fragment suggests that an optically allowed transition is involved. In the case that the energy needed for this transition is larger than about 11.8 eV (= LiF cut-off), Dyson's results do not contradict those of Braun et al. [17], even though we did not find any radiation of excited state(s) of CH_3 in our experiment. We may remark that the relevant dissociation process(es) in expression (5) probably lead to H atoms in their ground state (n=1), because at 100 eV impact energy the cross section for production of CH_3^* as estimated by Dyson is much larger than that for the total production of excited H atoms, measured by Vroom and De Heer [1].

As was pointed out in the previous section, the formation of the $CH(A^2\Delta)$ fragment proceeds at least partly

via an optically allowed transition. At the observed threshold of 14.6 ± 0.5 eV, energy considerations (cf. table III nrs. 3, 4 and 5) require the dissociation process involved to be:

$$CH_4^* \rightarrow CH(A^2\Delta) + H_2(X^1\Sigma_g^+) + H(n=1)$$

The difference between the calculated minimum energy for this process and the observed onset for emission of the $CH(A^2\Delta)$ radical indicates that some kinetic energy (~ 2 eV) is imparted to the fragments. The observed "structure" in the energy dependence of the CH radiation (see fig. 2) suggests that other dissociation processes contribute to the production of $CH(A^2\Delta)$ fragments at somewhat higher impact energies (cf. table III, nr. 4).

Other dissociative excitation processes, which are optically forbidden, are involved in the production of excited H atoms ($n \geq 2$) (see ref. 1). Considering the calculated values in table III for those dissociation processes leading to H(n=4) and the observed onsets for the relevant Lyman and Balmer radiation in table II, we conclude that some part of these H^* atoms is probably formed in the dissociation process:

$$CH_4^* \rightarrow CH_3(\tilde{X}^2A_2'') + H(n=4)$$

where some kinetic energy is imparted to the fragments. We conclude that a part of the H(n=3) and H(n=5) fragments are formed in a similar way, because there is little difference between our experimental onset energies for H(n) states with n=3, 4 and 5 and also for the calculated minimum energies (not shown in table III for n=3 and 5). These considerations apply also to H(n=2) as suggested by Sroka [2].

The similar energy dependence of the resulting Lyman and Balmer radiation (see ref. 1) as well as the absence of "structure" near the onset energy (see ref. 2 and fig. 2) and the slightly different values for their onset of emission (see table II) suggest that the relevant dissociation processes occur via only a few intermediate molecular states (Rydberg states).

The excitation energy of the molecular states of CH_4 leading to the excited H fragments as well those leading to CH(A) is larger than the ionization potential of CH_4, being 12.99 eV [10]. This indicates that so called super-excited states (see Platzman [19]) are involved in the excitation process, as was also concluded from other evidence by Vroom and De Heer [1] and Ehrhardt and Linder [20].

5.2. *Ethylene.* The emission spectrum of C_2H_4 is very similar to that of CH_4, i.e. we found radiation from the same dissociation products. Contrary to methane, the ultraviolet absorption spectrum of ethylene shows discrete structure superimposed on continua (see for instance refs.14 and 21). However, we did not find any emission (in our wavelength region) from the molecular states of C_2H_4 as found in absorption. In order to calculate the onset energies for formation of excited fragments of C_2H_4 we used in addition to the data in section 5.1: $D(HCCH-H_2)$ = 1.85 eV [16], $D(C_2H_3-H)$ = 3.85 eV [22] and $D(CH_2-CH_2)$ = 7.3 eV [10]. Because the latter two dissociation energies as well as D(CH-H) (see section 5.1) are only approximate values, we estimate that most of

the calculated minimum energies for excitation of C_2H_4 as given in table III have an accuracy of about 1 eV.

The experimental onset of 15.2 eV for formation of the CH(A) fragment indicates that at least some part of the CH radiation is due to the dissociation process (see table III):

$$C_2H_4^* \rightarrow CH(A^2\Delta) + CH(X^2\Pi) + H_2(X^1\Sigma_g^+)$$

where some kinetic energy is imparted to the fragments.

In the case of the formation of H(n=4) fragments both processes nrs. 3 and 4 in table III are compatible with the observed threshold of 23.2 eV. Our measurements do not allow us to distinguish between these two processes.

The measured onset energies for the H_β and the CH radiation are larger than the ionization potential of C_2H_4, 10.50 eV [10]. This indicates, similar as for CH_4, that superexcited states are involved in the excitation process.

Acknowledgments. We are indebted to Professors J. Kistemaker and L.J. Oosterhoff and Dr. T.R. Govers for their critical comments on the manuscript. We gratefully acknowledge the helpful discussions with Professor C.E. Brion on threshold measurements.

This work is part of the research programm of the Stichting voor Fundamenteel Onderzoek der Materie (Foundation for Fundamental Research on Matter) and the Stichting Scheikundig Onderzoek in Nederland (Netherlands Foundation for Chemical Research) and was made possible by financial support from the Nederlandse Organisatie voor Zuiver-Wetenschappelijk Onderzoek (Netherlands Organization for the Advancement of Pure Research).

REFERENCES

1) Vroom, D.A. and De Heer, F.J., J.chem.Phys. 50 (1969) 573.

2) Sroka, W., Z.Naturforsch. 24a (1969) 1724.

3) Carré, M., Thesis, University of Lyon (1967).

4) Aarts, J.F.M., Thesis, University of Leiden, to be published.

5) Moustafa Moussa, H.R., De Heer, F.J. and Schutten, J., Physica 40 (1969) 517.

6) Aarts, J.F.M. and De Heer, F.J., Physica, to be published.

7a) Moore, C.E., A Multiplet Table of Astrophysical Interest (Observatory, Princeton, 1945).

7b) Moore, C.E., An Ultraviolet Multiplet Table, NBS Circ. 488 (U.S. Government Printing Office, Washington, 1950).

8) Field, F.H. and Franklin, J.L., Electron Impact Phenomena (Acad.Press New York, 1957) p. 61.

9) Pearse, R.W. and Gaydon, A.G., The Identification of Molecular Spectra (Chapman, London, 1965) 3rd ed.

10) Herzberg, G., Electronic Spectra of Polyatomic Molecules (Van Nostrand, Princeton, 1966).

11) Bethe, H.A., Ann.Physik 5 (1930) 325.

12) Brongersma, H.H. and Oosterhoff, L.J., Chem.Phys. Letters 3 (1969) 437.

13) Metzger, P.H. and Cook, G.R., J.chem.Phys. 41 (1964) 642.

14) McNesby, J.R. and Okabe, H. in Advances in Photochemistry, Vol. 3 (Interscience, New York, 1964) p. 157.

15) Herzberg, G., Spectra of Diatomic Molecules (Van Nostrand, Princeton, 1966) 2nd ed., table 39.

16) Wagman, D.D., Evans, W.H., Parker, V.B., Halow, I., Bailey, S.M. and Schumm, R.H., Selected Values of Chemical Thermodynamic Properties, NBS Techn.Note 270-3 (U.S. Government Printing Office, Washington, 1968).

17) Braun, W., McNesby, J.R. and Bass, A.M., J.chem.Phys. 46 (1967) 2071.

18) Dyson, K.O., Preprint of paper presented at Int.Conf. Mass Spectrometry, Brussels (1970).

19) Platzman, R.L., Radiation Research 17 (1962) 419.

20) Ehrhardt, H. and Linder, F., Z.Naturforsch. 22a (1967) 444.

21) Merer, A.J. and Mulliken, R.S., Chem.Rev. 69 (1969) 639.

22) Chupka, W.A., Berkowitz, J. and Refaey, K.M.A., J.chem. Phys. 50 (1969) 1938.

SAMENVATTING

Het in dit proefschrift beschreven onderzoek heeft betrekking op metingen van de werkzame doorsnede voor emissie tussen 500 en 10000 Å bij bombardement van de moleculaire gassen N_2, CO, CH_4 en C_2H_4 door electronen met een energie variërend tussen de drempel en 5 keV. Deze doorsneden, die verwant zijn met de doorsnede voor aanslag van een electronentoestand, worden bepaald door meting van de intensiteit van de uitgezonden straling vanuit die toestand. De resultaten van het onderzoek zijn neergelegd in een zestal publikaties, waarvan er vier hier opnieuw zijn afgedrukt.

De publikaties worden voorafgegaan door een korte inleiding, hoofdstuk I. In dit hoofdstuk wordt tevens een beschrijving gegeven van het apparaat, dat voor de metingen met zogenaamde "lage energie" (0-100 eV) electronen wordt gebruikt. De experimentele werkwijze met dit apparaat is analoog aan die van het zogenaamde "hoge energie"-apparaat (100-5000 eV), dat reeds in een vroegere publikatie werd beschreven.

Hoofdstuk II bevat de resultaten van de doorsneden voor emissie van een aantal bandensystemen van N_2 en N_2^+ en multipletten van N I en N II.

Hoofdstuk III vermeldt de resultaten van emissiedoorsneden voor bandensystemen van CO en CO^+, waarvan een aantal analoog zijn aan die van N_2 en N_2^+.

De metingen, beschreven in de hoofdstukken II en III tonen aan dat mogelijke secondaire processen, zoals additionele aanslag door secondaire electronen en absorptie van resonantiestraling, gemakkelijk tot fouten kunnen lei-

den in de bepaling van de emissiedoorsneden. Bij de analyse van de meetresultaten bij hoge energie is gebruik gemaakt van de Bethe-Born benadering, waarmee in het geval van optisch toegestane aanslagprocessen oscillatorsterkten kunnen worden bepaald. Het energiegedrag van de emissiedoorsneden voor moleculaire bandensystemen is in overeenstemming met hetgeen voor de relevante aanslagprocessen in N_2 en CO te verwachten is op grond van de soort overgang, hetzij optisch toegestaan of verboden. De intensiteitsverhoudingen van de vibratiebanden van N_2 en N_2^+ electronenovergangen komen overeen met de waarden, die met Franck-Condon factoren berekend kunnen worden; voor een aantal CO en CO^+ overgangen treden afwijkingen op.

Voorts wordt in hoofdstuk II nog aangetoond dat het met behulp van de "molecular orbital" theorie mogelijk is de dissociatieve aanslag en ionizatieprocessen in N_2, die leiden tot de waargenomen N I en N II multipletstraling, althans voor een gedeelte toe te schrijven aan de vorming van bepaalde moleculaire toestanden.

Hoofdstuk IV bevat de resultaten van de emissiedoorsneden van CH_4 en C_2H_4. Van deze moleculen is slechts emissie van fragmenten waargenomen. Door meting van de drempelenergie voor de vorming van deze fragmenten is inzicht verkregen in de dissociatieprocessen.

Volgens het gebruik in de Faculteit der Wiskunde en Natuurwetenschappen volgt hier een kort overzicht van mijn academische studie.

Na het behalen van het einddiploma HBS-B aan het St. Aloysius College te 's-Gravenhage begon ik in september 1959 met de studie in de scheikunde aan de Rijksuniversiteit te Leiden. Het candidaatsexamen, letter f, werd afgelegd in oktober 1962, waarna de studie werd voortgezet onder leiding van de hoogleraren Dr.L.J. Oosterhoff, Dr. C.J.F. Böttcher en Dr.C. Visser. Het doctoraalexamen met hoofdvak Theoretische Organische Chemie werd afgelegd in juni 1966. In oktober 1966 begon ik in de onder de leiding van Dr.F.J. de Heer staande groep botsingsfysica van het F.O.M.-Instituut voor Atoom- en Molecuulfysica te Amsterdam aan een onderzoek van de lichtemissie van moleculen geproduceerd door botsingen met electronen. Alle experimenten, die in dit proefschrift zijn beschreven, werden in het F.O.M.-Instituut verricht.

Van januari 1965 tot oktober 1967 was ik achtereenvolgens als candidaat-assistent en doctoraal-assistent verbonden aan de Afdeling Theoretische Organische Chemie. Hierna was ik als wetenschappelijk medewerker in dienst van Z.W.O. (S.O.N.).

Professor Dr.J. Kistemaker, directeur van het F.O.M.-Instituut voor Atoom- en Molecuulfysica ben ik zeer erkentelijk voor de genoten gastvrijheid. De stimulerende omgang met het wetenschappelijk en technisch personeel en de hulp die ik van hen ontving, heb ik zeer gewaardeerd. In het bijzonder bedank ik de leider van de groep botsingsfysica, Dr.F.J. de Heer, die mij voortdurend heeft

begeleid en gestimuleerd tijdens het onderzoek. Dr.L. Vriens en Dr.T.R. Govers bedank ik voor de vele vruchtbare discussies.

De meetapparatuur, die geconstrueerd werd door de heren E. de Haas en M.J. Hoogervorst, werd vervaardigd in de instrumentmakerijen van het F.O.M.-Instituut te Amsterdam en van het Chemie Complex te Leiden, respectievelijk onder leiding van de heren A.F. Neuteboom en W.C. Bauer. De medewerking van de heren H.B.J. Marsman en J.W. Bakker bij de opbouw van het apparaat heeft veel bijgedragen tot het bereiken van de resultaten. De electronische afdeling van het F.O.M.-Instituut onder leiding van de heer P.J. van Deenen heeft bijgedragen tot het oplossen van electronische problemen. Dr.D.A. Vroom en de heer C.I.M. Beenakker bedank ik voor hun aandeel in de metingen.
Mijn erkentelijkheid gaat voorts uit naar mej. J. Pleysier die de figuren tekende, naar de heren F. Monterie en Th. van Dijk voor het fotografische werk en naar mevrouw C.J. Köke-van der Veer, die het manuscript typte.

De prettige samenwerking met de leden van de Afdeling Theoretische Organische Chemie is door mij bijzonder op prijs gesteld. Vooral de stimulerende discussies met Dr. H.H. Brongersma heb ik zeer gewaardeerd.

STELLINGEN

1. De bewering van Schwarzenbach en Michaelis, dat bij de reductie van Bindschedler's Grün in waterige oplossing de optredende kleuromslag van blauwgroen naar geel toegeschreven moet worden aan de vorming van het bis-(p-dimethylaminophenyl)-stikstof radicaal, is aan bedenkingen onderhevig.

   Schwarzenbach, G. en Michaelis, L., J.Am.Chem. Soc., 60 (1938) 1667.

   Neugebauer, F.A. en Fischer, P.H.H., Chem.Ber. 98 (1965) 844.

2. Het door Gerhart en Ostermann gepostuleerde mechanisme voor het ontstaan van kernspinpolarisatie bij radicaal-overdrachts-reacties is onwaarschijnlijk, daar het een relatief lang levende overgangstoestand van drie fragmenten met ontkoppelde electronenspins veronderstelt.

   Gerhart, F. en Ostermann, G., Tetr.Letters (1969) 4705.

3. Voor de bepaling van de kwantumopbrengst van een monochromator voor straling in het vacuum ultraviolet (1000-2000 Å) kan het gemis van een standaard-lichtbron ondervangen worden door gebruik

te maken van een moleculair bandensysteem, waarvan de emissiedoorsneden berekend kunnen worden met behulp van aanslag-doorsneden en Franck-Condon factoren.

Aarts, J.F.M. en De Heer, F.J., J.Opt.Soc.Am. 58 (1968) 1666.

Dit proefschrift, hoofdstuk IIC, IIIB.

4. Het is onmogelijk de unimoleculaire dissociatie van HeH^+ te verklaren met behulp van predissociatie door middel van rotatie (tunnelen) op grond van de gemeten werkzame doorsneden.

Houver, J.C. et al., Int.J.Mass Spectrom.Ion Phys. 4 (1970) 137.

5. Het mechanisme dat Hogeveen, Gaasbeek en Bickel veronderstellen voor waterstof- en deuterium uitwisseling van alkanen in zeer sterke zuren zou nader onderzocht kunnen worden door bijvoorbeeld de producten van de waterstofoverdracht van alkanen in zure media, die met deuterium en tritium zijn gesubstitueerd, naar het pentamethylbenzyl kation te analyseren.

Buck, H.M., Rec.Trav.Chim. 89 (1970) 794.

Hogeveen, H., Gaasbeek, C.J. en Bickel, A.F., Rec.Trav.Chim. 88 (1969) 703.

6. De waarde bepaald door Briegleb en Czekalla van het dipoolmoment van het complex tussen chlooranil en hexamethylbenzeen is gezien de experimentele condities onbetrouwbaar.

   Briegleb, G. en Czekalla, J., Z.Elektrochem. 58 (1954) 249.

7. De veronderstelling van Siegbahn et al. dat de aanzienlijk verbrede piek rond 40 eV in ESCA spectra van twee-atomige moleculen het gevolg is van vibratiestructuur en Coster-Kronig-processen is onwaarschijnlijk. Een mogelijke verklaring voor deze verbreding is, dat de desbetreffende aangeslagen iontoestand repulsief is.

   Siegbahn, K. et al., ESCA Applied to Free Molecules, North-Holland (Amsterdam, 1969) hoofdstuk 5.

8. Het verdient aanbeveling om de in de molecuulspectroscopie gebruikelijke notatie voor overgangen tevens te gebruiken in de atoomspectroscopie.

   Document U.I.P. (S.U.N. 65-3) (1965).

9. De in de regeringsverklaring van 31 augustus j.l. geuite beschuldiging van moord aan het adres van een groep Zuid-Molukkers dient als smaad of bele-

diging van deze personen te worden aangemerkt.
Europese Conventie ter bescherming van de Rechten van de Mens en de Fundamentele Vrijheden, Art. 6 lid 2.
Wetboek van Strafvordering, Titel XVI van het Tweede Boek.

10. De doelstellingen en selectienormen van het onderwijs aan kinderen met leer- en opvoedingsmoeilijkheden komen onvoldoende tot hun recht zolang zich - zoals thans het geval is - nog een zeer belangrijke invloed doet gelden van negatieve milieu-factoren op de schoolgeschiktheid, met name ten aanzien van het verbaal vermogen, van kinderen die aangemeld worden voor L.O.M.-scholen.

J.F.M. Aarts Leiden, 16 december 1970.

DE PROMOTIE VINDT PLAATS IN DE
SENAATSKAMER VAN DE RIJKSUNIVERSITEIT,
RAPENBURG 73, LEIDEN.

RECEPTIE NA AFLOOP VAN DE PROMOTIE
IN HET ACADEMIEGEBOUW